Solar Powered Beach Buggy Challenge

Group #1

Team Members:
Jared Cozart
Jose Rosales
Robinson Charles
Tony Jimogaon

Spring 2018
4/27/18
Sponsored by Duke Energy

List of Figures

List of Tables

Table of Contents

1. Executive Summary

In recent years, there has a been a growing interest in both the public and commercial sectors with regards to the viability of automated motor vehicles. While there has been much research and prototyping done in the realm of converting traditional, on-road vehicles into self-driving cars, our team was unable to find anything concerning the automation of cars for non-standard terrain, such as sand. As a result, we have decided to create an automated, single passenger buggy for use on a populated beach. It will also be entirely operated on solar power, in order to demonstrate the viability and low power consumption of environmental detection and recognition systems.

The buggy will consist of a chassis, able to carry a passenger weighing a minimum of 120 lbs, across the beach at approximately 3 miles an hour. Through a combination of stereoscopic camera vision and Lidar, it will be able to conclusively detect and identify objects, communicate with an onboard Arduino unit, and through there affect the rotational speed of the wheels in order to turn the buggy away from a collision course with the object. Through the use of solar panels, as well as two onboard batteries, it will be able to operate for a minimum of 10 hours, assuming ideal weather conditions and functional components.

Lidar will be used as a primary method of surveying the landscape. Due to it's basis on time-of-flight technology, it is an ideal method for quick and precise distance measurements to within one centimeter. It can generate a 'point cloud', or a series of data points with differing distances and angles from the origin, that are within its field of view and are constantly updated, and these data points can be fed into the arduino in order to identify objects. The system will also utilize two stereoscopic cameras on the front of the buggy, giving us a rudimentary three-dimensional image which can be analyzed by image recognition software running on the Arduino unit. Through the use of both systems in unison, we can be certain of any objects that could potentially obstruct the path of the buggy, and program the buggy to move around them.

In an effort to emphasize the general independent nature of the buggy, and with consideration to the bright environment it will be operating in, it will be powered by a solar panel placed on a platform located at the rear of the buggy. The panel selected will be chosen for its ability to operate at a maximum efficiency in the bright sunlight, and for the capability to output a sufficient level of wattage, so as to properly run the motors, Arduino, location and navigational systems onboard. The solar cell will also turn slightly, using two smaller solar cells in a wedge pattern in order to detect the general location of the sun and maximize the amount of sunlight incident on the surface at any given point in time.

The primary goal of this project is to demonstrate the feasibility of both solar energy and automated vehicles, while simultaneously aiding beachgoers during their visit. The most costly aspects of our design will be the motors operating the wheels, and as a result we hope to showcase an efficient and cost effective way to provide self-driving capabilities to conventional vehicles.

This project is of course being done in conjunction with a group of mechanical engineers. Their role in the project will be in designing the chassis we will use as a basis for our electronic components, and in helping select the motors we will use to operate the buggy.

2. Project Description

The following section provides a general description of the project, listing all of the constraints and engineering requirements we were given by our sponsor. It will also describe the limitations on the components we will choose as we prototype our design.

2.1 Block Diagram

The diagram below in Figure 2.1 is a block diagram illustrating the general layout of the operating components, as well as their inputs and outputs. At the time of writing, none of the components have yet been acquired. As the project is still in the design phase, it is also possible that certain components may be altered slightly in order to produce a more efficient system. We intend to optimize our system to the best of our ability, and so our current design has been constructed with the understanding that the parts are not necessarily final. In an attempt to organize the workflow for this project, a list detailing the individual components of the project and the respective members who are responsible for that component's successful development is included blow in Table 2.1.

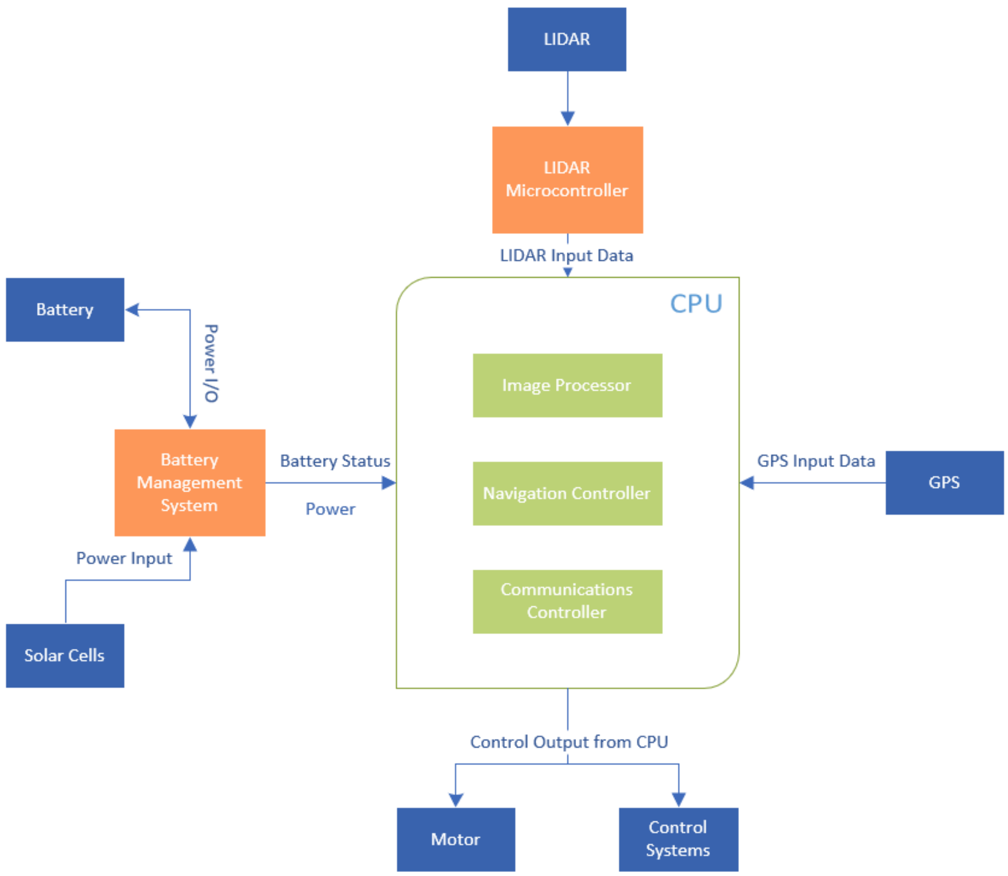

Figure 1 - The block diagram of the electrical system for the buggy.

Component Description	Team Member(s) Responsible	Component Status
Lidar	Jose Rosales, Jared Cozart	In Development
Lidar Microcontroller	Jose Rosales, Jared Cozart	In Development
Antenna	Robinson Charles	In Development

Battery Management Systems	Robinson Charles	In Development
Solar Cells	Robinson Charles	In Development
Communication Systems	Tony Jimogaon	In Development
Image Processor	Tony Jimogaon	In Development
Navigation Controller	Tony Jimogaon	In Development

Table 1 - A list of each of the components of the block diagram, the team member or members responsible, and their status

2.2 Requirement Specifications

Our buggy has a well defined set of criteria it must meet in order to be deemed a success. In terms of its power source, it must be able to run entirely on solar power for the entirety of time spent in operation. While in operation, it must not exceed speeds of 3 miles per hour, and it must be able to undergo a 10 mile trip along the beach, and successfully make the return trip. It must be designed to be able to withstand a carrying capacity of a 120 pound passenger. It must be able to operate without causing any harm to the environment, local wildlife or beachgoers, and it must be constructed on a budget that does not exceed our established budget of $2000.

2.3 Project Constraints

- Ability to operate under suboptimal weather conditions, such as a cloudy sky
- Ability of solar panels to adequately power all necessary subsystems for the duration of the trip
- Must be able to identify and steer away from ocean

2.4 Economic and Time Constraints

Given the scale of this project, there are significant economic restraints that need to be taken into consideration. We were given a budget of approximately $2000. Despite appearing as a sizeable amount of money, this budget is then split between the electrical and mechanical engineering teams, to be allocated on the basis of importance to the overall function of the system. For reference, typical automated vehicles using LIDAR spend between $12000 and $75000 for a single LIDAR system operating on a single vehicle. As a result, many difficult decisions concerning the allocation of the budget had to be made, with the most costly components appearing to be the tires and motors for the buggy.

As for our time constraint, significant consideration for the time requirement is a must. Our group alone will be working on the second semester in realizing the buggy. That means that we will not have the Mechanical or Computer Science teams working with us. While the absence of the Mechanical team can be remedied with the purchase of a subsystem that has most of our Mechanical requirements (such as a Power Wheels children's vehicle), the subsystem handled by the Computer Science team will still need to be handled by our team, as it is considered a vital component of the system. Without it, the buggy will not be an autonomous buggy.

Another consideration is that our second semester is a summer semester. Therefore, it has considerably less break time allotted to us than normal. Most teams will have the break between Fall-Spring or the summer between Spring-Fall to polish their plan, order their parts, and start assembly while our team will have only one week in between Spring-Summer.

And lastly, the summer semester itself is only about 12 weeks--4 weeks less than a Spring or Fall semester. As such, our team will have to design our system in such a way that it can be quickly assembled and tested once it is finalized. Specifically, the stereoscopic vision, LIDAR, and solar cells need to be able to be fine tuned and improved in a very short amount of time if the need arises.

2.5 Ethical, Health, and Safety Constraints

Given the relatively innocuous nature of our project, we see no serious ethical issues which need to be taken into consideration prior to development of this project, or which would be likely to present themselves in the course of the buggy's construction. Given the slow speed limited by both the specifications and the hardware, our buggy holds no real capability to be used in a military capacity, or as a weapon of any kind, as it is explicitly designed to avoid collision with objects. If anything, our buggy's primary use lies in its utility as a tool of leisure by allowing people to travel along the beach without any strenuous physical activity, which would be especially helpful for the elderly or the physically disabled. It could also be used to assist people who have been injured on the beach by allowing them to be transported to distant medical professionals. In both cases, there are no serious ethical considerations that would complicate the design of the buggy.

A major concern of this project is safety, specifically with regards to the people on the beach and the wildlife. As the vehicle will be driving autonomously, it is paramount that the image recognition systems be able to detect any moving object from a safe distance and steer well clear of it. As a result, we will incorporate both a remote and a manual 'kill switch' into our design, in order to ensure that the vehicle can be stopped in the event that either an error occurs with our prototyping, or a passenger riding in the vehicle feels that they are unsafe and need to bring the buggy to a stop.

Given the populated nature of the beach, and the electronics on board, it's also paramount that the buggy does not drive into the water. This is a massive potential safety hazard, and in order to counteract this we intend to program our LIDAR system to identify the scattered, haphazard point cloud it would likely receive from a large body of water like the ocean as a positive identification for a body of water, and automatically steer clear of it, providing that there is nothing in its way. This same logic will be used in order to stop the buggy from travelling away from the beach, into the mainland.

Bystanders should be made aware that the buggy is autonomous and should not be blocked or disturbed to prevent any unforeseen consequences. The buggy should also consider pedestrians that are not aware of the presence of the buggy. The buggy might trip or run over (albeit slowly) unaware pedestrians. A safe way to ensure that the buggy maintains a safe operating environment is to post watchers that can monitor the buggy and alert and pedestrians that may endanger the pedestrian, the buggy, or both.

Health-wise, the buggy does not emit any harmful elements (radioactive energy or carbon emissions). Health considerations were researched and our team has found none.

2.6 Environmental, Social, and Political Constraints

In much the same way that we were unable to identify any legitimate ethical concerns with regards to the design of our buggy, we find no political issues which would impact our design process. Our buggy is meant as a tool to assist beachgoers, and as a result has a very apolitical purpose. The only potential effect that politics could have on our designs are the country's use of tariffs on other powers which may or may not make certain components of our design more expensive.

The buggy, powered by solar cells, has a zero direct carbon footprint. Global environmental considerations are thus not a concern for this project. However, considerations are made for the small flora and fauna that might cross the buggy's path. Prior observation of the buggy's path of travel should be done to ensure that no endangered species or any flora or fauna are at risk of being trampled or hit by the buggy. Should there be environmental concerns that may cross the buggy's path, steps will be done to ensure that the buggy does not endanger them by either avoiding them or by the manual intervention of the team.

As the buggy is designed from well-accepted standards and methods, the buggy poses no threat to the fabric of society and does not have any opposition from any social group. Social considerations were researched and our team has found none.

2.7 Manufacturability and Sustainability constraints

Manufacturability constraints limit our procurement of materials and parts to ones that can be manufactured either by ourselves or through a third-party. Should a part prove to be something that we cannot manufacture ourselves or if it is more efficient to be purchased, it will be purchased. Our designs uses parts that are commonly and easily obtainable and thus pose no manufacturability constraint.

Our parts also use commonly available materials and poses no sustainability issues in both manufacturing and the sustainability of ecological balance.

2.8 House of Quality

After considering the engineering requirements we were tasked to work around, we constructed a house of quality, as shown below in Figure 2, in order to determine which areas of our design were the most vital, and which aspects of the design conflicted with each other the most.

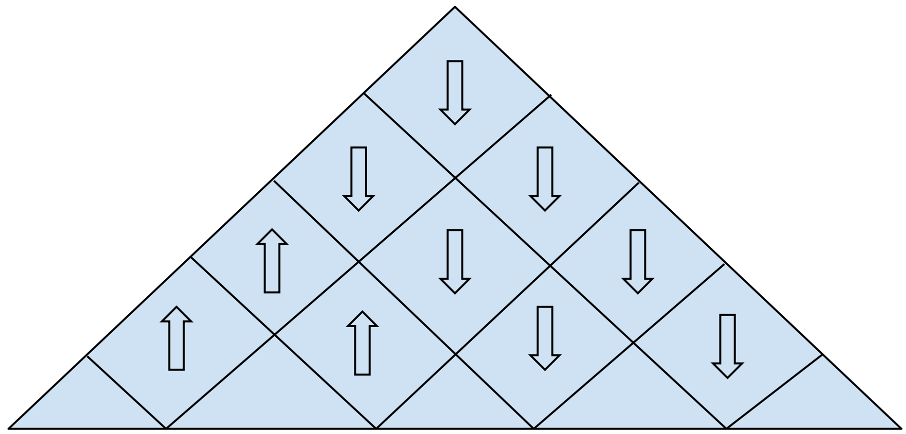

		Durab-ility	Structural Integrity	Speed	Power Use	Cost
		+	+	+	-	-
Object Detector	+			⇊	⇈	⇈
Cost	-	⇊	⇈	⇈	↑	⇈
Safety	+	⇈	↑	⇊	↑	⇈
Weight	+	⇊	⇈	⇊	⇈	↑

Targets for Engineering Requirements	Able to travel for 20 miles	Can carry a minimum of 120 lb	Max of 3 MPH	Self sufficient for 8 hours min.	Max of $2,000

Figure 2 - House of Quality

2.9 Objectives

This project has many objectives set forth by the client, Duke Energy. Namely, they are: To create a vehicle capable of traversing a beach while autonomously detecting moving and inanimate objects; To have the buggy travel at a maximum speed of 3 miles per hour, travel 10 miles, and carry a weight of approximately 120 lbs; To have it run entirely on solar power; To do no harm to the environment, or any beachgoers; and to be produced with a budget of $2000. These design goals ensure that the buggy can be a positive addition to the beach going experience, and can demonstrate the viability of low-cost Lidar and solar systems for autonomous transportation purposes.

A key feature of the buggy is its ability to automatically detect objects and move around them, and for that purpose we chose to incorporate a Lidar system into our design. While other autonomous vehicles chose to incorporate traditional rangefinders into their designs as a way of detecting objects, the ability of Lidar to generate a point cloud and recognize individual objects makes it a superior, if more complex, choice. It also allows us to continuously scan an entire field of view, as opposed to simply measuring distances along a single vector. In the interest of ensuring safety, we have also opted to incorporate a redundant form of image recognition in the form of stereoscopic vision, by way of two cameras placed at the front of the buggy. Through the use of both the Lidar and the stereoscopic vision, we can be certain that the buggy will not collide with any people or objects, assuming all components are functional.

In the interest of safety, several design decisions have been implemented. The primary safety feature will be several ‘kill switches’ placed in easily accessible areas of the buggy. One will be reachable by the passenger, another on the side of the buggy so as to be available to a passerby, and a remote ‘kill switch’ available to us as we monitor the buggy. For safety reasons, the maximum speed of the buggy is also limited to 3 miles per hour, so as to give us time to react in the event of some unforeseen design failure.

The primary purpose of this project is to create a novel mode of transportation that will stoke the public interest in the capabilities of both solar power and autonomous navigation. To this end, we intend to have a large solar panel on the rear of the buggy, which will provide power into one of two on-board batteries. The batteries will power the motor and electrical systems, and will each alternate between powering the buggy and receiving a charge from the solar cells. The solar panel will also be outfitted with servos, which will slightly adjust it's pan and tilt until it is maximizing the exposure of the solar cells to the sun. This will be done by taking two smaller solar cells and placing them in a wedge formation, allowing light to be incident on both faces. When both cells report an equal amount of light, that will indicate an optimal angle for the larger panel.

3 Initial Research

The following section contains a description of the research each of the team members has done in preparation for the design phase of the project. This includes a discussion on the fundamental, conceptual aspects of some key features of the project, such as solar power, Lidar, stereoscopic vision, electric motors, and so on.

3.1 Mechanical Components

This section details the research done into the mechanical engineering aspects of the buggy, such as the materials used to create the chassis and the suspension system. These components are as vital to the successful operation of the buggy as the electrical components, and so an extensive amount of research was done in order to determine the most effective solution to each individual concern.

3.1.1 Chassis

There are a couple main concerns when designing this chassis: the structure and the material properties. The structure itself has multiple components that must be designed around. The chassis will need to hold all of the components, its cargo, withstand the forces coming from the driving surface, and withstand the torque from the drivetrain. Another design topic is arrangement of the chassis members. The chassis must hold photovoltaics, wiring, computers, sensors, motor, drivetrain, suspension, and seat a 120 lb human within reasonable size. As long as all goals are met, smaller and lighter will typically be better. When a vehicle is made more compact, transport is easier but serviceability maybe sacrificed. With tighter arrangements of components, to access one part others might need to be removed in the process. When making a vehicle lighter, it will put less stress on mechanical components and the power of the motor will be used more efficiently.

The electrical properties of the chassis material come into play when electrical components come into contact with the chassis. Most vehicles use a conductive chassis to utilize it as an electrical ground around the vehicle. High end vehicles might use some fibrous composite, in which case a different grounding system must be used. However, a composite would not be useful for this buggy because it is not conductive and expensive. So, for this buggy steel or aluminum are being considered. Steel is inexpensive, works as a ground, and has high strength. On the other hand, steel is very heavy which which require stronger motors. Aluminum is light, even higher conductivity than steel, but more expensive.

Most chassis, whether it is a buggy or automobile, do not typically fail without being in a crash. Manufacturing a chassis is almost always welded together. Machining is not feasible because chassis are too large. When a weld is done properly, it should retain the strength of the member material from one member -- through the weld -- and to the other member. Welding provides strength in all directions instead of bolts, which vary in yield strength depending on the direction of forces act upon them. There are uncommon cases where the top mounting areas, of the rear subframe and/or spring and strut assemblies, will fatigue causing cracks or mushrooming. Depending on region and type of use, rust and corrosion can form. This is a very common occurrence in snowy regions because the salt on the roads corrode not only the chassis but any ferrous components on the vehicle. In the buggy's case, there will be salt and moisture which accelerate corrosion. Fortunately, this is a negligible issue for such short run time.

3.1.2 Suspension

The suspension will include control arms, swing arm, shocks, and springs. A spring will mount between a lower control arm and the chassis. The weight of the buggy partially compresses the springs when static. If the buggy encounters a bump under one tire while in motion, the spring will compress and the chassis will remain more level than if there was no suspension. If the buggy encounters a hole under one tire while in motion, the tire will dip inside as the spring extends providing the chassis with stability. The shocks will prevent excessive oscillation of the springs. While this design would be ideal for performance, the budget could be used in more important areas. So, one design in the works for the rear is a monoshock, swing arm, and solid-rear-axle setup. Figure 3 below shows the UFP Baja from Brazil with the same setup that might be implemented [1]. As it seems, it is very simple and cost effective. Considering the 3 MPH speed limit and relatively smooth terrain, there is not much of a performance loss. So, this design is a good candidate.

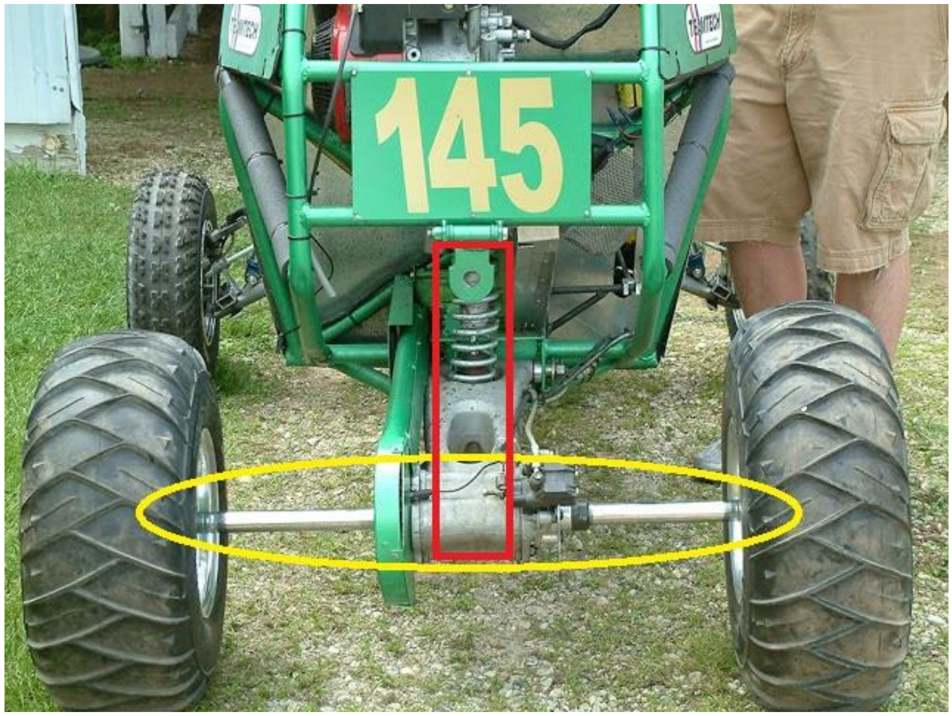

Figure 3 - UFP Baja presenting solid-rear-axle (yellow oval), monoshock (red rectangle), and swingarm design.

3.1.3 Drivetrain

Initially, the drivetrain would be a belt or chain running from the shaft of the motor to the rear axle(s). Instead of the price and weight of an independent rear end, a solid-rear-axle (SRA) might be used. A chain will likely be used over a belt because the chain is much cheaper. The belt would last longer with sand exposure, but the duration of service is short and one time. So, endurance of the chain will likely perform as needed. Figure 4 below shows the independent axles which can be compared to the SRA shown in figure 01. If the SRA is used, there will have to be design and analysis comparing a steel versus an aluminum axle and diameters. This is done to assure torque from the motor can be withstood. Given the beach as the surface being driven on, it would be helpful to not have a slipping differential to keep from getting stuck. The looseness of the sand will almost entirely ease the binding of tires from a locked differential. Since there is no longer a significant need for a conventional or limited-slip differential, the buggy does not need a differential at all. Now, the buggy will be simpler, lighter, and cheaper. Another possible design is differential steering where typical axles are not necessary. In this case, each drive wheel is electronically controlled, providing power as well as the ability to steer. Just an axle beam as part of the swingarm setup will suffice to tie components together. Since electric motors have a very broad range of RPM of usable torque, a transmission is not necessary.

Figure 4 - Baja with independent axles (yellow circles).

3.1.4 Frame Structure and Material Selection

To begin with, a trend that is observed when scrutinizing different low budget beach buggy models is that the frame merely consists of a few metal tubes arranged to resemble a truss, and welded together to successfully encase and protect the internal components, such as the engine, and the passengers aboard. The frames composing these specialized sand vehicles constituted the exterior appearance, possessing virtually no body panels to enhance the vehicle's aesthetic. While it is possible to locate elegant beach buggies possessing decorative body panels, convenient windows, and functional doors, these amenities are not essential to building a competent beach roaming vehicle, adding unnecessary costs and mass to the buggy. A prime example of a beach buggy showcasing this simple, yet functional patterned metal frame is shown below in Figure 5 for reference.

Figure 5 - A vehicle composed of a simple strutted frame [2]

A popular frame, shown in the image above, utilized in the construction of a sand buggy is known as a space frame, which is a three-dimensional frame structure formed from multiple struts arranged in a triangular pattern that effectively converts bending moments into tension and compression forces due to its specific geometric arrangement [3]. The mechanical function of the triangular pattern of a space frame is demonstrated and elaborated upon below in Figure 6.

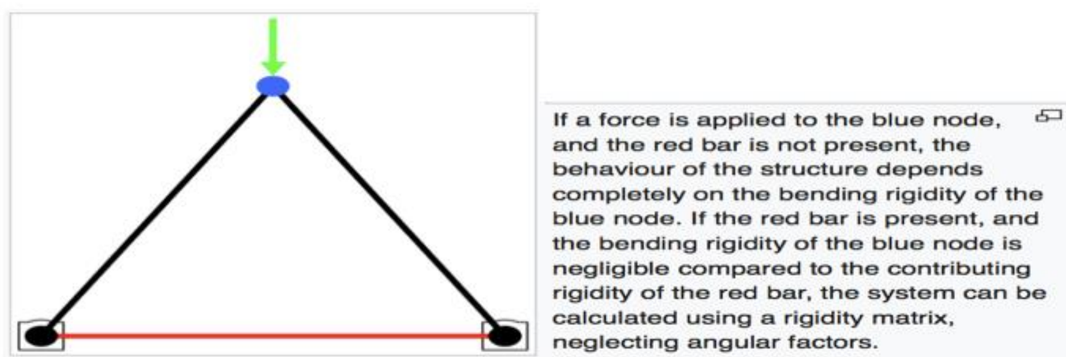

Figure 6 - The function of a space frame explained [4]

A space frame structure contributes the necessary rigidity to ensure the safety and sturdiness required by a beach buggy while also remaining lightweight and cost effective, two qualities desired when recalling the relatively sparing budget and the requirement that this rover remain completely powered by solar energy. Without a doubt, the students must consider this form of patterned frame, and similar arrangements, when constructing the beach buggy.

Furthermore, the metal frame must be composed of a sturdy, lightweight, and inexpensive metal that can withstand the loads generated by the passengers, required to be specifically 120 pounds for this task, and the internal components. Common properties that describe a metal's suitability for this task include:

- Density- the ratio of a metal's mass to its volume
- Modulus of Elasticity- the ratio of a given tensile stress applied to the produced stress
- Yield Strength- the maximum stress a metal can withstand before plastically deforming

- Ultimate Tensile Strength- the maximum stress a metal can withstand before fracturing

The students researched these specific properties of common metals utilized in the formation of metal frames and the data is displayed in Table 2 below [5].

Metal	Density (g/cc)	Modulus of Elasticity (Gpa)	Yield Strength (Mpa)	Ultimate Tensile Strength (Mpa)
Aluminum	2.6989	69	95	110
Steel	7.75-8.05	180	502	860
Iron	7.87	210	120-150	180-210
Copper	8.96	117	70	220

Table 2: A table showing various properties of common metals

The table shown above states that aluminum is the lightest metal of the group, but steel possesses a higher Modulus of Elasticity. The students must analyze the data carefully and select the metal best suited to form the frame of the beach buggy.

3.1.5 Beach Buggy Tires

Moreover, an additional defining characteristic of a beach buggy that the students noticed are their massive, uniquely shaped wheels. A beach buggy needs to be equipped with special blade tires in the front, which possess a blade profile in the center of the wheel to enhance flotation above the sandy terrain and increases the maneuverability and traction of the beach buggy. In addition, the beach vehicle requires wide paddle tires, named after the paddle shaped rubber pattern that they possess, in order to provide elite traction [6]. These blade and paddle tires are shown below in Figure 7. The students must utilize these specialized tires to produce an efficient beach vehicle.

Figure 7 - A blade tire, left, and a paddle tire, right, shown [6]

3.1.6 Motors

When it comes to electric motors, two main types will be considered: DC (direct current) and AC (alternating current). First though, it is best to understand the parts of a simple motor. These include:

- Armature or rotor (electromagnet)
- Commutator
- Brushes
- Axle
- Field Magnet (permanent magnet)
- DC power supply

Magnets and magnetism is the driving factor in electric motors. The attracting and repelling forces are utilized to create rotational motion.

The guidelines of this challenge involve the team to be able to transport 120 lbs a distance of 10 miles at a max speed of 3mph. Due to these requirements, there are certain aspects of the vehicle that should be calculated to determine the size of the motor that will be needed; such as torque required, rpm, voltage and amps.

1. Figure out the number of revolutions of the tire per mile. Circumference equals distance per 1 revolution. Convert tire circumference to revolutions per mile.
2. Calculate wheel rpm for desired speed.
3. Calculate estimated weight of vehicle and determine power required to operate at desired speed continuously.
4. Determine the power needed for initial acceleration.
5. Sum continuous power with acceleration power to get peak power.
6. Calculate wheel torque.
7. Choose the gearbox/differential ratios then divide the torques by gear ratio to get the required motor torques. Multiply the wheel rpm by the gear ratio to get required motor speed.
   [8]

The two options for electric motors are either direct current (DC) or alternating current (AC). Alternating current describes the flow of charge that changes directions periodically, where as DC provides a constant voltage or current (Most electronics that use batteries relies on DC). [9]

Type of Motor	Advantages
AC	● Faster acceleration ● Higher RPM rates, generate higher top speed ● More power for hill climbing ● Lower maintenance costs ● Improved downhill braking

	power
DC	• Widespread availability • Easy installation • Cheaper • Offers all of its toque from standstill • Ability to overdrive

Table 3 - A comparison of AC and DC motors

The option to use AC motors is there for the team, but their advantages do not apply to our project. Opting out of AC leaves us with the DC motor as the prefered choice. Within the DC family though, there are two main motor categories: Brush and brushless. Brushless motors are usually much better than their counterpart. They are more efficient, have a higher power output, quieter, have a longer lifespan, and are overall more stable. The optimal choice, due to the apparent advantages and also previous controlling knowledge, will be the brushed DC motor. The characteristics of a Brushless DC motor is displayed below in Figure 8.

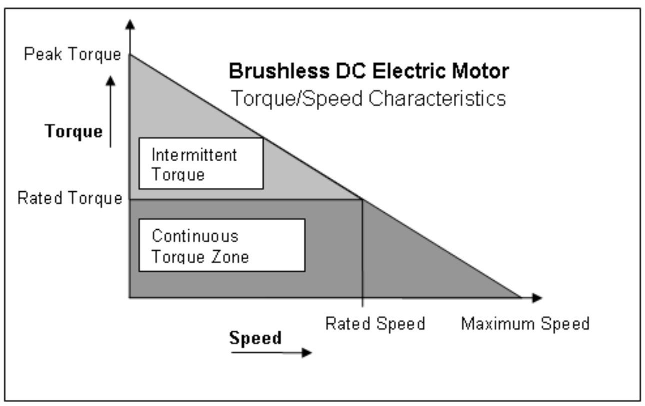

Figure 8 - Brushless DC Motor Characteristics [7]

When considering obtainable options for the buggy's motor, it appears that Go-Cart motors will be the easiest to purchase. Depending on possible car designs, like whether the buggy will have a differential or not, will determine the amount of motors needed for the vehicle. The average cost of motors range from $100-$400.

Table 4 below shows a comparison between a brush and brushless motor.

	AmpFlow E30-400	Motenergy ME-0907	NPC4200	Motenergy ME-0909

Motor Type	Brushed	Brushless	Brushed	Brushed
Weight	5.9 lbs	22lbs.	15.7lbs.	24lbs.
Voltage	12-24V	12-72V	24-36V	24-48V
Peak current	266A	220A	470A	300A
Peak Torque	11Nm	38 Nm	N/A	N/A
Peak Horsepower	2.1hp	N/A	3.8hp	15hp
RPM	5700rpm @24V	5000rpm	3400rpm	4850rpm
Price	$109	$392	$339	$385
Efficiency	79%	90%	N/A	95%

Table 4 - Brush and brushless motor comparison

Although a brushless motor is more efficient and requires less maintenance, a brushed motor will be the most economical choice for this application. As a result, the AmpFlow E30-400 will be the motor that will power the solar beach buggy.

3.1.7 Batteries

In the process for designing an autonomous solar powered beach buggy, it is of utmost importance to develop great understanding of batteries and the uses they can have in the development of designing a beach buggy. This beach buggy will be need to traverse a 10 mile stretch, so it will be necessary to have the optimal battery for the journey. This technical memo will be used to explain how batteries can be used to store energy collected from the sun and how batteries can be used to power motors.

In order to understand how a vehicle can be run using the power from the sun, it is first necessary to know how to collect the energy from the sun and converting that energy into electricity. This process of collecting the sun's energy is accomplished using photovoltaic cells or PVCs. PVCs are the components in solar paneling that convert the sun's energy into electricity. PVCs are made up of semiconductors that are absorb the light and are usually made out of silicon. The energy from the sun then frees the electrons in the semiconductors, when then creates the flow of electrons. The flow of electrons then generates the electricity that powers the battery or powers the motor directly.

A key element in this Solar Beach Buggy Challenge is understanding batteries. The primary functions of batteries in a PV systems are to store electrical energy when it is produced by the PV array, to supply power to electrical loads at stable voltages and currents, and to supply high peak operating current to appliances.

Each battery type has its individual strengths and weaknesses. Table 5 below compares some of the characteristics of the battery types in consideration. In PV systems, lead-acid batteries are most common due to their wide availability in many sizes, low cost and well understood performance characteristics. Nickel-cadmium cells are used in low temperature applications, but their high costs limit their use in most PV systems.

Battery Type	Cost	Deep Cycle Performance	Maintenance
Flooded Lead-Acid			
Lead-Antimony	low	good	high
Lead-Calcium Open Vent	low	poor	medium
Lead-Calcium Sealed Vent	low	poor	low
Lead Antimony/Calcium Hybrid	medium	good	medium
Captive Electrolyte Lead-Acid (VRLA)			
Gelled	medium	fair	low
Absorbed Glass Mat	medium	fair	low
Nickel-Cadmium			
Sintered-Plate	high	good	none
Pocket-Plate	high	good	medium

Table 5 - Battery Types: Cost, Deep Cycle Performance, Maintenance

Lead-Antimony batteries are a type of lead acid battery which use antimony (Sb) as a primary alloying element with lead in the plate grids. The advantages of these types of batteries include providing greater mechanical strength than pure lead grids, and excellent discharge and high discharge rate performance. Lead-antimony grids also limit the shedding of active material and have better lifetime than lead-calcium batteries when operated at higher temperatures. The disadvantages of lead antimony are a high self-discharge rate, and as the result of necessary overcharge, require frequent water additions depending on the temperature and amount of overcharge. Most lead-antimony batteries are flooded, open vent types with removable caps to permit water additions. They are well suited to application in PV systems due to their deep cycle capability and ability to take abuse, however they do require periodic water additions. The frequency of water additions can be minimized by the use of battery designs with excess electrolyte reservoirs.

Lead-calcium batteries are a type of lead-acid battery which use calcium (Ca) as the primary element with lead in the plate grids. The advantages to these type of batteries include providing greater mechanical strength than pure lead grids, low self-discharge rate, and reduced gassing results in lower water loss and lower maintenance requirements than for lead antimony batteries. The disadvantages include poor charge acceptance after deep discharges and a shortened battery life at higher operating temperatures.

Lead-Antimony/Lead-Calcium hybrid are typically flooded batteries, with capacity rating of over 200 ampere-hours. This design combines and advantages of both lead-calcium and lead-antimony design, including good deep cycle performance, low water loss and long life.

Captive electrolyte lead-acid batteries are another type of lead-acid battery, and as the name implies, the electrolyte is immobilized in some manner and the battery is sealed under normal operating conditions. Electrolyte can not be replenished in these battery designs, therefore they are intolerant of excessive overcharge. Captive electrolyte lead-acid batteries are popular for PV applications because they are spill proof and easily transported, and they require no water additions making them ideal for remote applications where maintenance in infrequent or unavailable. However, a common failure mode for these batteries in PV systems is excessive overcharge and loss of electrolyte, which is accelerated in warm climates. For this reason, it is essential that the battery charge controller regulation set points are adjusted properly to prevent overcharging. The benefit of captive or immobilized electrolyte designs is that they are less susceptible to freezing compared to flooded batteries. In the US, about one half of the small remote PV systems being installed use a captive electrolyte or sealed batteries. The two most common captive electrolyte batteries are the gelled electrolyte and absorbed glass mat designs (AGM). The advantages and disadvantages of battery types are further displayed in Table 6.

Battery Type	Advantages	Disadvantages
Flooded Lead-Acid		
Lead-Antimony	low cost, wide availability, good deep cycle and high temperature performance, can replenish electrolyte	high water loss and maintenance
Lead-Calcium Open Vent	low cost, wide availability, low water loss, can replenish electrolyte	poor deep cycle performance, intolerant to high temperatures and overcharge
Lead-Calcium Sealed Vent	low cost, wide availability, low water loss	poor deep cycle performance, intolerant to high temperatures and overcharge, can not replenish electrolyte
Lead Antimony/Calcium Hybrid	medium cost, low water loss	limited availability, potential for stratification
Captive Electrolyte Lead-Acid		
Gelled	medium cost, little or no maintenance, less susceptible to freezing, install in any orientation	fair deep cycle performance, intolerant to overcharge and high temperatures, limited availability
Absorbed Glass Mat	medium cost, little or no maintenance, less susceptible to freezing, install in any orientation	fair deep cycle performance, intolerant to overcharge and high temperatures, limited availability
Nickel-Cadmium		
Sealed Sintered-Plate	wide availability, excellent low and high temperature performance, maintenance free	only available in low capacities, high cost, suffer from 'memory' effect
Flooded Pocket-Plate	excellent deep cycle and low and high temperature performance, tolerance to overcharge	limited availability, high cost, water additions required

Table 6 - Battery Type: Advantages and Disadvantages

Table 7 below shows a list of batteries of different type that is being considered.

Type	Brand	Weight (lbs.)	Dimensions LxWxH(in)	Capacity (AH)	Voltage (V)	Price ($USD)
FLA	USBattery US12VXC	86	13.13 x 7.07 x 11.38	155	12V	$178.87
FLA	Trojan T1275	82	12.96x7.13x11.25	150	12V	$189.95
AGM	Universal Battery	69.9	12.12 x 6.61 x 9.16	100	12V	$164.99
Gel	Renogy	66	13 x 6.8 x 9.0	100	12V	$229.99
SLA	NPP	59.5	12.1 x 6.7 x 8.2	90	12V	$162.99

Table 7 - Lead acid battery comparison

As part of the requirement, the solar beach buggy must have the ability to travel up to 10 miles; therefore, the battery must have the capacity to store a lot of charge it receives from the solar panel. The USBattery US12VXC is the best choice for this application mainly because it has more capacity and it is fairly inexpensive.

Once a particular type of battery has been selected, it is then best to consider how to configure and maintain the battery for optimal performance; considerations in battery subsystem design include the number of batteries in series and parallel, over-current and disconnect requirements, and selection of the proper wire sizes and types.

Batteries connected in a series circuit have only one path for the current to flow. Batteries are arranged in series by connecting the negative of the first battery to the positive terminal of the second battery. The negative of the second battery to the positive of the third battery, and so on for as many cells in the series string. The total voltage is the sum of the individual battery voltages, and the total capacity is the same as for one battery. If batteries or cells with different capacities are connected in series, the capacity of the string is limited to the lower battery capacity.

Batteries connected in parallel have more than one path for current to flow, depending on the number of parallel branches. Batteries are arranged in parallel by connecting all of the positive terminals to one conductor and all the negative terminals to another conductor. For similar batteries connected in parallel, the voltage across the entire circuit is the same as the voltage across the individual parallel branches, and the overall capacity is sum of the parallel branch capacities.

Battery manufacturers recommend that their batteries be operated in as few parallel strings as possible. If too many parallel connections are made in a battery bank, slight voltage differences between the parallel strings will occur due to length, resistance and integrity of the connections. The results of these voltage differences can lead to inconsistencies in the treatment received by each battery in the bank, potential causing unequal capacities within the bank.

3.1.8 Frame Materials

To build a solar powered vehicle, a desert buggy needs to be purchased. The weight of the buggy must be kept in mind thought the entire design process. Whether it's made from plastic, wood, different alloys, mild steel or manufactured types of steel durability and safety is the top priority. As seen in the Figure below, HREW has a yield strength of 30,000 to 45,000 psi and an ultimate strength of 42,000 to 62,000 psi. [10] DOM ranges from 60,000 to 70,000 yields and 70,000 to 80,000 ultimate strength. Most of the metals used to build the frame of the buggy are formed and welded by using a tube bender and tig/mig welder. Any unnecessary parts can be removed from buggy leaving just a unibody shell that fused body, fenders and frame. Figure 9 below shows the differences between potential frame materials. Heavy wheels, batteries location, electric motor, and solar panels must all be considered when designing a buggy. The chassis composes a major issue because of its metal construction, narrow front, and limited spacing for batteries, charger and controller.

Figure 9 - Car Frame Materials

3.1.9 Steering

In the rack-and-pinion system, a small pinion (gear wheel) is inside a housing at the base of the steering column. Its teeth mesh with a straight row of teeth on a rack - a long transverse bar. Turning the pinion makes the rack move from side to side. The ends of the rack are coupled to the road wheels by track rods. This system is simple, with few moving parts to become worn or displaced, so its action is precise. A universal joint in the steering column allows it to connect with the rack without angling the steering wheel awkwardly sideways.

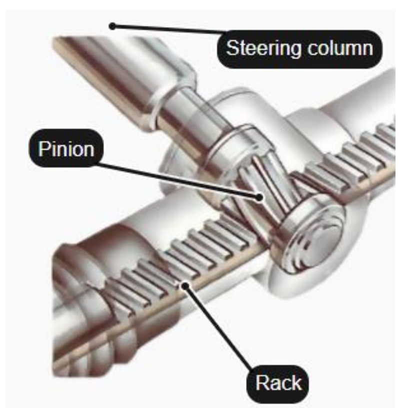

Figure 10 - Rack and Pinion System

Differential steering allows a vehicle to move on tracks by increasing or decreasing the speed at which one side of the tracks moves. This method may be more cost/labor efficient as it only requires two motors which can be used for both driving and steering compared to a rack-and-pinion system which requires a motor to drive and a separate system for steering.

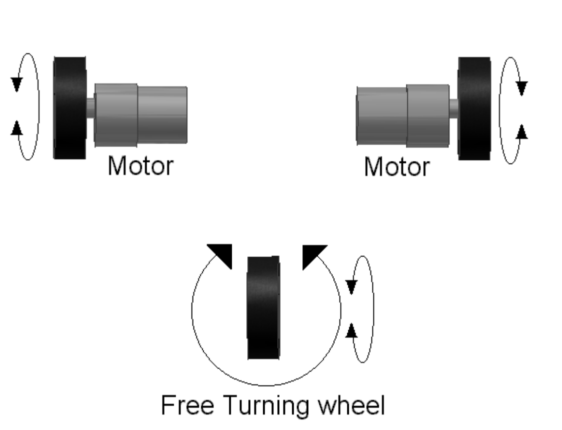

Figure 11 - Differential Steering

3.2 Electrical Components

In this section we will describe the research conducted into the electrical components which will be considered for our final design. Much like the mechanical components, combining the proper electrical components in their proper configuration is vital to the successful construction and completion of this project. This section will contain a discussion of the systems which will be used in order to survey the environment, communicate the correct signals to the appropriate devices, and interact with the motors in order to move the buggy in the necessary manner.

3.2.1 Solar Cells

In this section we will discuss some of the operating characteristics of solar cells, as well as the primary distinctions between different types of solar cells, in order to be able to select the appropriate cell for our needs. Solar cells form a central tenet of our design, and as such it is necessary to select a cell that most adequately aligns with our goals in regards to power output, efficiency, heat tolerance, durability, and price.

The basic operating principle of a solar cell relies on the use of a photodiode to capture light emanating from the sun and transform it into a current. This is possible due to a scientific phenomenon known as the photoelectric effect, which describes the emission of electrons or other free carriers when light shines upon an object. This occurs because the light passes through an area of the material known as the depletion region, wherein a photon of light is absorbed by an electron, which causes it to escape the depletion region and escape from the semiconductor as current.

A photodiode is a semiconductor device, meaning that they are typically made of materials such as silicon or gallium. These materials are then doped by other materials such as boron or phosphorus, giving them an excess amount carriers, which refers to either electrons or holes. These materials are then referred to as either n-type or p-type, respectively. When placed in contact with each other, these materials create a ‘depletion region’ where a built in electric field causes the movement of excess carriers. As such, when a photon of sufficiently high energy is incident on the depletion region, it creates an electron-hole pair, which are then carried off in different directions by the electric field, generating a photocurrent. Depending on how the photodiode is biased, it can also generate a voltage. However, a solar cell is operated under zero bias conditions.

There are three different types of solar panels that are typically used for commercial use: Monocrystalline silicon, polycrystalline silicon, and thin-film solar panels. There are also more niche types of solar panels, such as translucent cells and high efficiency cells, which are capable of reaching efficiency rates as high as 40%. Although research is constantly being done on these panels and their price is steadily decreasing, these solar cells are not yet commercially viable, and so will not factor into our designs as a serious option.

Monocrystalline silicon cells are created using sheets or cylindrical wafers of silicon ingots. It is produced via a manufacturing technique called the Czochralski process, which is a long, technical process which gives the monocrystalline silicon cell a higher price than some alternative panels. As a result, however, they boast a relatively high efficiency rate, in the range of 15-20%. They are also space efficient, and boast a better performance than polycrystalline silicon cells in low light conditions, as well as generally low failure rates. In particular, they suffer noticeably less degradation in efficiency when exposed to high temperatures than other types of solar cells. This makes them a viable candidate for our design.

Polycrystalline silicon cells do not use silicon ingots or the Czochralski process, instead being produced by pouring molten silicon into square molds which are then cooled and made into wafers. As a result, they prove to be a cheaper, more cost effective alternative to monocrystalline silicon cells, although they prove to have a slightly lower average efficiency, at around 15%. This also makes them less space efficient than some alternatives.

Thin-film solar cells are created by depositing multiple layers of photovoltaic materials onto a substrate. They can also be further classified by the photovoltaic material deposited onto the substrate, namely: Amorphous Silicon (a-Si), Cadmium Telluride (CdTe), Copper Indium Gallium Selenide (CIS/CIGS), and organic photovoltaic cells (OPC). Thin-film solar cells are a fairly new, rapidly developing form of solar cell, and as a result they have among the lowest operating efficiency, achieving a maximum efficiency of around 7%. However, the production process is relatively simple, meaning that thin-film solar cells have a significantly lower cost than more traditional solar cells. They are also more flexible, and suffer less negative effects as a result of extreme temperatures.

From our research, it was determined that a monocrystalline solar cell would be the most appropriate for our needs. Despite being among the more expensive options, it proved to have the highest efficiency in converting incident sunlight into useful energy, which is of vital importance to our project, as the solar cells are responsible for powering the entire buggy. This efficiency also makes it the most space-efficient, which is also a key aspect of our decision as every foot of space on the panel needs to be accounted for in the design of the buggy's chassis. Monocrystalline solar cells have also demonstrated relatively little drop in efficiency in response to changes in temperature, which is of special concern to us, seeing as the buggy needs to operate continuously on a hot, humid, and crowded Florida beach. An image of a monocrystalline cell is displayed below in figure 12.

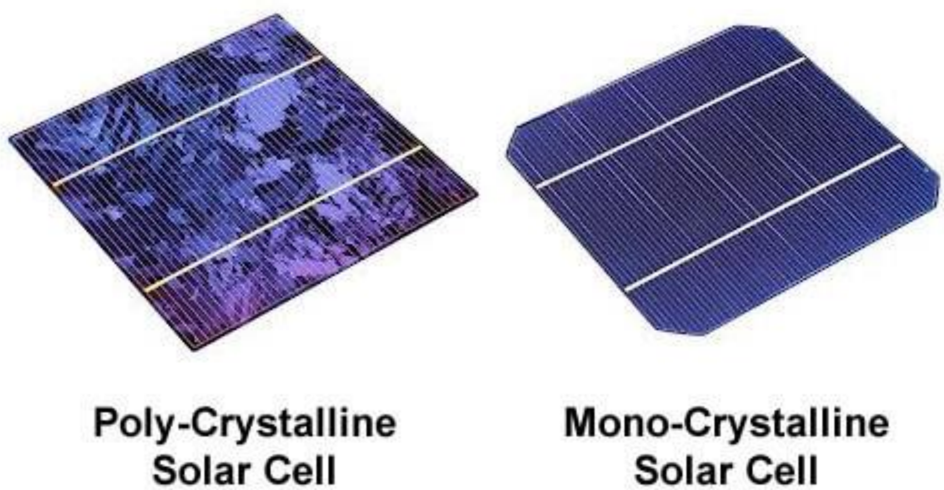

Figure 12 – A comparison of the appearance of a polycrystalline versus a monocrystalline solar cell

3.2.1.1 Advantages

Solar energy boasts many significant advantages over forms of energy creation such as fossil fuels. It's a renewable, clean energy source that is readily available from anywhere in the globe and can be harnessed quickly and easily, using equipment that requires relatively little in the way of maintenance. As research progresses and energy needs grow, solar energy continues to look more and more like a viable, and in many ways necessary, source of power.

Solar energy can prove to be a useful energy source in volatile areas where complicated, high maintenance machinery is not viable, due to its ability to be decentralized, off-grid and operate with next to no management. It's especially useful for areas near the equator, where sunlight is both prevalent for most of the year and especially intense. The standalone nature of a solar panel station also insulates it from difficulties involving changing economic conditions, such as might heavily affect energy production through the use of fossil fuels. Not only are solar cells useful for small scale power generation, they're also proving to be a viable source of large scale energy production, with solar farms generating over 50 GW of power in the U.S. alone.

With regards to our needs, a monocrystalline solar cell has many advantages over systems utilizing traditional battery power or fossil fuels. The nature of our buggy makes it ideal for emergency situations, wherein it could allow beach patrons to reach safety when they would otherwise be rendered unable to move. In such a crisis, it would be catastrophic if the buggy were to suddenly and unexpectedly stop moving due to a lack of sufficient battery charge or an empty gas tank. A total reliance on solar energy ensures that, provided sufficiently sunny weather conditions and regular maintenance to ensure all parts of the buggy are in proper working order, our buggy would be able to operate from first light at dawn to sunset without ever having to slow down or recharge.

3.2.1.2 Disadvantages

Solar energy faces a few limitations. For one, it is extremely limited by location, as only regions which experience large amounts of unobstructed sunlight on a regular basis can generate a useful amount of power. It's also limited by the fact that it is only capable of generating power during the day, and night time activities need to either be conducted on battery power or through the use of other energy sources. It also requires a significant allocation of land which could potentially be used for other purposes. Moreover, although it is advancing rapidly, solar panels remain a costly investment. These are issues that will disappear with time as solar cells become more efficient, both in terms of cost and power generation, allowing them to occupy less space.

For our purposes, these are both reasonable but not insurmountable obstacles. While the buggy is heavily dependent on optimal weather conditions, Florida is known for an abundant amount of sunshine, particularly in the summer seasons when attendance at a beach would be at their highest points. As such, the buggy would be able to operate, without incident, more often than not. This design also takes advantage of the fact that beach attendance is traditionally down during periods of unfavorable weather, meaning that, with less beachgoers in general on days of overcast or rain, the buggy is less likely to be needed during the periods in which it would have difficulty operating. As far as cost of investment goes, the system we're proposing is fairly cheap when the total amount of functionality is considered, and a minimal amount of regular maintenance would be required in order for the buggy to remain functional. The solar cells themselves have guarantees in excess of 25 years, ensuring that they could provide a massive return on investment.

As global demand for energy rises, and a public call for more renewable energy becomes lauder, solar energy is poised to become a primary source for the world's power needs. For our purposes, understanding the strengths and limitations of solar energy is vital to creating an efficient, functional design. As our buggy will be operating on a beach, ideally on a sunny day with no overcast clouds, we foresee no issue in acquiring sufficient light to power our design, only in selecting the appropriate solar cell and power configuration to make it viable for the duration of our journey.

3.2.2 Inverters

This section will discuss the various types of inverters that are commercially available, as well as their properties, benefits, and drawbacks. Inverters are a vital component for any system using photovoltaic cells. As our solar cell is only capable of putting out DC current, and we need it to operate many different, highly complex electrical components with as much efficiency as is possible, it is necessary for us to incorporate an inverter in order to convert the DC current to AC current.

Inverters are also useful in other respects. By utilizing a maximum power point tracking system, the inverter can analyze the non-linear DC current from the solar cells and output a steady, maximized power for the system. Because the solar cells follow a characteristic I-V curve for their output, the inverter is able to sample the I-V curve at the location of the maximum of the current/voltage product, in order to output the maximum power.

3.2.2.1 String Inverters

This section will discuss the basic properties of a string inverter, and how they relate to our project. Inverters can prove to be a key component to the success and efficiency of system involving solar panels, and so it is necessary that we examine all the various types that exist in order to determine which type will be able to most satisfactorily meet the needs of our system.

String inverters are among the most cost effective inverter options available, as they have been in use for many years in solar systems. A basic diagram of a string inverter is shown below in figure 3.2.1. They are typically used in systems involving multiple solar panels. They essentially function by taking the combined output of many different solar cells in series and inverting the current to AC. This has major implications in terms of lowering costs and complexity of the system.

However, it can also cause problems if one or more of the panels in the system becomes shaded and ceases to work, drastically reducing the amount of power produced by the solar cells. Due to this limitation, and our inability to predict weather patterns once the buggy is in motion, we will seek out an alternative type of inverter.

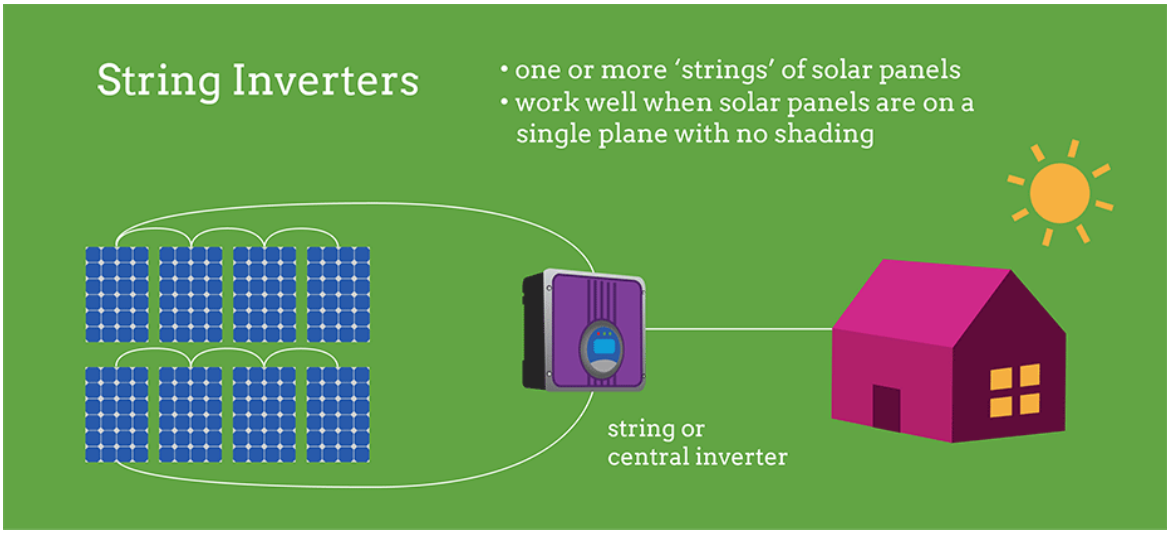

Figure 13 - Basic diagram of a string inverter
Image courtesy of EnergySage.com

3.2.2.2 Micro Inverters

This section will detail the key features of the micro inverter, it's typical applications and how it compares to other types of inverters.

A micro inverter differs from the string inverter in one key area. Rather than providing a single inverter to convert the entire output of a solar system into AC current, an individual micro inverter is connected to each solar panel in the system, and is responsible for converting the output of that panel alone into AC. A diagram of the micro inverter is shown below in figure 3.2.2. Due to this independence, the total output of the system is no longer capable of being severely diminished by the effects of optical blocking on one or more of the solar panels, leading to greater overall efficiency. However, as a result of the extra parts required in setting up multiple micro inverters, this can prove to be a more costly solution. As we are only interested in one or two panels, this is a non-issue, but the increase in efficiency makes it a viable choice over a string inverter.

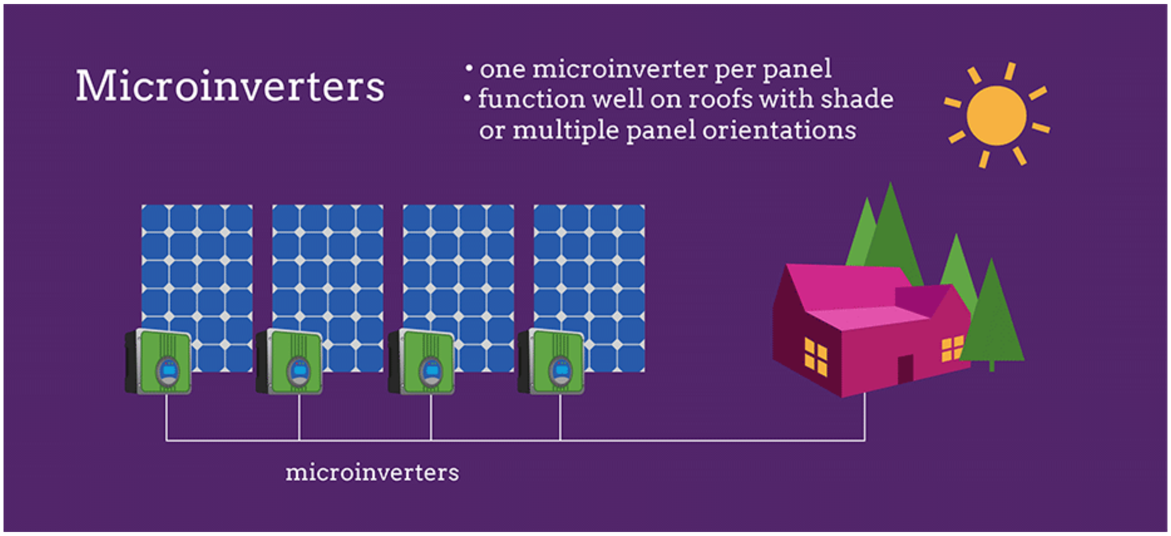

Figure 14 - Basic diagram of a microinverter system
Image courtesy of EnergySage.com

3.2.2.3 Power Optimizers

This section will detail the construction and implementation of power optimizers in a system of solar cells, and how it compares in terms of cost, efficiency, and practicality for our purposes with the other types of inverters available to us.

A power optimizer is a device that monitors the output of a solar cell and tracks it's maximum point in order to ensure that the cell is outputting at the largest amount of power it can. I does this through a process called maximum power point tracking, wherein it monitors the output of the array and adjusts the load it presents to the system in order to keep the system operating at its peak efficiency point. They are fairly inexpensive, and so can be considered as viable solutions in our design process.

A power optimizer setup can almost be thought of as a combination of a string inverter and a micro inverter. A basic diagram is shown below in figure 3.2.3. It functions by placing a power optimizer at the output of each solar panel, and then connecting all the outputs of the power optimizers in series into an central string inverter. In this way it is able to easily convert all the DC current produced by the solar panels into AC current without suffering the severe decreases in efficiency due to partial shading of one or more solar panels. Due to these properties, it can be thought of as a happy medium between the two previous inverters, and sits somewhere between the two in terms of cost. For our purposes, this type of inverter seems to be ideal, as cost is a significant issue in our designs, as well as maximum efficiency in all foreseeable conditions. It would likely be a much cheaper solution to purchase two power optimizers than it would be to purchase two micro inverters, and we will only suffer a negligible amount of power loss as a result.

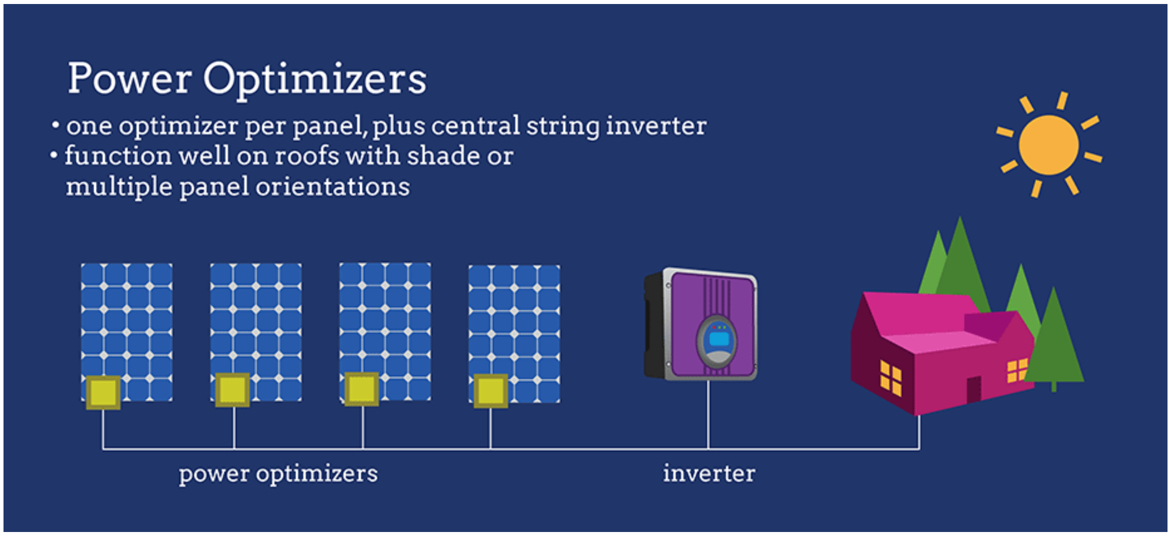

Figure 15 - Basic diagram of a solar system utilizing power optimizers
Image courtesy of EnergySage.com

Table 8 below compares the different solar panels under consideration.

	Ram	Renogy	Renogy	Grape	Nature Power

		sond SP100	RNG-100P		Solar	
Maximum Power (W)		100	100	100	100	100
Peak Voltage (V)		18.5	17.79	18.9	18	17.85
Peak Current (A)		5.41	5.62	5.29	5.56	5.6
Effiency (%)		17	-	-	17.4	-
Cell Technology		Mono	Poly	Mono	Poly	Poly
Number of cells		36	36	36	36	36
Weight (lbs.)		16.5	16.5	16.5	18.11	20.4
Dimensions (in)	L	47	39.7	47	40.16	41
	W	21.63	26.7	21.3	26.37	27
	T	1.56	1.4	1.4	1.37	2
Cost (USD)		140	114.99	124.99	89.99	179.99

Table 8 - A comparison table of different Solar panels

The Grape Solar is the best candidate for this project mainly because of its price. Table 8 shows it has similar specification compared to the other panels in considerations.

3.2.3 Single Board Computer

In selecting the proper hardware system in providing a backend for the software required to operate the robot, the following must be considered: its weight, its power draw, its processing power, and its architectural capabilities. The hardware should be powerful enough to be able to control and process the different sensors and imaging devices on the buggy without having too much overhead, allowing a real-time autonomous operation of the vehicle but at the same time, its power draw should be conservative in such a way as to not overdraw from the solar panels and the batteries as power might be needed elsewhere.

For the buggy, a single-board computer provides the ability to satisfy our requirements as it has the ability to have an operating system installed, along with the ability to use the programs considered in operating our robot (elaborated in the 3.3 Software Components section).

As opposed to microcontrollers that tend to be specific to only one application, A single-board computer contains the necessary, more powerful, components (especially a more powerful CPU and CPU architecture; a GPU, however, is not required) to run the software that will manage the buggy as well as the architecture that can support installing an operating system that will be the backend to our image processing and robot-control software.

Table 9 compares the different single-board computers in consideration which are: the Asus Tinker Board S (Figure 16a), the nVidia Jetson TX1 (Figure 16b), and the Raspberry PI 3 Model B+ (Figure 16c).

Single-board Computer	Asus Tinker Board S	nVidia Jetson TX1	Raspberry PI 3 Model B+
CPU	Quad core 32-bit 1.8 GHz ARM Cortex-A17	64-bit quad-core ARM A57 CPUs	1.4GHz 64-bit quad-core ARM Cortex-A53 CPU
GPU	600 MHz Mali-T760 MP4 GPU	1 TFLOP/s 256-core Maxwell	
RAM	2GB dual channel LPDDR3	4 GB LPDDR4 (25.6 GB/s)	1GB LPDDR2 SDRAM
Storage	16GB eMMC + removable MicroSD slot	16 GB eMMC	Micro SD
Networking	Gigabit LAN (not shared with USB bus)	10/100/1000Mbit Ethernet	Gigabit Ethernet over USB 2.0 (max 300 Mbps). Power-over-Ethernet support (with separate PoE HAT).
Wireless	Bluetooth V4.0 + EDR, 802.11 b/g/n Wi-Fi, with IPEX antenna header	802.11ac wireless LAN, Bluetooth-enabled	Dual-band 802.11ac wireless LAN (2.4GHz and 5GHz) and Bluetooth 4.2
Power Input	5V @ 2~2.5A	5.5 V-19.6 V DC (6.5 W-15 W)	5V @ 2.5A
Weight	55g	88g	
Other IO	GPIOs, SPI, I2C, UART, PWM, PCM/I2S, 5V and 3.3V power pins, ground pins	GPIOs, I2C, I2S, SPI	GPIO, I2C, I2S
Price	$80	$299	$35

Table 9 - A comparison of some of the single-board computers being considered

Figure 16a: Asus Tinker Board S

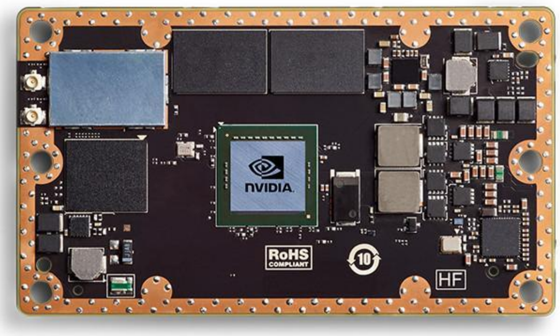

Figure 16b: nVidia Jetson TX1

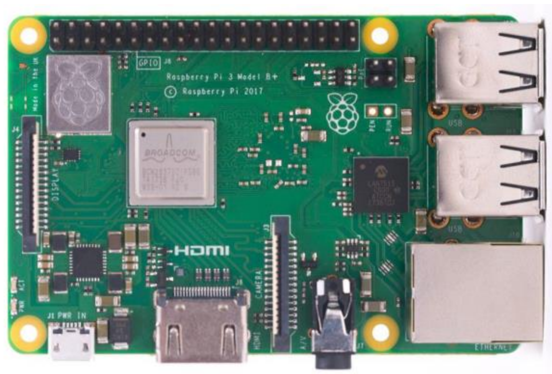

Figure 16c: Raspberry Pi 3 Model B+

The most promising candidate for selection is the Raspberry Pi 3 Model B+ mainly because of its price and its ability to still decently run the required software implementations for the buggy. The nVidia Jetson TX1, while impressively powerful, has an MSRP of ~$300. Compared to the Asus Tinker Board S, the Raspberry Pi 3 Model B+ has been in the market longer and has more support from the manufacturer and the community, making computational hardware and software implementation less time and resource consuming.

3.2.4 GPS Tracking Unit

While Image and sensor processing alone can allow a robot to operate safely by avoiding obstacles, true autonomy can only be achieved if the robot knows where exactly it is. A GPS tracking unit is a device that allows just that.

A GPS tracking unit uses the Global Positioning System (GPS) to track the device's movements at intervals to determine its location and, when attached to the vehicle, its carrier.

GPS currently consists of 31 satellites in semi-synchronous orbits around the earth. GPS satellites continuously transmit data about their current time and position. The satellites have atomic clocks on board to keep accurate time. General and Special Relativity predict that differences will appear between these clocks and an identical clock on Earth; that is, time will run faster on GPS satellites than that of clocks on earth due to General Relativity predicting that time appears to run slower under stronger gravity. Also, Special Relativity dictates that due to the speed of the satellites relative to a clock on earth, satellite clocks will appear to run slower.

A GPS tracking unit monitors multiple satellites and uses triangulation to determine its position along with its deviation from true time. It does this by receiving GPS signals (carrier wave with modulation) that includes:

- Pseudorandom bits that is known to the tracking unit. By time-aligning a receiver-generated version and the receiver-measured version of the code, the time of arrival of a defined point in the code sequence, called an epoch, can be found in the tracking unit clock time scale
- A message that includes the time of transmission of the code epoch (in GPS time scale) and the satellite position at that time

The tracking unit measures the times of arrival of at least four satellite signals. From the time of arrival and the time of transmission, the tracking unit forms four time of flight values which are approximately equivalent to the distance between the tracking unit and the satellite. The tracking unit then calculates its three dimensional position from this.

Two GPS trackers are in consideration: the Adafruit Ultimate GPS HAT for Raspberry Pi (Figure 17a) and the Adafruit Ultimate GPS Breakout (Figure 17b). Both of which are identical to each other except the HAT (Hardware Attached on Top) is an add-on board specifically for Raspberry Pi B+ that conforms to a specific set of rules that make life easier for users. A significant feature of HATs is the inclusion of a system that allows the B+ to identify a connected HAT and automatically configure the GPIOs and drivers for the board. The disadvantage is that the GPS HAT takes over the Raspberry Pi's hardware UART to send/receive data to and from the GPS module so if you the RX/TX pins are used with a console cable, this HAT cannot be used in conjunction.

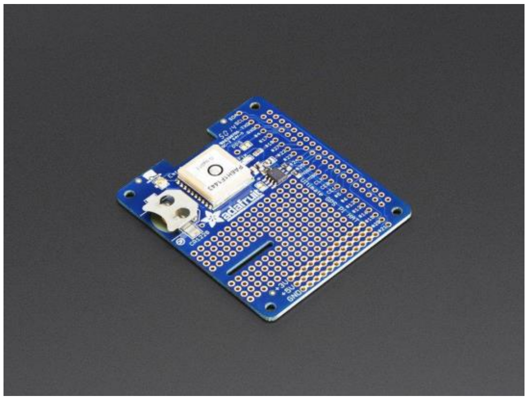

Figure 17a. Adafruit Ultimate GPS HAT for Raspberry Pi

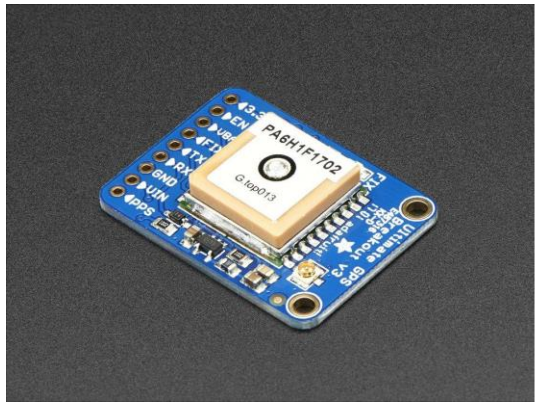

Figure 17b. Adafruit Ultimate GPS Breakout

Among their features, it includes:

- 165 dBm sensitivity, 10 Hz updates, 66 channels
- 5V, 20mA current draw
- Breadboard friendly + two mounting holes
- RTC battery-compatible
- Built-in datalogging
- PPS output on fix
- Internal patch antenna + u.FL connector for external active antenna
- Fix status LED

Table 10 lists detailed specifications for the GPS chipset.

GPS Solution	MTK MT3339

Frequency	L1, 1575.42MHz
Sensitivity[1]	Acquisition: -148dBm, cold start Reacquisition: -163dBm, Hot start Tracking: -165dBm
Channel	66 channels
TTFF	Hot start: 1 second typical Warm start: 33 seconds typical Cold start: 35 seconds typical (No. of SVs>4, C/N>40dB, PDop<1.5)
Position Accuracy	Without aid:3.0m (50% CEP) DGPS(SBAS(WAAS,EGNOS,MSAS)):2.5m (50% CEP)
Velocity Accuracy	Without aid : 0.1m/s DGPS(SBAS(WAAS,EGNOS,MSAS,GAGAN)):0.05m/s
Timing Accuracy (1PPS Output)	10 ns(Typical)
Altitude	Maximum 18,000m (60,000 feet)
Velocity	Maximum 515m/s (1000 knots)
Acceleration	Maximum 4G
Update Rate	1Hz (default), maximum 10Hz
Baud Rate	9600 bps (default)
DGPS	SBAS(defult) [WAAS, EGNOS, MSAS,GAGAN]
QZSS	Support(Ranging)
AGPS	Support

Power Supply	VCC：3.0V to 4.3V；VBACKUP：2.0V to 4.3V
Current Consumption	25mA acquisition, 20mA tracking
Working Temperature	-40 °C to +85 °C

Table 10 - GPS Specification table

3.2.4.1 GPS Antennae

A GPS system work by receiving signal from a network of satellites, and an antenna makes it possible. Most GPS unit come with an antenna that is built-in or inside the case that works fine when they have clear view of the sky. Others come with the option to use an external antenna. While many units don't need an external GPS antenna, others, due to obstructions and interference, need an external antenna.

There are currently two types of GPS antennas today: passive and active. Passive GPS antennas simply receive the satellites signal and send it to the GPS navigation device. However, an active GPS antenna boost the power of the signal it receives with an amplifier circuit, which nearly doubles the GPS signal strength.
Active GPS antennas are expensive compared to the passive antenna and are better suited for use with a larger vehicle.

Table 11 compares the different antennas in consideration.

	ADA 2460	ADA 2461	ADA 960
Type	Passive	Passive	Active
Supply Voltage(V)	*	*	2.3~5.5
Supply Current(A)	*	*	0.0066~0.0166
Gain (dBi)	-2	1	28
Wire Lenght (mm)	50	50	5000
Weight (g)	2.4	5.5	*
Dimensions (mm)	9x9	15x15	41.2x38.5
Interface	IPX uFL	IPX uFL	SMA
Price (USD)	4.95	3.95	12.95

Table 11 - GPS antennas comparison table

After careful consideration of the antennas in Table 11, the ADA2461 will be the antennas of choice for the project due to its price.

3.2.5 Wireless Networking

While the buggy is intended to operate autonomously, being able to communicate with it is a priority considering that it is important to gather the buggy's telemetry data such as its current position, speed, and energy status when not near its vicinity. It is also imperative that the buggy's operation can be aborted should it pose a threat to itself, to property, or to others.

The implementation details of which wireless technology to use depends on the bandwidth, range, and power consumption requirements for the buggy. Three technologies are considered: WiFi, GSM, and Bluetooth Low Energy.

Wi-Fi is a technology based on IEEE 802.11 standards, with 802.11ac as the latest standard as of writing. It is a trademark of the Wi-Fi alliance. Depending on standard implementation, Wi-Fi can reach a single-link theoretical throughput of at least 500 Mbit/s (802.11ac). Both 802.11n and 802.11ac have similar maximum ranges of around 230 feet. While 802.11ac and 802.11n do not differ much when it comes to range, 802.11ac provides superior throughput in longer ranges than

802.11n. Wi-Fi has a modest power consumption rate which averages around 0.5-2 W.

Global System for Mobile Communications, or GSM, provides a virtually unlimited range where the buggy can be communicated from anywhere around the world. However, GSM is subscription based and requires a subscriber identification module (SIM) for both the buggy and the human operator. Current devices primarily communicate on the subscriber network over the Long-Term Evolution (LTE) standard, which is based on GSM. LTE has a theoretical net bit rate capacity of up to 100 Mbit/s in the downlink and 50 Mbit/s in the uplink, with realistic bit rates of half of that. LTE has the most consumption rate of the technologies considered, which averages around 1 — 3.5W.

Bluetooth Low Energy, or Bluetooth LE, is a wireless technology designed and marketed by the Bluetooth Special Interest Group. Bluetooth LE is based on the “classic” bluetooth but is not backwards compatible. Compared to Classic Bluetooth, however, Bluetooth LE is intended to provide considerably reduced power consumption and cost while maintaining a similar communication range. Bluetooth LE has a max theoretical range of 330 feet and has an over the air data rate of up to 0.27 MBit/s throughput. While its throughput is nowhere compared to WiFi or LTE, it shines the most in its power consumption-- a mere 0.01-0.50 W with peak current consumption of 15 mA.

Table 12 compares the different wireless technologies discussed:

	WiFi	Bluetooth LE	GSM
Frequency	2.4 GHz or 5 GHz	2.4 GHz	600 MHz - 2300 Mhz (Depending on carrier and LTE band)
Throughput	500 Mbit/s (802.11ac)	0.27 MBit/s	100 Mbit/s downlink 50 Mbit/s uplink
Range	105 feet	330 feet (theoretical)	Unlimited over land
Power Consumption	0.5-2 W	0.01-0.50 W	1 — 3.5W

Table 12 - Wireless Technologies Comparison Table

The ultimate choice in wireless technology will depend on which factor is important the most: throughput, range, or power consumption. There is an advantage of choosing Bluetooth or WiFi over GSM as the former technologies are already built-in to the Single-board computers in consideration.

3.2.7 Voltage Regulator

A voltage regulator is an electronic circuit that provides a constant output voltage for an electronic design regardless of changes to its input voltage or load conditions. It is very important in any electronic circuits to provide stability and efficiency. Any fluctuation in output currents can damage sensitive electronic components. Some of the reasons why variations in output current may occur: appliances turning on and off, time of day, weather, to only name a few. In this project, many of the components in considerations require a specific voltage. Microcontrollers and sensors need to operate mainly on 3.3V and 5V while the motors require 12V to operate and current as high as 1000W.

3.2.8 Linear Voltage Regulator

Linear voltage regulators work by varying the resistance in accordance to the load which results in keeping the output voltage fixed. They are a good choice for low power applications. Even though they are simple, easy to use, and inexpensive, they are very inefficient.

From the equation 1 of the power dissipation below, the smaller the difference between the input and output voltage the better the linear regulator is. Therefore, a linear regulator is not a good option for our application as high-power devices will be used.

Power dissipation = (input-output) Voltage * load current (equation 1)

3.2.9 Switching Regulators

In a switching regulator, a transistor is used to control the regulator. It works by rapidly switching a series of element on and off. When the transistor is off, there is no current flowing through it therefore no loss of energy; on the other hand, when the transistor is on, it is fully conducting and again there is little or no power dissipations.

Unlike linear voltage regulators, switching regulators are very efficient; whether they are conducting or not there is almost no power dissipation. They are also able to generate multiple output voltages from a single input or output higher voltages than they take in.

3.2.10 Voltage Regulator Circuits

In this design, a switching regulator will be used since it offers the advantages of higher power conversion efficiency that we are looking for. A boost converter will be used to lower the input voltage from the battery or solar panel to 5 volts and 3.3 volts to power the microcontrollers, IR sensors, LIDDAR, and cameras. For the 5V, the LM22670 will be used. The same chip will be used for the 3.3 V with only a few modifications from the circuit. Figures 18 and 19 below show the circuit diagrams for two voltage regulators which will lower the voltage to 5V and 3V, respectively.

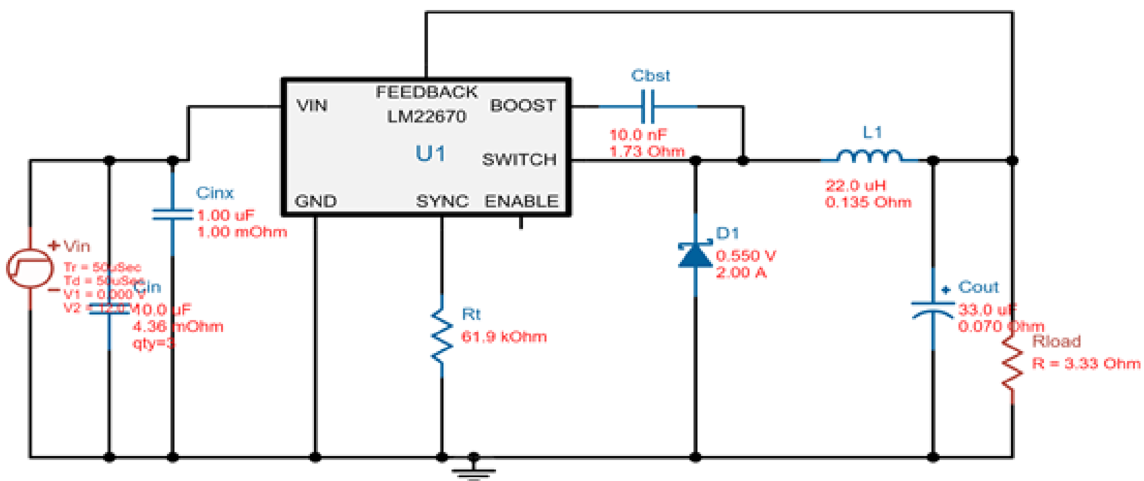

Figure 18 - Buck converter voltage regulator circuit with a 5V output. Reprinted with permission from Texas Instruments.

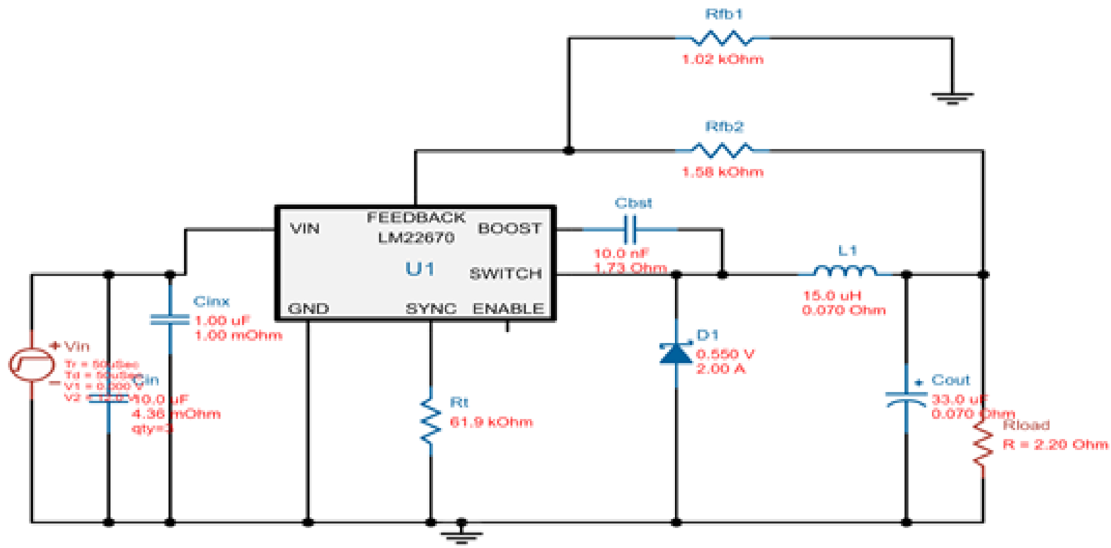

Figure 19 - Buck converter voltage regulator circuit with a 3.3V output. Reprinted with permission from Texas Instruments.

3.2.11 Motor Controller

A motor controller is an electronic device that controls the performance of a DC motor. The controller is necessary in our project because the microcontroller we are going to use can only provide less than 1 A of current whereas our choice of DC motors require a minimum of 60A continuous and 120A peak.

3.2.12 Motor Controller Selection

For this application, finding a motor controller capable of providing sufficient power to the motor was very important. First, it must have a dual driver motor; second, it has to be able to handle a motor with at least 700W of power. The following table will compare 3 motor controllers that can supply high current to a DC motor.

The following Table 13 compares the different motor controllers in consideration. Figure 20 illustrates the different motor controllers in consideration.

	Sabertooth dual 25A	Sabertooth dual 32A	Sabertooth dual 60A
Price	$124.99	$124.99	$189.99
Weight(g)	90g	125g	240g
DC input(V)	6-30V	6-30V	6-30V
Weight Rating	300 lbs.	300 lbs.	1000 lbs.
Board Size(mm)	65 x 80 x 21 mm	70 x 90 x 25 mm	76 x 89 x 46 mm
Peak Current(A)	25A	32A	60A
Continuous Current(A)	50A	64A	120A

Table 13 - Specifications for 3 DC motor controller

Figure 20a - Sabertooth Dual 25A Motor Driver

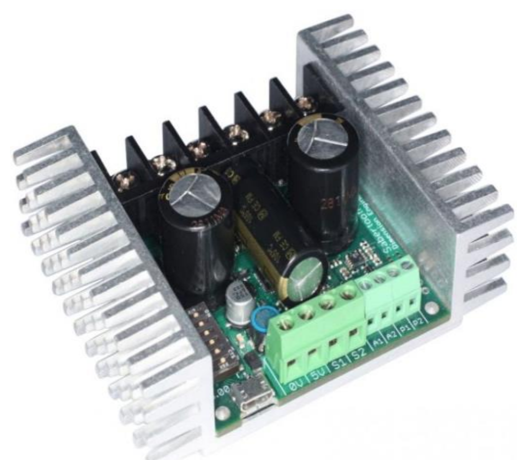

Figure 20b - Sabertooth Dual 32A Motor Driver

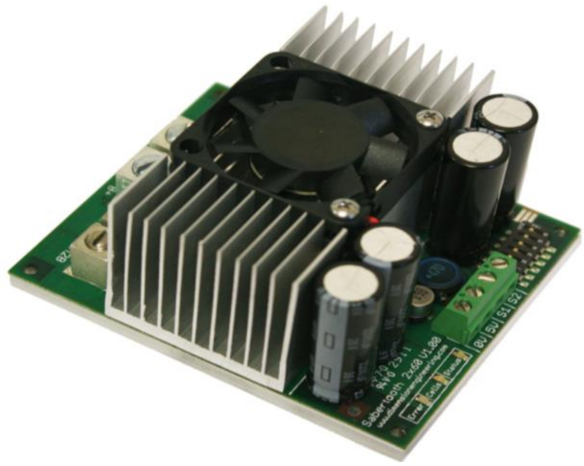

Figure 20c - Sabertooth Dual 60A Motor Driver

Based on the Table 11 above, it is clear that the Sabertooth dual 60A is best fit for our application. The other two motor controllers do not generate enough power to supply high current motors. The Sabertooth dual 60A can supply two DC brushed motors up to 60A of continuous current each and up to 120A peak currents per channel for a few seconds. In addition to a dual motor driver, the controller comes with thermal and overcurrent protection. This is an important feature for a controller to have since an overheating board can have a negative effect on other electrical components. The motor controller allows the control of the two motors using analog, radio, serial and packetized serial control. The controller also has a build in switch mode converter that can supply power to a 5V DC source like microcontrollers, receivers, as well as up to 4 analog servos.

3.2.12 Solar Charge Controller

A battery bank is simply storing energy from the solar panel. When the battery reaches its storing capacity, it will be overcharged and get damaged. Because a solar panel is not producing energy constantly during the day, for that reason, a controller that regulates the amount of charges to the battery is needed.

A solar charge controller, as the name implies, is an electronic module which controls the amount of charges to and from the battery and regulates the performance of the battery. The charge controller offers many benefits to any systems. It charges the batteries at the correct voltage level. This helps preserves the life of the batteries. Other benefit of having a charge controller: it protects the batteries from overcharging and over discharging; it also blocks reverse current and protect the system from electrical overload.

Solar charge controllers perform many major functions. They charge the battery bank. When the battery bank is fully Charge, they indicate it using either an LED indicator or arrays of LED's. They monitor the input and output of the battery bank; if the charge is below the minimum level, the supply to the load is cut off. However, if the battery bank is full, it will ensure the charging switch is in off position.

3.2.13 Types of Solar Charge Controller

There are two types of charge controllers. They are pulse width modulated (PWM) and Maximum power point tracking (MPPT).

3.2.13.1 PWM

PWM controllers work by lowering the input voltage they receive from the solar panel to charge the battery bank. Their charging features are very basic compared to the MPPT. When the battery voltage is low, the controller pulled down the voltage of the panel from 18 V to the battery voltage. Due to loss in power, PWM charge controllers are only 75-80% efficient. PWM is suitable for small systems and provide low cost solutions. Figure 21 illustrate the wiring diagram.

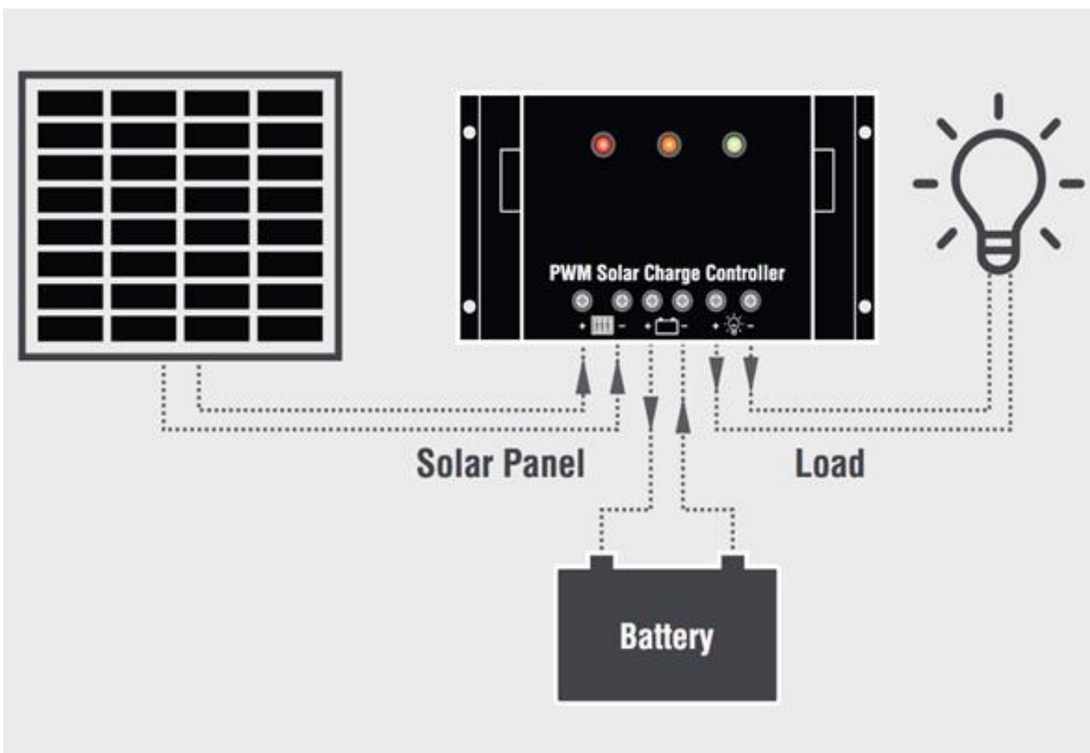

Figure 21 - PWM Solar Charge Controller Wiring Diagrams

3.2.13.2 MPPT

MPPT controllers work by regulating the electrical module state in order to charge the battery bank with the maximum power output. Unlike PWM, MPPT controllers are very efficient. They can accept a higher input voltage than the battery can handle and step it down to match the battery bank voltage for a correct charge. The MPPT controller convert any excess voltage to current making the battery charges faster.

While MPPT provides the best solution for high power systems, it is very expensive. It is best to use it when the solar panel voltage is higher than the battery bank.

In order to determine the best controller for this project, we will be looking at various charge controllers.

The very first one is TI charge controller known by TIDA00120.

The TIDA 00120 is a solar MPPT (Maximum Power Point Tracking) charge controller. It is a 20A MPPT solar charge controller that can take a solar charge inputs between 12-24V DC and outputs up to 20A current to either a 12 or 24V batteries. It is designed for small and medium solar systems. It is scalable to a 48V and up to 40A current by just replacing a few MOSFETs. The controller has lots of features built including reverse battery protection and software programmable alarms. It has an efficiency of over 97% at full load in a 24V systems and uses less than 10mA of standby currents while operating from battery.

The charge controller has a current sense and a cut-off circuit. The circuit will check the voltage in the battery; if it's at least 12.7V meaning it is fully charged, the circuit will prevent any more charge going to the battery. On the other hand, if it is less than fully charged, the circuit will send the appropriate charge to the battery until it reaches a fully charged state.

The operating efficiency of the design reaches well above 96% in a 12V and 24V systems, as illustrated in Figure 22.

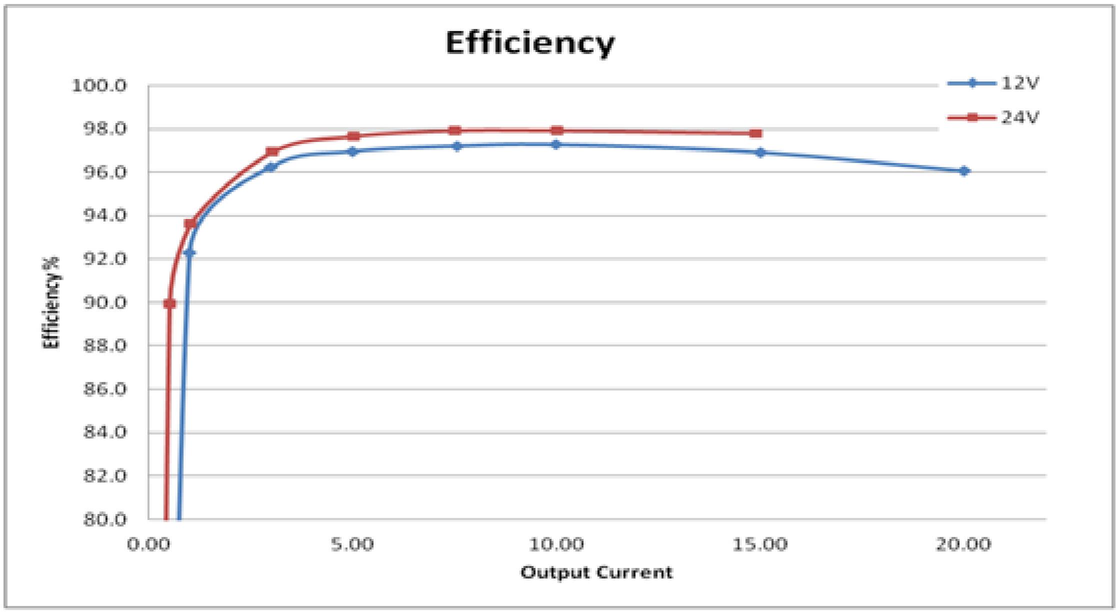

Figure 22 - Efficiency Curve Vs Output Current

The second charge controller we will be looking at is the Rover, illustrated in Figure 26. The Rover is an MPPT charge controller; it has a 12-24V DC input and is available in 20A and 40A. it features a die-cast aluminum shell that allows heat to dissipate and provides protection for the device. It is an intelligent controller capable of tracking power efficiently up to 99%. It can also self-diagnose system faults.

Some of its key features:

- Automatically detects 12V or 24V DC system voltages
- Compatible with various Deep Cycle battery options: Sealed, Gel, Flooded, and Lithium
- Innovative MPPT technology with high tracking efficiency up to 99% and peak conversion efficiency of 98%
- Electronic protection against reverse polarity, overcharging, over-discharging, overload, short-circuiting, and reverse current
- LCD screen and multiple LED indicators for displaying system operation information, customizable parameters, and error codes
- Features diverse load control; also capable of charging over-discharged lithium batteries
- Die-cast aluminum design allows for efficient heat dissipation
- RS232 port allows the Rover to communicate with the BT-1 Bluetooth

Figures 24, 25, and 26 illustrate the various graph properties of this controller.

Figure 23 - Rover 20A MPPT Solar Charge Controller

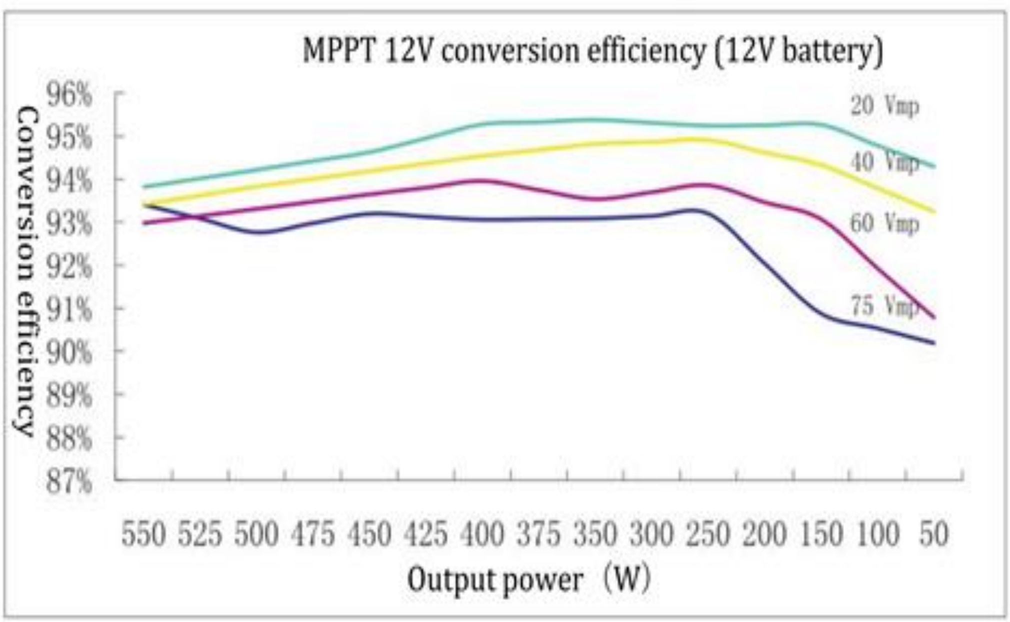

Figure 24 - Efficiency Vs. Output power(12V)

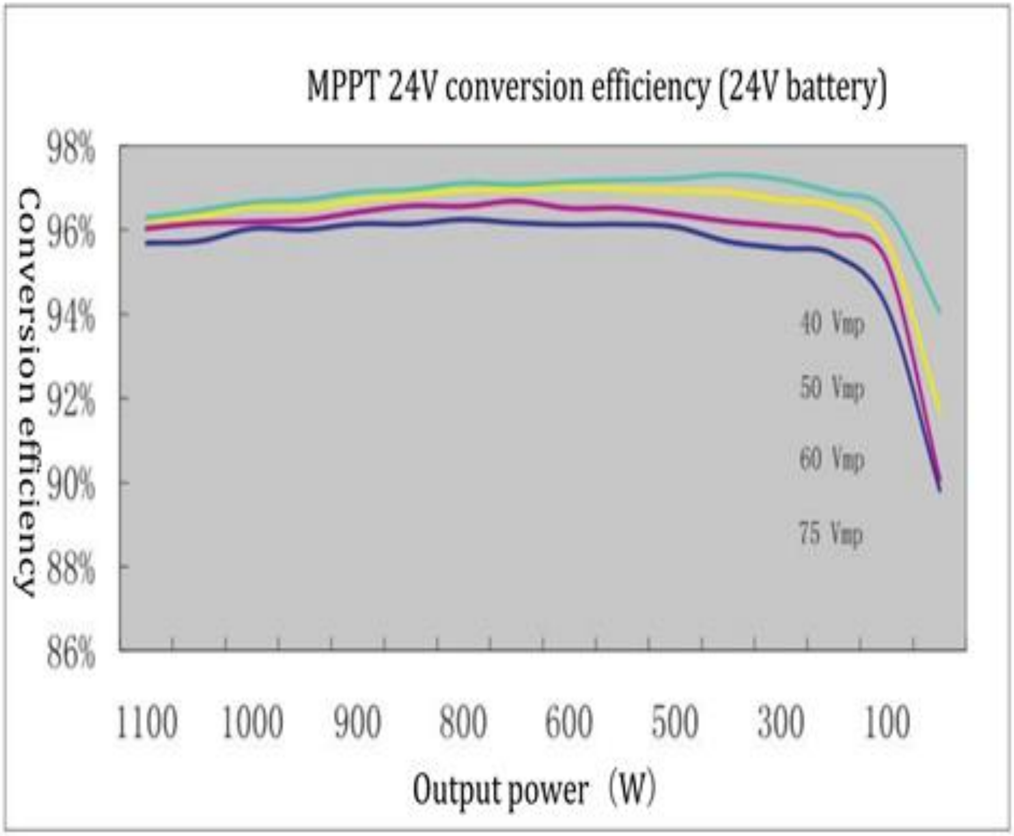

Figure 25 - Efficiency Vs. Output power(24V)

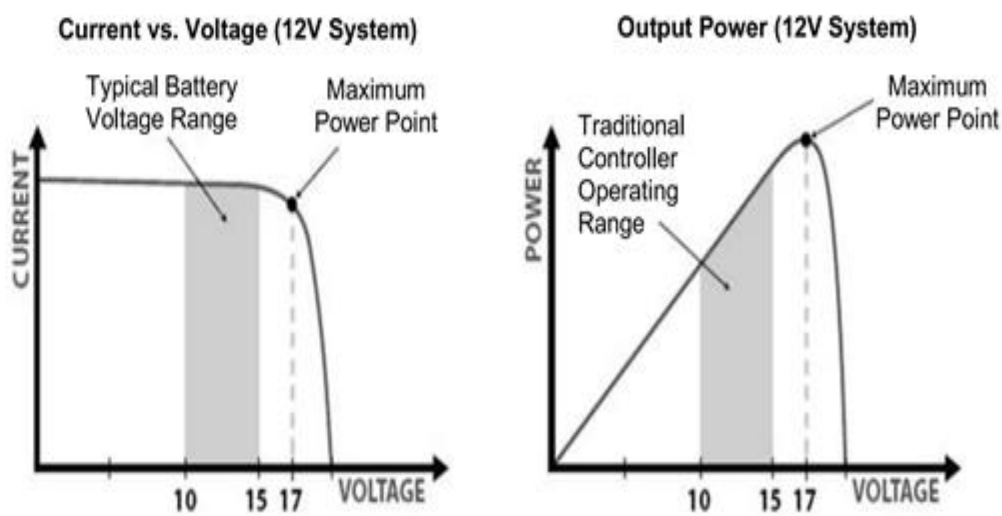

Figure 26: Current Vs. Voltage(left); Power Vs. Voltage(right)

In the following section, Table 14 compares the different solar charge controllers in consideration.

	Renogy Rover 20A	Renogy Rover 40A	Tristar TS-60	Tristar TS-60	ZHCSolar
Type of Regulation	MPPT	MPPT	PWM	MPPT	PWM
Load Current Rating	20A	40A	60A	60A	80A
System Voltage	12-24V	12-24V	12-24-48V	12-24-36-48V	12-24V
Output Voltage	12-24V	12-24V	*	8-72V	12-24V
Price	$129.99	$209.99	$220.00	$579.00	$73.00

Table 14 - Comparison table of solar charge controller

The ZHCSolar is the likely candidate compared to the other choices. It is inexpensive and can provide four times more current to the battery bank. Unlike the TIDA00120, the ZHCSolar is a fully assembled board with enclosure and is available to purchase. Although the TIDA00120 can be designed and assembled for less than $30, other readily available product on the market can be purchased for less and still provide more output current to the battery.

3.2.14 LIDAR

LIDAR stands for “light detection and ranging” and is often used for machine vision. It works by sending out laser pulses and recording the time it takes for the pulse to return. Sending out many quick pulses while moving the laser around allows the LIDAR to create a real-time 3D map of its environment. Figure 30 visualizes the parts of a typical LIDAR system.

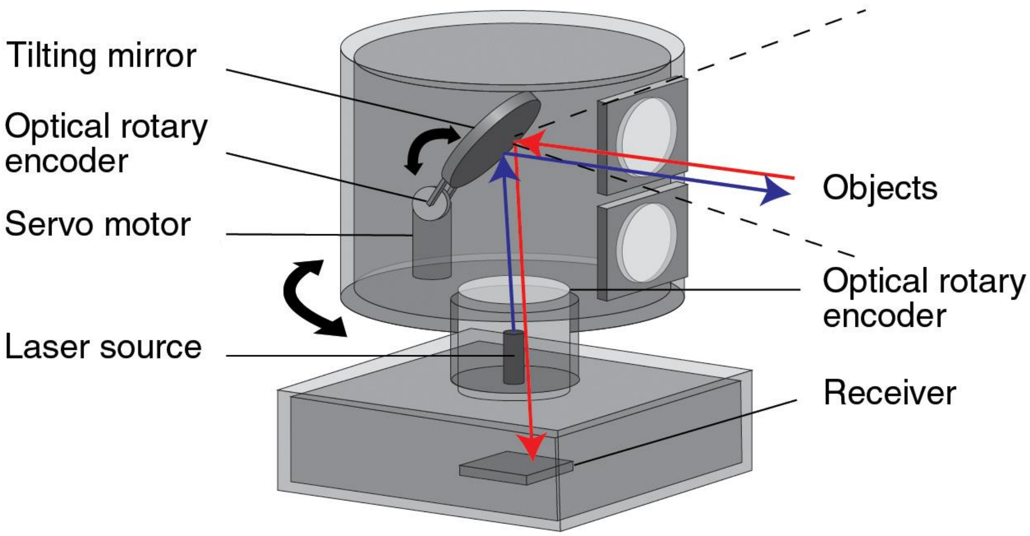

Figure 27 - Diagram of a typical LIDAR system

In principle, a lidar must consist of a transmitter and a receiver. Short light pulses with lengths of a few to several hundred nanoseconds and specific spectral properties are generated by the laser. Light pulses with lengths ranging from a few to several hundred nanoseconds and specific spectral properties are generated by the laser. Many systems also use a beam expander within the transmitter unit to reduce the divergence of the light beam. At the receiver end, optics are used to gather the returning signal. An optical analyzing system can be used which, depending on the application, selects specific wavelengths or polarization states out of the collected light.

Wavelengths used in lidar depend on the application and usually extend from about 250nm to 11µm. Ruby, nitrogen, copper-vapor, and CO2 lasers were mainly used in the early years, but high-power excimer and Nd:YAG lasers have been growing in use since the 1980s. Excimer lasers produce ultraviolet radiation, while the Nd:YAG crystal emits in the infrared spectral region at a wavelength of 1064nm. Frequency doubling and tripling with nonlinear crystals is often used to convert the wavelength of Nd:YAG radiation to 532 and 355nm. Quadrupling to 266nm is also utilized. The doping of crystalline lattices, e.g., yttrium aluminum garnet (YAG), yttrium lithium fluoride (YLF), lutetium aluminum garnet (LuAG), or of glasses with active ingredients such as Nd, Ho, Tm, Cr, Er, or Yb, creates a wide range of infrared wavelengths, some of which are particularly well suited for Doppler lidar. Presently, new laser types such as slab, microchip, waveguide, and solid-state Raman lasers are under investigation for their possible use in lidar.

Large systems have as many as 64 emitter/receiver pairs, also known as “channels”. Multiple channels enable the system to generate more than a million data points per second. However, 64 stationary channels aren’t enough to be able to map an entire environment. It would just give very clear resolution in focused areas. Adding more of these channels is expensive due to the precision required in the optics, so increasing the number of channels above 64 just increases cost faster. Instead, many Lidar systems use rotating assemblies, or rotating mirrors to enable the channels to sweep around the environment 360 degrees. Usually, each of the emitter and receiver pairs are angled above or below horizontal to blanket more of the environment in the field of view of the lasers.

Semiconductor lasers are favorable compared to other solid-state lasers in pulsed TOF (time-of-flight) laser radars because they are small, mechanically stable, relatively cheap, and have good efficiency. One of the most important requirements for a laser being used for LIDAR is that it must make short, powerful optical pulses. Laser Diodes are capable of the peak powers and pulse durations needed.

A quickly-switching circuit is needed to pulse the laser diode. A schematic diagram of a basic avalanche transistor laser pulser is shown in Figure 28.

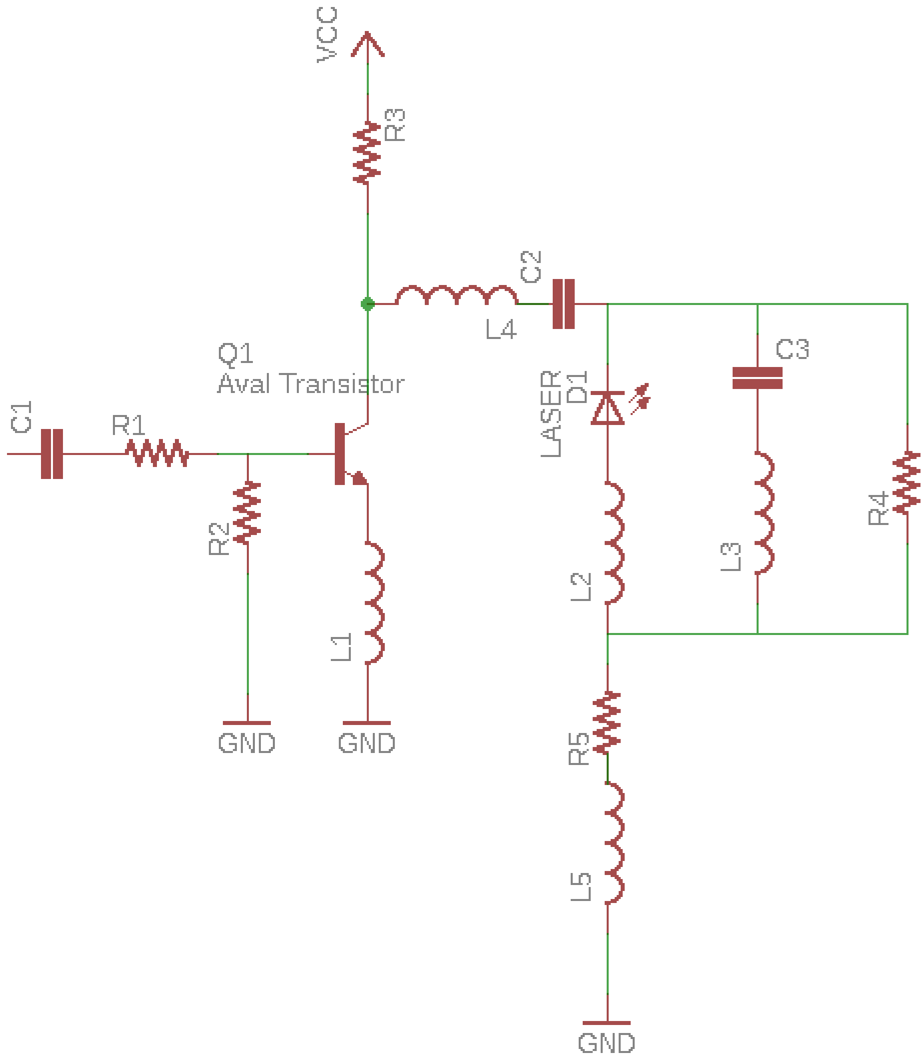

Figure 28 - Schematic diagram of a typical avalanche pulser.

Redesigned in Eagle for clarity.

A study performed by Ari Kilpelä and Juha Kostamovaara at the University of Oulu compares the parameters of different avalanche transistor circuits used for time of flight laser radars. Figure 32 below shows a comparison for the max peak current pulses that different avalanche transistors are capable of producing, while Figure 33 shows the output of laser diodes LD-65 and CVD-197 with full bandwidth of the system and from LD-65 with 100 MHz bandwidth.

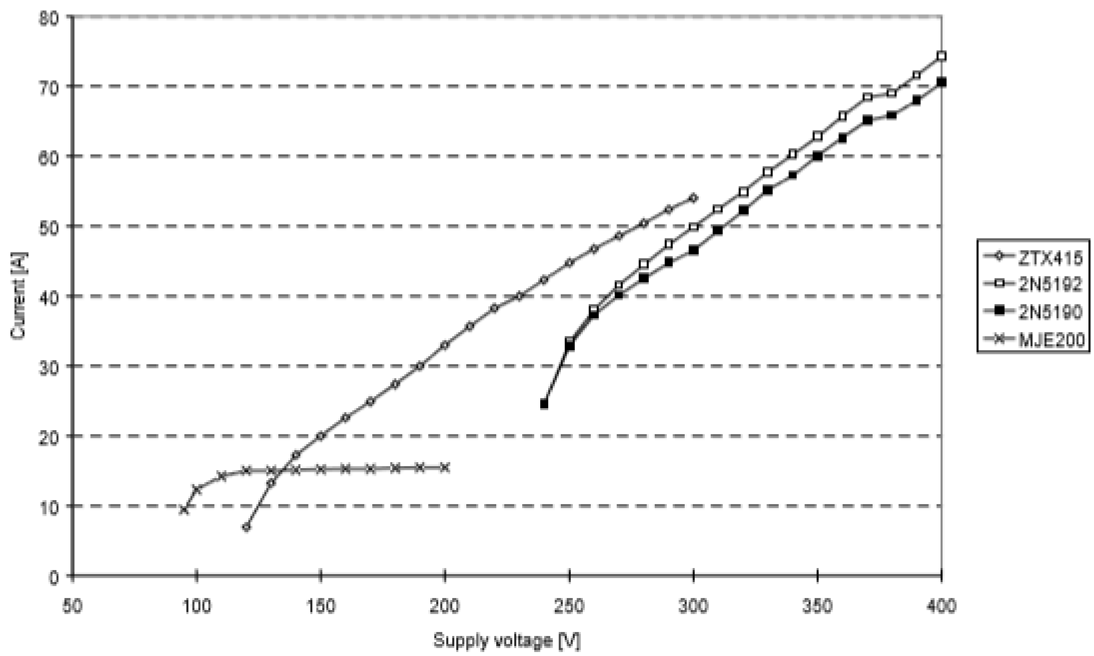

Figure 29 - The peak amplitudes of current pulses as a function of supply voltage

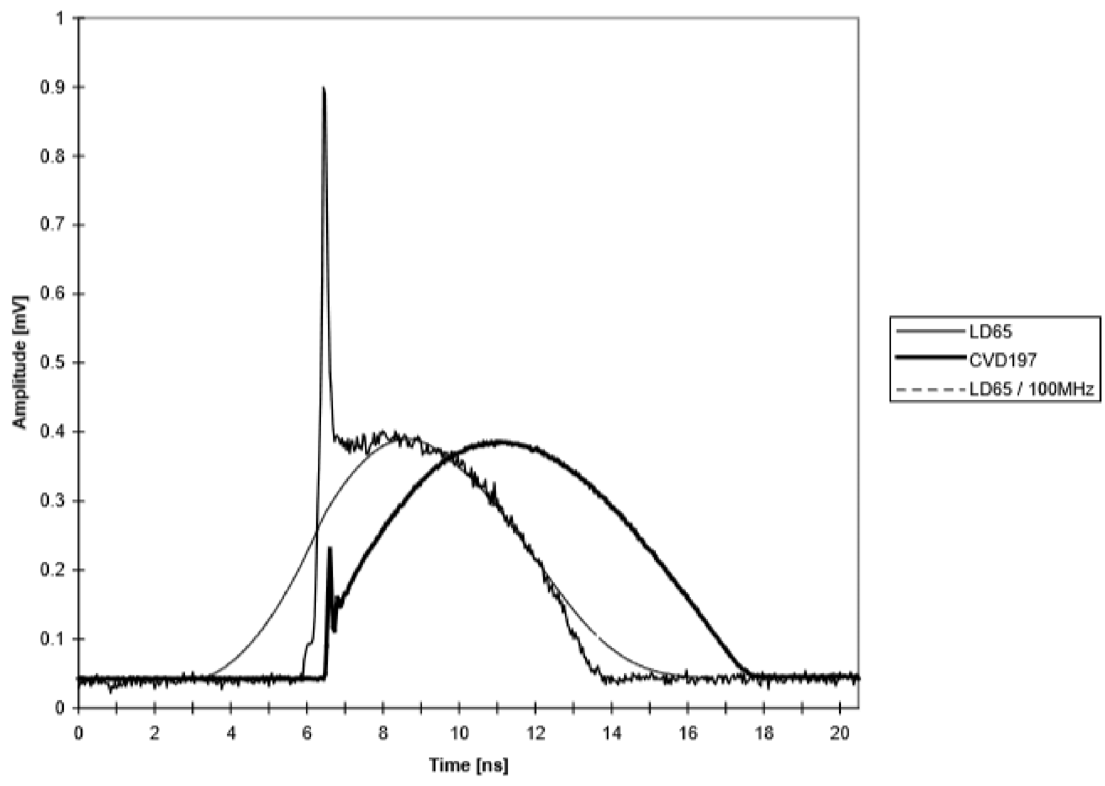

Figure 30 - Output of Laser Diodes at full and 100 MHz Bandwidth

Table 15 shows measurement results of current and optical pulses from a circuit, in which a capacitor has been used in parallel with laser CVD197.

	Current of series resistor			Optical pulse	
Capacitance	I_{peak} (A)	t_{rise} (ns)	t_{width} (ns)	t_{width} (ns)	P_{peak} (W)
0 pF	29.6	3.8	9.2	8.9	57
100 pF	30.9	5.5	9.0	8.7	58
200 pF	26.5	2.7	10.5	7.2	72
300 pF	26.7	2.4	12.4	7.2	72
400 pF	28.3	2.5	13.8	7.5	70

Table 15 - Measurements of Current, Power and Width in nanoseconds of optical pulses from a circuit

The data above shows that laser diodes with avalanche transistor circuits are capable of producing laser pulses with adequately short pulse durations and high enough peak intensities that they can be used for range finding.

3.2.15 Power Calculation

In order to meet the requirements of the design, it is important to calculate how much power the various components of the beach buggy will consume. Based on this calculation, a proper battery configuration can be selected to meet the project requirements.

Table 16 shows the power consumption of all electrical components used in the system.

Components	Supply Voltage	Number of Components	Net Current
Buggy Motors	12 VDC	2	29A
Servo	4.8 VDC	2	150mA
Motor Controller	12 VDC	1	60A
Rapsberry Pi3	5 VDC	1	2.5A
GPS Antenna	3.3 VDC	1	negligible
IR Sensors	3.3 VDC	1	10 mA
Ultrasonic Sensor	3.3 VDC	1	15 mA
LIDAR	12 VDC	1	275mA
GPS	5 VDC	1	negligible
TK1	12 VDC	1	5A
ODROID	5 VDC	1	4A
Total current draw			130 A

Table 16 - Power consumption by parts

3.3 Software Components

For hardware to work, it must have software. While the CPU provides the brain of the buggy and its other parts as its limbs, eyes, and hands, the software is its mind. The following software considerations were researched to provide the command and control of the buggy, to make it the autonomous robot that it needs to be.

3.3.1 Programming Language

Two programming languages were considered: C and Python.

C is an imperative procedural language that provides low-level access to memory, provides language constructs that map efficiently to machine instructions, and requires minimal run-time support. By design, C provides constructs that map efficiently to typical machine instructions, and therefore it has found lasting use in applications that had formerly been coded in assembly language, including operating systems, as well as various application software for computers ranging from supercomputers to embedded systems.

Python is an interpreted high-level programming language for general-purpose programming. Python features a dynamic type system and automatic memory management. It supports multiple programming paradigms, including object-oriented, imperative, functional and procedural, and has a large and comprehensive standard library. Python has a design philosophy that emphasizes code readability, notably using significant whitespace. It provides constructs that enable clear programming on both small and large scales.

Due to the nature of our system, and the middleware required for robot control (section 3.3.4), Python is considered to be the most optimal choice in our programming design language.

3.3.2 Image Processing

For data from a camera to be useful, a frontend software must be implemented to understand what we human see as Red, Green, and Blue values that compromises an image which, to a robot, is just a series of bits.

OpenCV (Open Source Computer Vision), originally developed by Intel, is a library of programming functions mainly aimed at real-time computer vision and has proven to be one of the most powerful libraries when it comes to real-time computer vision computation. It has extensive support and can be interfaced easily with our choice of Robot Control software.

3.3.3 Robot Control

Robot Operating System (ROS) is robotics middleware (i.e. collection of software frameworks for robot software development). It is not an operating system but it provides services designed for heterogeneous computer cluster such as hardware abstraction, low-level device control, implementation of commonly used functionality, message-passing between processes, and package management. Running sets of ROS-based processes are represented in a graph architecture where processing takes place in nodes that may receive, post and multiplex sensor, control, state, planning, actuator and other messages. Despite the importance of reactivity and low latency in robot control, ROS, itself, is not a real-time OS (RTOS), though it is possible to integrate ROS with real-time code.

ROS has extensive developer and community support, allowing the use of many libraries and packages that can be used to process the various data output from our sensors such as from our main sensor, LIDAR.

3.3.4 Operating System

The Robot Operating System (ROS), being middleware, requires an underlying Operating System to run. Its only supported Operating System is Ubuntu, an open source operating system.

Ubuntu is a Linux distribution based on the Debian architecture. It is usually run on personal computers, and is also popular on network servers, usually running the Ubuntu Server variant, with enterprise-class features. Ubuntu runs on the most popular architectures, including Intel, AMD, and ARM-based machines.

4.0 Related Standards

Standards are very important in today's technological world as not only do they provide a blueprint for designers and manufacturers to follow, but it also allows the ease of use for consumers by allowing interoperability and interdependency. Standards also provide major safety guidelines that prevent any harmful effects from the use of products or from the implementation of technology.
Many organizations provide standards. Examples of such organizations are the American National Standards Institute (ANSI), a private non-profit organization whose mission is "to enhance U.S. global competitiveness and the American quality of life by promoting, facilitating, and safeguarding the integrity of the voluntary standardization and conformity assessment system"; the IPC (Association Connecting Electronics Industries), a trade association whose aim is to standardize the assembly and production requirements of electronic equipment and assemblies; and the IEEE (Institute of Electrical and Electronics Engineers), "The world's largest technical professional organization for the advancement of technology".

Standards from these organizations will be looked at and discussed in relation to this project.

4.1 PCB Standard

The IPC-2221B Generic Standard on Printed Board Design (PCB) establishes the generic requirements in designing organic printed boards and other forms of component mounting or interconnecting structures. The requirements in the standard establishes design principles and recommendations that shall be used together with the detailed requirements of another specific sectional standard.

The standard identified generic physical design principles and is supplemented by other various sectional standards that focuses on specific aspects of printed board technology that includes:

IPC-2222 Rigid organic printed board design
IPC-2223 Flexible printed board design
IPC-2225 Organic, MCM-L, printed board design
IPC-2226 High Density Interconnect (HDI) printed board design

The standard itself is not a performance specification for finished printed boards.

The standard allows us to create PCBs that are oriented properly, allowing an efficient and error-free soldering process; placed properly, preventing things such as components on the solder side of a board resting behind plated through-hole components; organized, allowing the PCB to be efficient, look clean, and minimize assembly steps due to standards such as requiring that Surface Mount (SMT) components be placed on the same side of board, and all through-hole (TH) components on the top side the board; and minimized interference due to guidance such as separating the power ground and control ground for each power supply stage.

4.2 Software Testing Standard

The ISO/IEC/IEEE 29119 series consists of five standards that define an internationally agreed set of standards to support software testing. The standard allows developers to create software that meets industry specifications, as well as proper testing of functionalities to ensure proper operation of the system.

Two parts of this standard is discuss in relation to this project: ISO/IEC/IEEE 29119-2 (Part 2) - Test Processes and ISO/IEC/IEEE 29119-4 (Part 4) - Test Techniques.

4.2.1 ISO/IEC/IEEE 29119-2 (Part 2) - Test Processes

This part defines a generic process model for software testing that is intended for use by organizations when performing software testing. It comprises test process descriptions that define the software testing processes at the organizational level, test management level and dynamic test levels. Each testing process is described using a standard template.

The purpose of the organization level is to develop and maintain organizational test specifications, such as a test policy and organizational test strategy. “Organization” in our context, is our group members. This process allows us to implement a test specification based on stakeholder requirements.
The management level describes test planning, test monitoring and control, and test completion. Test planning involves understanding the context of the test and its scope, wherein one should then organize test plan development. Risks should then be identified and incorporated in to the design test strategy. Once a strategy is in place, staffing and scheduling should be determined, along with documenting the test plan. Once a test plan is documented and approved, the test plan is ready for test monitoring and control.

Once testing begins, test monitoring and control allows revisions or updates on previous test plans to allow for accounting of factors that may not have been considered previously. This allows the creation of new test plans that can be cycled again through test monitoring and control; repeating the process if necessary. As with previous test plans, new test plans must confirm with organization test process guidelines. Once testing is complete, the test completion process can be executed.

The test completion process involves the dynamic test process which, similar to the test management process, involves test design and implementation. Additionally, the dynamic test process includes a processing for testing environment requirements, setting up the test environment, and then test execution. Once test execution is done, the results can be reviewed and, if any incidents arise, be reported so the rest of the group can be aware. Figure 34 illustrates the Test Management Process, as illustrated by ISO/IEC/IEEE 29119-2

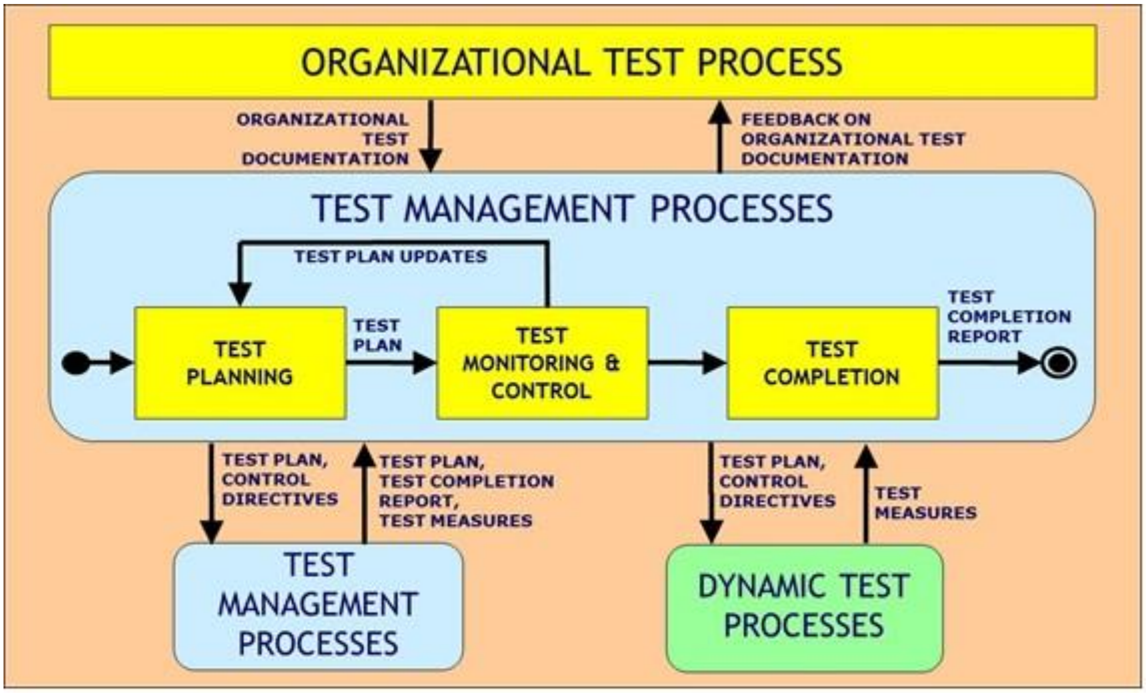

Figure 31. The Test Management Process

4.2.1 ISO/IEC/IEEE 29119-4 (Part 4) - Test Techniques

This part defines standard definitions of software test design techniques (also known as test case design techniques or test methods) that can be used during the test design and implementation process that is defined in ISO/IEC/IEEE 29119-2. Techniques of part 4 are intended to support part 2 or can be used without part 2.

The techniques in the section are categorized into three categories: Specification-Based Test Design Techniques, Structure-Based Test Design Techniques, and Experience-Based Test Design Techniques. Each category has different techniques wherein the identification of relevant test aspects and the derivation of test inputs and test cases varies by technique used. Consideration of these technique categories and the techniques within can allow our group to thoroughly, properly, and effectively test the requirements and operation of our buggy.

Specification-Based Test Design Techniques base on the (functional) specification of the system under test. They are also called black-box testing. These techniques examine the functionality of an application without knowing its internal structures or workings. The tester is aware of what the software is supposed to do but is not aware of how it does it.

Structure-Based Test Design Techniques base on the (internal) structure of the system under test. They are also called white-box testing. These techniques tests internal structures or workings of an application, as opposed to its functionality. These techniques are especially useful in knowing the flow of program code within the software so that any discrepancies between blocks or functions can be corrected.

Experience-Based Test Design Techniques rely on the experience of the human tester. The standard list only one technique in this category--Error guessing. It is a test method in which the test cases used are established based on experience in prior testing. Typical errors include divide by zero, null pointers, or invalid parameters. Error guessing has no explicit rules, and its scope can vary widely depending on the situation.

5.0 Project Hardware and Software Design Details

After an extensive discussion on the base elements which will be necessary to the successful operation of the buggy, this section will detail the current plans the team has with regards to the actual design of the electrical components which will be used on the beach buggy. This is obviously a vital part to ensuring the success of the overall design, and so it is important to be as detailed as possible.

5.1 LIDAR

This section will discuss the implementation of the Lidar system onto our buggy. This will incorporate a laser diode and photodiode, as well as driving and receiving circuits that will operate the diodes. The output of this system will be fed into an arduino and an analysis will be carried out on that data in order to determine distances and create a rudimentary point cloud which will allow us to identify objects in the path of the buggy.

The Lidar module will consist, broadly, of two components: A laser emitter which will periodically emit a pulse of light out into the environment we wish to scan, and a receiver module, which will focus a portion of the laser light reflected directly back from the environment. By using a periodic step function as a method of time-keeping, the difference in time between the output of a pulse of the laser diode and the registered input of the photodiode can be recorded and converted into a distance traveled, which can in turn be fed into an arduino for computational purposes. This method of laser rangefinding is referred to as time-of-flight tracking, and for our purposes, we have chosen it as the most efficient and easily developed method of laser rangefinding. A visual depiction of the basic operation of the Lidar system is shown below in figure 35.

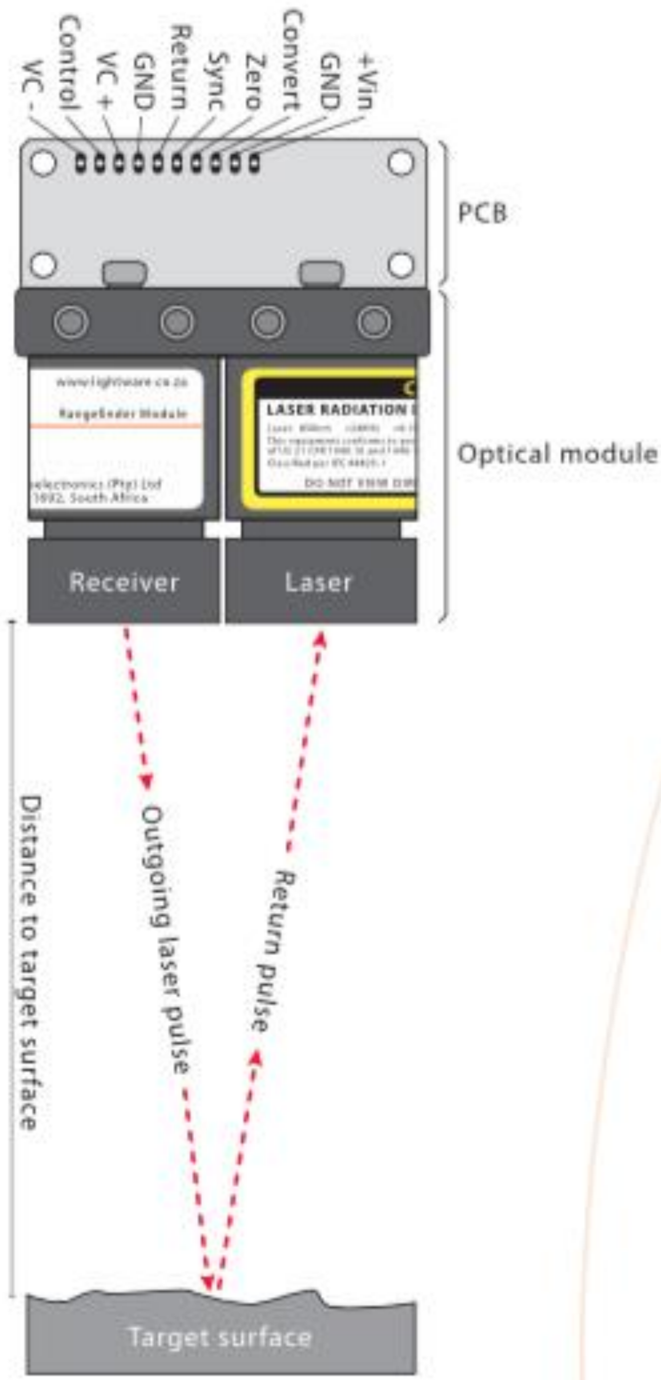

Figure 32- A basic diagram of the operation of the Lidar system
Courtesy of Lightware Optoelectronics

As stated above, the Lidar module will consist of two major components: The laser emitter and the photodiode receiver. The laser emitter is a fairly simple set up, being driven by a laser driving circuit that produces a regularly pulsed signal, which is kept in sync by the sequential equivalent time sampling circuit. This pulse is sent to the laser diode, and produces an output which is then passed through a collimating lens before being sent out into the environment. The photodiode receiver is also a relatively simple circuit design, as it only needs to incorporate a detector that is sensitive enough to receive the minute amounts of light reflected off of the surfaces in the environment, and an amplifier to turn the received signals into a useful pulse waveform. A rough block diagram for our system is displayed below in figure 33.

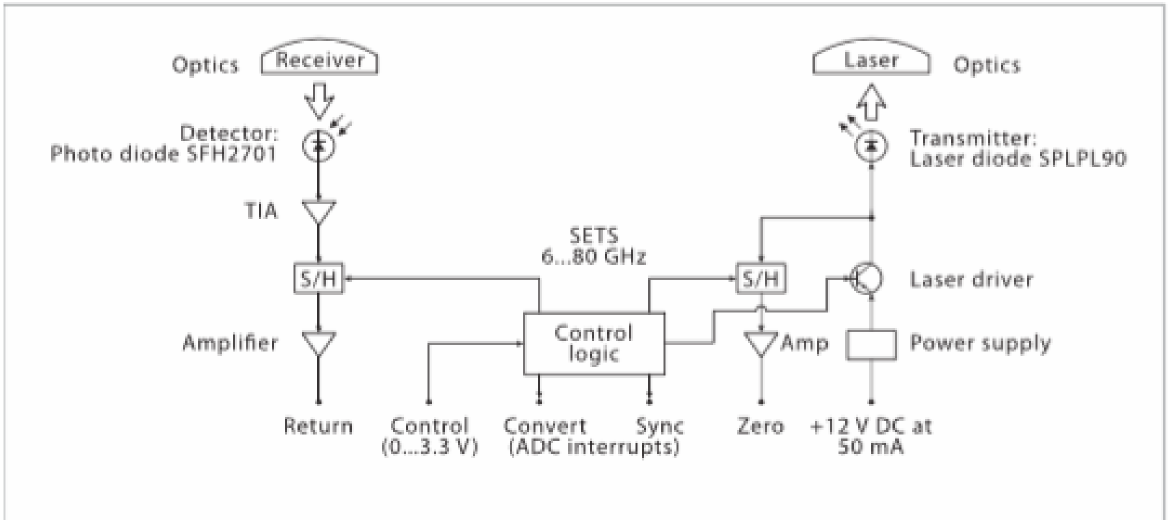

Figure 33 - A basic block diagram of the Lidar system

Courtesy of Lightware Optoelectronics

One of the most important aspects of our Lidar set up is the timing circuits, referred to as the sequential equivalent time sampling circuit. Given the high frequency at which light pulses need to be generated, received, and calculated, an efficient and dependable timing circuit is vital to the successful operation of our device. As we are dealing with a system that would require clocking speeds on the order of 15 GHz in order to maintain a resolution of 1cm, it would be impractical to incorporate a direct timer to track our pulses. In order to design around the expensive equipment that a direct sampling method would require, the sequential equivalent time sampling circuit operates by establishing a discreet timebase of our own choosing, which can then be used to sample the outgoing and incoming pulse waveforms and convert high speed signals onto the slower timebase that we have established, thereby allowing the computations to be done with less expensive, power intensive hardware. The slowed down signals operate on a timebase that is around 100,000 times slower than the real-time signals, and the amount of timebase expansion can be modified to change the resolution of the measurements and the update rate.

The real-time span of the timer in our timing circuit is approximately 122 ns, but can be stretched to more than 20 ms using the timebase adjustment we had previously mentioned. This gives us an operational distance of approximately

18.33 m, which is more than sufficient for our purposes. A square sync signal is provided, the falling edge of which marks the end of one measurement and the start of another on our expanded timebase. The period of the sync signal is always equivalent to 18.33 m, meaning that distances between signals on our expanded timebase can be calculated as proportions of the period of the sync signal. The relationship between the sync signal and our output/input signals is illustrated below in figure 37. This period can be altered by a change in the control voltage input, which alters the timing and results in a faster or slower expanded timebase. In addition, the two analog signals that represent the outgoing laser diode pulse and the return signal are on the same timebase as the sync signal, due to the fact that the timing circuit performs a timebase expansion of each of the signals, with the sync being an expanded image of the real-time timer. In addition, there is a convert reference that can be used to trigger successive ADC conversions on a host controller. This convert signal is synchronous with our timing circuit and will help reduce noise in the digitised signals.

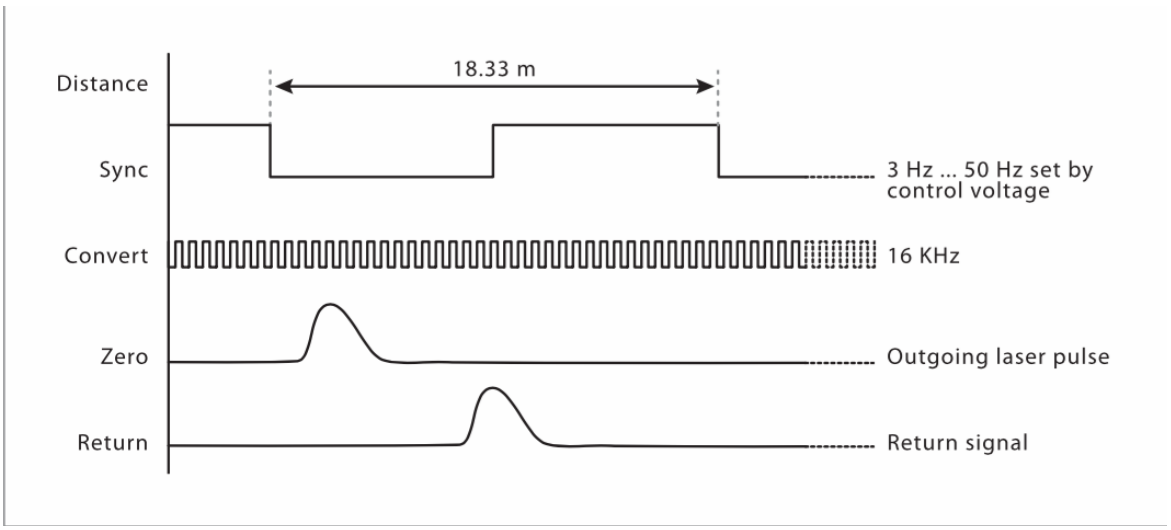

Figure 34 - An illustration of the timing relationship between signals

Courtesy of Lightware Optoelectronics

On an expanded timebase, the signal to fire the laser diode is sent at the exact same moment as the falling edge of the sync signal. However, because there is an inherent delay between the signal being received and the diode producing light, there is a noticeable delay on the expanded timebase. There is also the fact that the pulses have a width associated with their real-time generation and travel. This means that we can not utilize the full range of the sync signal for rangefinding, and our effective location distance will be slightly below 18.33 meters. Despite this minor limitation, it should not prove to be a significant detriment to our design, as the distances we are concerned with fall well within our operating potential.

SETS (sequential equivalent time sampling):

The time between the outgoing laser pulse and the return signal needs to be measured with very high precision in order to calculate the distance. The SETS circuit slows down these signals so that they can be viewed on a much lower frequency.

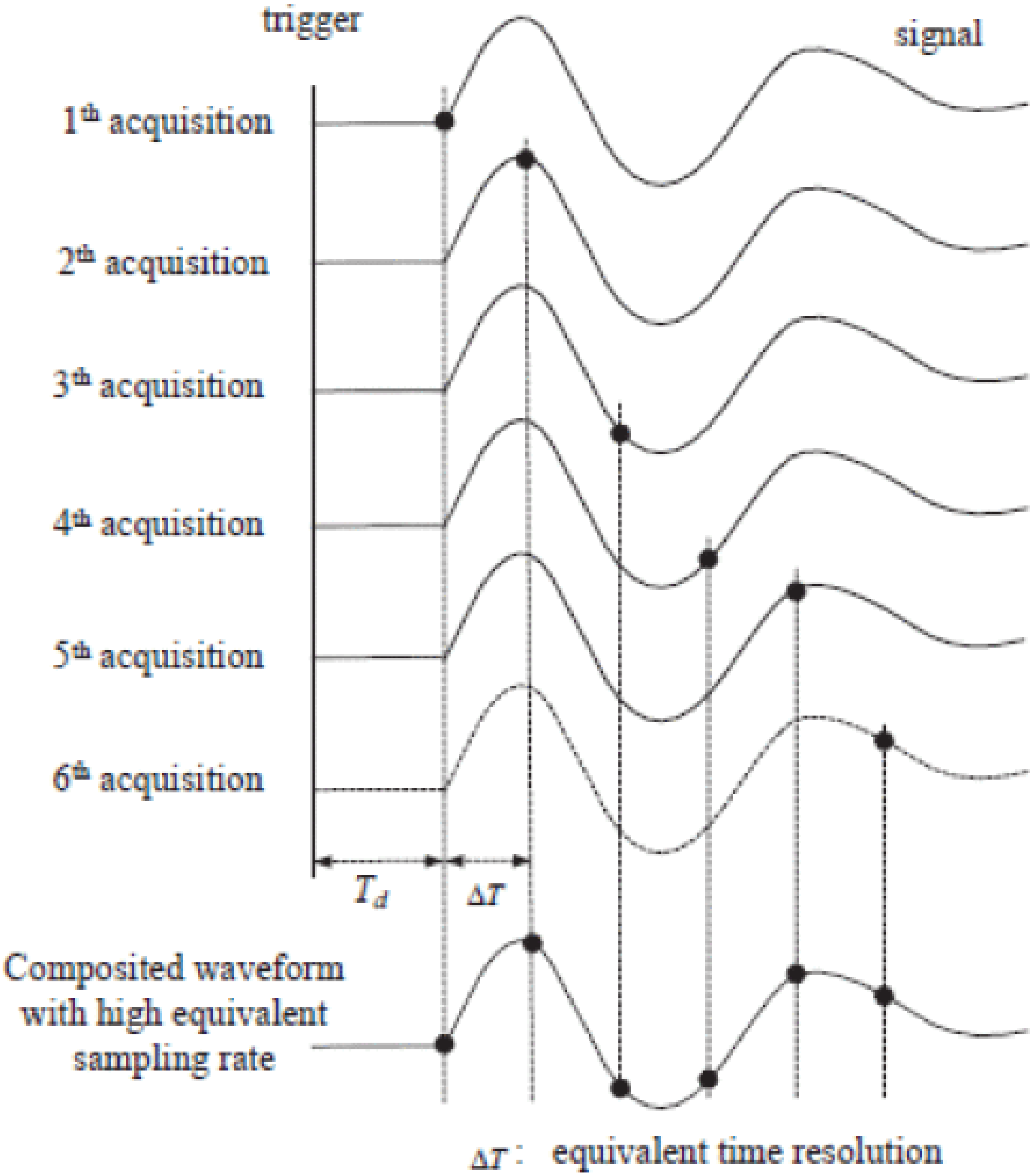

Figure 35. Basic principle of SETS sampling

The basic principle of SETS sampling is illustrated in figure 38. In SETS, the test signal should be periodic or repetitively generated. SETS system captures one sample at each acquisition. When the trigger signal is detected, the first samples is taken after a fixed time delay. At the next acquisition, after trigger signal, the second sample is taken after a slightly longer time delay. After enough samples are collected, the signal is reconstructed by time aligning the samples

Software Timing Strategies:

After analogue to digital conversion (ADC), the digital signal can be analyzed using different software algorithms. The simplest strategy is to define a threshold voltage on and then to count the number of ADC samples from the falling edge of the sync reference to the rising edges of the zero and return that reach this threshold. Each ADC sample is counted, and these counts give the relative time to the edges measured on the expanded timebase. The number of ticks between falling edges of the sync reference allow the distance can be calculated as follows:

distance_to_target = ((ticks_to_return - ticks_to_zero) / ticks_between_Sync_edges) * 18.33m

One limitation to this strategy is that the return signal will change size and shape depending on the color and distance of the measured object. These changes will cause differences in both the height and the width of the digitized signal and therefore the point at which the leading edge crosses the threshold. This effect can be minimized by setting a dynamic threshold that is set at a fixed proportion of the height of the return signal.

Another strategy is to use constant fraction discrimination (CFD). This method uses both the rising edge and the falling edge of the return signal, as they are timed as they cross a fixed threshold. The true position of the return is then defined as midway between these points.

The current pulse first goes through a transimpedance amplifier, labeled as IC13 in Figure below, which turns the input current signal into an input voltage. This voltage then goes through the sequential-equivalent-timing circuits to slow down the voltage before it is amplified and then outputted. The receiver circuit is illustrated in figure 39 below.

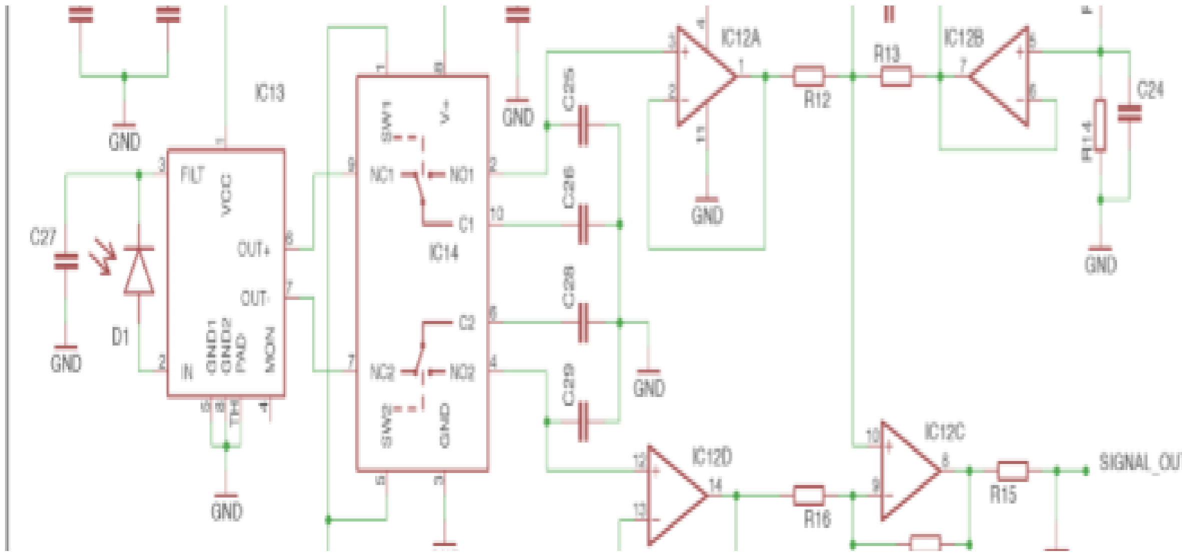

Figure 36. Receiver Circuit

Once the signal travels through a laser driver, it must be also be sent to a sequential-equivalent-timing circuit and through an amplifier so that it can be outputted for timing purposes. Figure 40 , shown below, shows the circuit schematic of the sequential-equivalent-timing circuit and the buffer used to slow down the signal.

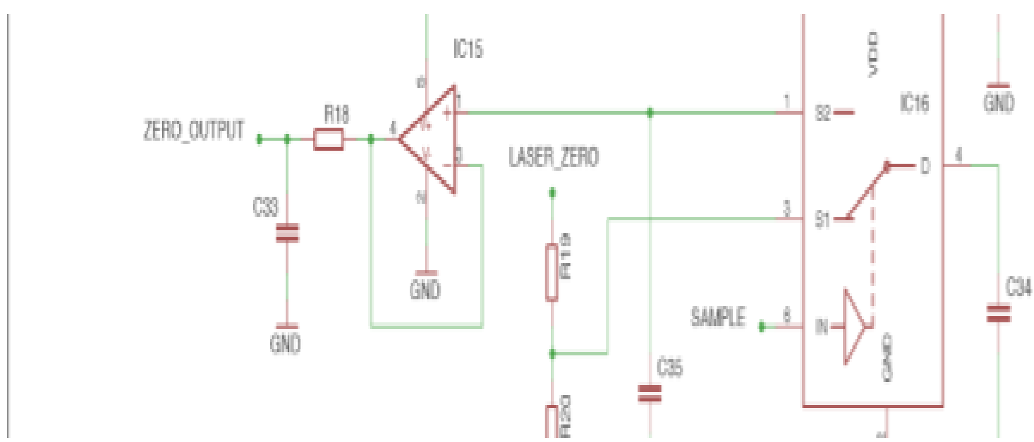

Figure 37. Circuit Schematic of the Sequential-Equivalent-Timing Circuit

In order for the transmitting and receiving sides of the optics to produce slowed-down signals that can be outputted for timing purposes, it is controlled by circuitry designed to control the sequential-equivalent-timing-circuits on both the transmitting and receiving sides. It is also responsible for controlling the laser driver on the transmitting end. Figure 41 shows the schematic of this control logic, while figure 42 shows the laser driver.

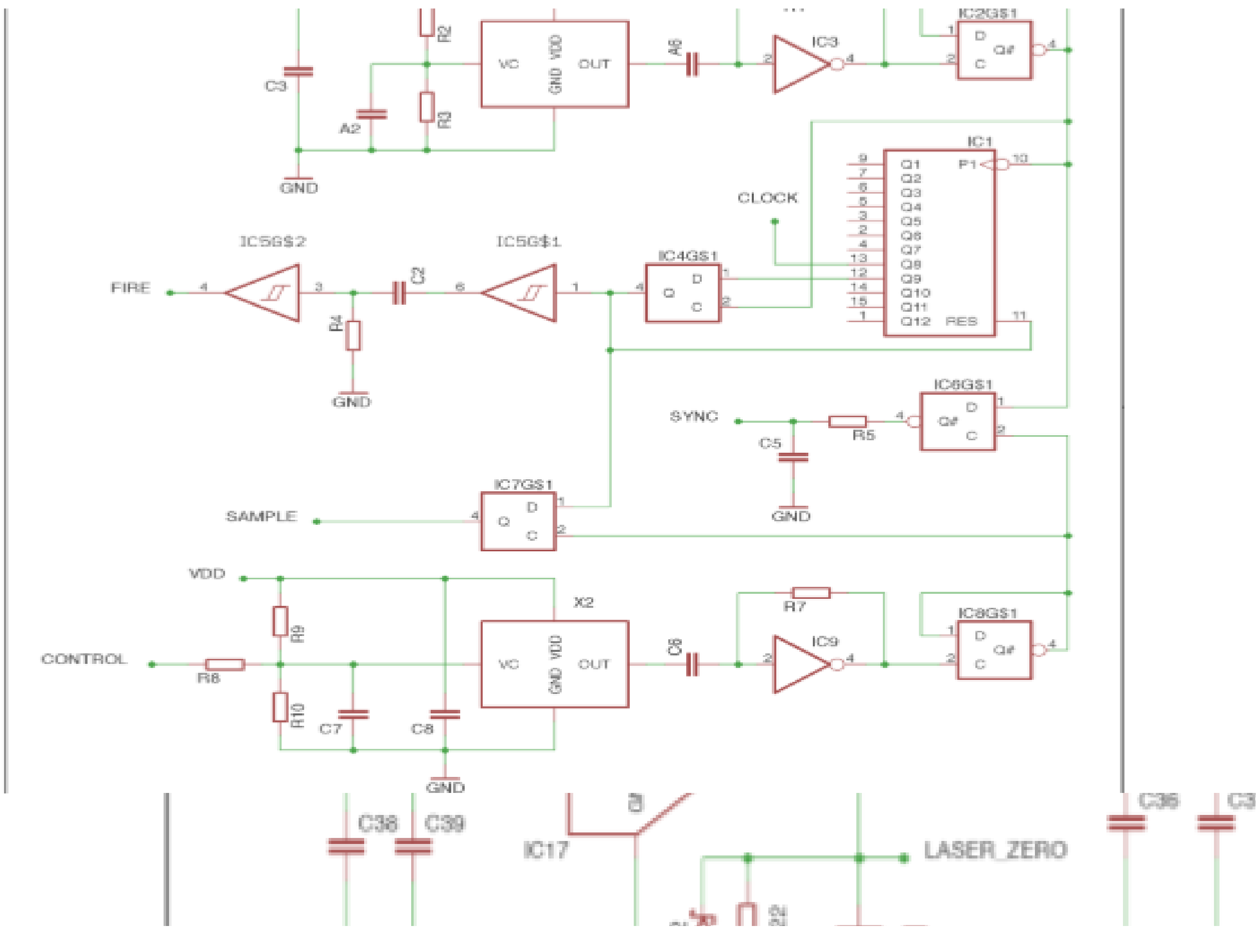

Parts list: Table 17 shows all the components that will be on the PCB

1		Reference	Description	Package	Supplier	Part code
2	Capacitors	C1	1nF, 50V, X7R	402	RS Components	723-5266
3		C2	120pF, 50V, X7R	402	RS Components	723-5376
4		C3	100nF, 16V, X7R	402	RS Components	723-5228
5		C4	100nF, 16V, X7R	402	RS Components	723-5228
6		C5	1nF, 50V, X7R	402	RS Components	723-5266
7		C6	1nF, 50V, X7R	402	RS Components	723-5266
8		C7	1uF, 10V, X5R	402	RS Components	723-5199
9		C8	100nF, 16V, X7R	402	RS Components	723-5228
10		C9	100nF, 16V, X7R	402	RS Components	723-5228
11		C10	100nF, 16V, X7R	402	RS Components	723-5228
12		C11	100nF, 16V, X7R	402	RS Components	723-5228
13		C12	100nF, 16V, X7R	402	RS Components	723-5228
14		C13	100nF, 16V, X7R	402	RS Components	723-5228
15		C14	100nF, 16V, X7R	402	RS Components	723-5228
16		C15	100nF, 16V, X7R	402	RS Components	723-5228
17		C16	100nF, 16V, X7R	402	RS Components	723-5228
18		C17	100nF, 16V, X7R	402	RS Components	723-5228
19		C18	10uF, 16V, X7R	1206	RS Components	723-6565
20		C19	10uF, 16V, X7R	1206	RS Components	723-6565
21		C20	1uF, 10V, X5R	603	RS Components	391-040
22		C21	100nF, 16V, X7R	402	RS Components	723-5228
23		C22	100nF, 16V, X7R	402	RS Components	723-5228
24		C23	100pF, 50V, X7R	402	RS Components	624-2929
25		C24	1uF, 10V, X5R	402	RS Components	723-5199
26		C25	1nF, 50V, X7R	402	RS Components	723-5266
27		C26	22pF, 50V, COG	402	RS Components	723-5408
28		C27	1nF, 50V, X7R	402	RS Components	723-5266
29		C28	22pF, 50V, COG	402	RS Components	723-5408
30		C29	1nF, 50V, X7R	402	RS Components	723-5266
31		C30	100pF, 50V, X7R	402	RS Components	624-2929
32		C31	100pF, 50V, X7R	402	RS Components	624-2929
33		C32	100nF, 16V, X7R	402	RS Components	723-5228
34		C33	1nF, 50V, X7R	402	RS Components	723-5266
35		C34	22pF, 50V, COG	402	RS Components	723-5408
36		C35	1nF, 50V, X7R	402	RS Components	723-5266
37		C36	2 x 22nF, 50V, COG	603	RS Components	391-195
38		C37	2 x 22nF, 50V, COG	603	RS Components	391-195
39		C38	10uF, 16V, X7R	1206	RS Components	723-6565
40		C39	0.1uF, 25V	603	RS Components	147-538
42	Resistors	R1	100k, 1%, 100ppm	402	RS Components	667-8977
43		R2	10k, 1%, 100ppm	402	RS Components	678-4697
44		R3	10k, 1%, 100ppm	402	RS Components	678-4697
45		R4	200R, 1%, 100ppm	402	RS Components	667-8628
46		R5	200R, 1%, 100ppm	402	RS Components	667-8628
47		R6	200R, 1%, 100ppm	402	RS Components	667-8628
48		R7	100k, 1%, 100ppm	402	RS Components	667-8977
49		R8	10k, 1%, 100ppm	402	RS Components	678-4697
50		R9	10k, 1%, 100ppm	402	RS Components	678-4697
51		R10	4k7, 1%, 100ppm	402	RS Components	667-8794
52		R11	10k, 1%, 100ppm	402	RS Components	678-4697
53		R12	1k, 1%, 100ppm	402	RS Components	667-8680
54		R13	10k, 1%, 100ppm	402	RS Components	678-4697
55		R14	1k, 1%, 100ppm	402	RS Components	667-8680
56		R15	10k, 1%, 100ppm	402	RS Components	678-4697
57		R16	1k, 1%, 100ppm	402	RS Components	667-8680
58		R17	10k, 1%, 100ppm	402	RS Components	678-4697
59		R18	10k, 1%, 100ppm	402	RS Components	678-4697
60		R19	470R, 1%, 100ppm	402	RS Components	678-9355
61		R20	200R, 1%, 100ppm	402	RS Components	667-8628
62		R21	100R, 1%	1210	RS Components	679-2373
63		R22	27R, 1%	603	RS Components	679-0099

65	Integrated Circuits	IG1	SN74HC4040PWG4, 12 stage counter	TSSOP-16	RS Components	663-2105
66		IG2	SN74LVC1G80DCK, D-flip-flop, Q#	SC-70	RS Components	662-8803
67		IG3	74LVC1GU04DCK, inverter	SC-70	RS Components	662-6670
68		IG4	SN74LVC1G79DCK, D-flip-flop, Q	SC-70	RS Components	662-8806
69		IG5	SN74LVC2G17IDCK, dual, ST, buffer	SC-70-6	RS Components	662-8948
70		IG6	SN74LVC1G80DCK, D-flip-flop, Q#	SC-70	RS Components	662-8803
71		IG7	SN74LVC1G79DCK, D-flip-flop, Q	SC-70	RS Components	662-8806
72		IG8	SN74LVC1G80DCK, D-flip-flop, Q#	SC-70	RS Components	662-8803
73		IG9	74LVC1GU04DCK, inverter	SC-70	RS Components	662-6670
74		IG10	L78L08, 8V, linear regulator	SC-89	RS Components	686-9476
75		IG11	L78L33, 3.3V, linear regulator	SC-89	RS Components	686-9426
76		IG12	MCP6L04, quad, op-amp	TSSOP-14	RS Components	768-1404
77		IG13	MAX3658, transimedance amplifier	TDFN8	Digikey	MAXIM
78		IG14	TS5A23157DGSRG4	MSOP-10	RS Components	662-2788
79		IG15	LMV321IDCKRG4	SC-70	RS Components	660-9603
80		IG16	TS5A3157DCKRG4	SC-70-6	RS Components	662-2798
81		IG17	MIC44F18, MOSFET driver	MSOP EP-8	RS Components	453-205
83	misc	CON1	10x1 male header	0.1"		
84		D1	SFH2701, photodiode	3216	RS Components	665-5338
85		D2	1N5819, diode	SOD123	RS Components. In parallel with R22	708-2197
86		LAS1	SPL_PL90, 25W laser	N/A	Jameco	OSRAM 2192763
87		LED1	LED, red	1206	RS Components	700-7893
88		Q1	BSP318S, avalanche SIPMOSFET	SOT223	RS Components	753-2816
89		X1	16.369MHz, VCTCXO	2.5x2 PQFN	DigiKey	535-11784-1-ND
90		X2	16.369MHz, VCTCXO	2.5x2 PQFN	DigiKey	535-11784-1-ND

Table 17. Parts List

Table 18 shows the specifications of the open source LIDAR system OSLRF-01, which heavily inspired our system:

	OSLRF-01
Range	0.5 … 9 m
Resolution	Adjustable
Update rate	Adjustable: 3 … 50 readings per second
Accuracy	Adjustable
Power supply voltage	12 V (10 … 16 V)
Power supply current	50 mA
Outputs & interfaces	Timing & laser signal outputs
Dimensions	27 x 56 x 65 mm
Weight	57 g
Mounting	4 x M3 (3.2 mm diameter) mounting holes
Connection	0.1 in. pitch header
Optical aperture	53 mm
Beam divergence	50 mm at 9 m (approx.)
Laser power	14 W (peak), 6 mW (average), Class 1M
Operating temperature	- 20°C … + 60°C

Table 18. Open Source LIDAR Specification

5.2 Solar Cells

In this section we will describe the functional solar panel circuit designs which we will be implementing in our final buggy platform. After an extensive study of similar projects which involved significant dependence on solar power, we were able to incorporate a rough design which would be able to adequately distribute the power generated in the solar cells to the rest of our system. As the solar cell is the lifeblood of our buggy, it is vital that the implementation of the solar panel circuit be well-defined and secure.

Our basic system will consist of two monocrystalline solar panels, placed in prominent positions on top of either the buggy itself or a platform designed for the sole purpose of raising the the solar panels to a safe altitude, where they can be made to pan and tilt in order to maximize their efficiency. From there, the current generated in the photovoltaic cells by the impact of the incident sunlight will pass through to a charge controller, which will limit the rate that the current is passed through to the batteries, ensuring safe operation and charge speeds. This current will pass through to one of two batteries, which will charge over time as the other battery discharges in order to power the necessary operational elements of the buggy. These batteries will switch roles as they get discharged, ensuring that the buggy is always operational, provided a bountiful and consistent amount of sunlight.
From the battery that is being used to power the buggy, a current will pass through an inverter, which will convert the DC current provided by the battery to an AC current which can be utilized by the various electrical components of the buggy to function. As we had discussed in the prior sections, we have various promising candidates for the parts we will need to develop and implement this circuit.

5.3 Code Design

This section will detail the design aspects of the current model for the software that will be used to operate the buggy. Just as the physical hardware and materials of the chassis and wheels are vital to ensuring the durability of teh buggy, the coding aspects of the computer systems onboard are vital to ensuring that the buggy is able to operate effectively and efficiently once it is assembled, and so it is necessary for us to develop a thorough model of how it is to operate once it is compiled into a single system.

5.3.1 Robot Operating System

ROS is fundamentally a full-featured message passing interface intended for use with robotics. Message passing interfaces are, as implied by the name, a system where one component can send some kind of information to one or more other components or make it available for other components to read. There are numerous predefined messages that can be used which can store data as simple as a single integer or as complex as a fully colored image. In addition, ROS offers the ability to create messages from a user made template if a suitable message type can't be found.

5.3.1.1 Nodes

Every component in ROS is a "Node"; specifically, they are defined as a unit that does computation. They may additionally be publishers, subscribers, or both. Publishers are able to post messages of a specific type to specific topics, usually at a regular, fixed speed (although they can post as quickly as possible, or only in response to something else). Subscribers listen for messages posted to a specific topic or topics, and generally are event-driven.

5.3.1.2 Advantage of ROS

First and foremost, ROS is the largest, most common framework for programming robots today. Not only that, but it's also been around since 2007, meaning it's very stable and well supported both by the Open Source Robotics Foundation and by community developers. From a development perspective, the biggest benefit is that nodes can be written in any programming language (although primarily C++ and Python). This means that we can write low-level C++ nodes to get camera frames, while using Python to abstract the neural network to an extent and take advantage of the Python machine learning libraries and examples available online, rather than trying to slog through in C++.

5.3.1.3 Limitations

ROS is a very powerful framework for robotics; however, users are limited to the Linux operating system. At times Linux is not as intuitive as other operating systems. A basic understanding commands from the Linux terminal is required. As shown above, installation is not as simple as downloading a file from a web browser. In addition, each node, including ROScore, must be run from their own terminal window.

In addition, compiling a single node can be a little daunting. Each node must be made within a catkin package. It is compiled using a Cmake file which must find the ROS package in addition to any other packages that are needed and link them. The build dependencies must also be listed in an XML file located within the catkin package. While the catkin tool does generate these files with comments to help understand the system, it can be a lot to take in at once.

5.3.1.4 Data Flow

This section details the method in which data input to the system will be processed, and describes which nodes will perform what action in order to perform to the expectations we had established.

1. Hardware/Framework

Boxes represent physical hardware and the ROS framework; things that we didn't make and won't change.

2. Nodes

Nodes are represented by circles; some of them are just labeled "Publisher" or "Subscriber" because they only format raw data into messages before posting to a topic, or because (in the case of the subscriber) it's effectively just a hardware abstraction.

3. Serial Node

The serial node is how ROS sees the entire Arduino; it is part of a *rosserial_python* library, and effectively just pipes the Arduino serial output into a ROS node.

4. Navigation Node

The navigation node reads all data from the Arduino, through the serial node, and converts it into useful heading delta data. This heading delta, plus information about distance to the next waypoint and location within the travel corridor, will be sent to the main neural network. It also may be given the task of controlling additional cooling fans based on the INS temperature readings.

5. Camera Publisher Node

This node connects to the attached cameras using OpenCV's VideoCapture class. It then takes frames from the video streams and stitches them together into one large image to be processed. In order to send this image through ROS, the OpenCV image is packaged using the *image_transport* package offered by ROS and sent through the camera/image topic.

6. Avoidance Node

The avoidance node will contain a small neural network of some flavor that will take in the raw camera images and apply transformations to turn it into useful data. In the future, this node may be merged with the Neural Network node.

7. Neural Network Node

The neural network node takes in the rectified images along with heading delta and range information, and runs all of it through an end-to-end deep neural network to generate steering instructions. These steering instructions are then posted to a control topic that goes through the serial node to the Arduino subscriber, which sends the actual control signals to the electric motors.

8. Topics

Arrows are labeled with topic names, and indicate what node publishes to that topic and what node is reading from that topic. The only arrow that doesn't follow this rule is the *node_health* topic, which will be used by every node.

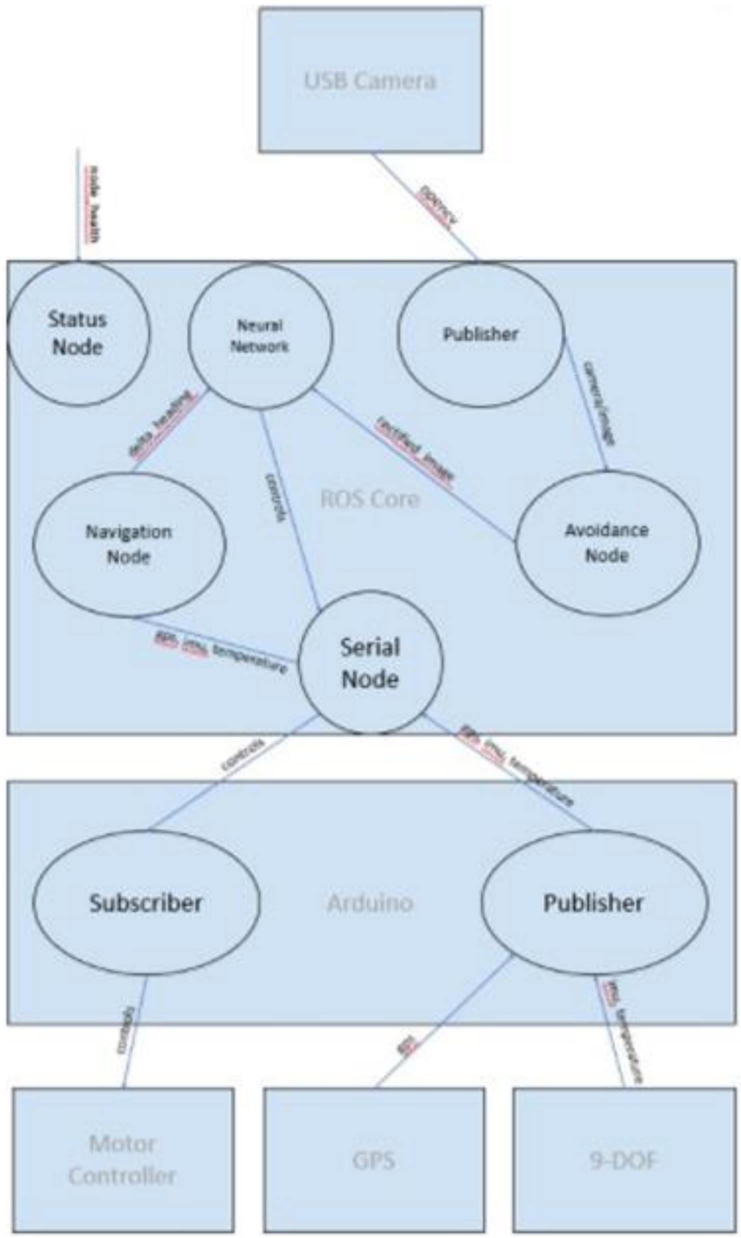

Figure 40: ROS Core Data Flow

5.4 Sensor Design

This section will discuss the composition of the sensor technologies, used to interpret data collected by the Lidar system in order to detect objects and maneuver around them. This is the heart of our design, and so requires an extensive design process.

5.4.1 Components

1. Single Board Computer:

In selecting the proper hardware system in providing a back-end for the software required to operate the robot, the following must be considered: its weight, its power draw, its processing power, and its architectural capabilities. The hardware should be powerful enough to be able to control and process the different sensors and imaging devices on the buggy without having too much overhead, allowing a real-time autonomous operation of the vehicle but at the same time, its power draw should be conservative in such a way as to not overdraw from the solar panels and the batteries as power might be needed elsewhere.

The Raspberry Pi 3 was initially the optimal choice due to its price and its ability to still decently run the required software implementations for the buggy. The Nvidia Jetson TX1, while impressively powerful, was originally turned down since it has an MSRP of ˜$300. The issue with the price ended up being resolved due to a student discount which brought the price down to a reasonable level. This price reduction caused us to go with the Nvidia Jetson TX1 as our official computer system.

2. GPS tracking unit:

While Image and sensor processing alone can allow a robot to operate safely by avoiding obstacles, true autonomy can only be achieved if the robot knows where exactly it is. A GPS tracking unit is a device that allows just that. A GPS tracking unit uses the Global Positioning System (GPS) to track the device's movements at intervals to determine its location and, when attached to the vehicle, its carrier. A GPS tracking unit monitors multiple satellites and uses triangulation to determine its position along with its deviation from true time. It does this by receiving GPS signals (carrier wave with modulation) that includes:

- Pseudorandom bits that is known to the tracking unit. By time aligning a receiver-generated version and the receiver-measured version of the code, the time of arrival of a defined point in the code sequence, called an epoch, can be found in the tracking unit clock time scale
- A message that includes the time of transmission of the code epoch (in GPS time scale) and the satellite position at that time

The tracking unit measures the times of arrival of at least four satellite signals. From the time of arrival and the time of transmission, the tracking unit forms four time of flight values which are approximately equivalent to the distance between the tracking unit and the satellite. The tracking unit then calculates its three dimensional position from this.

5.5 Navigation Design

This section will concern the design of the navigation system of the buggy, which will be used to ensure that the buggy does not leave a safe area of the beach and enters, say, open traffic. Such a malfunction would be disastrous to the safety aspects of this project, and so it is necessary to ensure that they are rock solid.

5.5.1 Components

The navigation system is based on two chips; an Adafruit Ultimate GPS Breakout v3 chip, and an Adafruit 9-DOF Absolute Orientation IMU Fusion Breakout INS chip.

1. **Adafruit 9-DOF Absolute Orientation IMU Fusion Breakout INS Chip**

The INS chip is primarily going to be used to verify GPS data- for example, if the GPS reports that the buggy has suddenly lurched 30 feet to the right but the INS says it hasn't, that GPS data is discarded. The secondary use of the INS chip is to monitor the temperature of the single-board computer and turn on and off additional cooling fans as needed. The INS chip does have a magnetometer that could make available usable heading information, however the team is concerned that the amount of metal in the buggy would interfere with the magnetometer enough to make it unreliable.

2. **Adafruit Ultimate GPS Breakout v3 Chip**

The GPS chip is going to be the core of the general navigation system. The team plans to make a series of GPS waypoints hardcoded into the buggy, which will describe a "safe" general path. The waypoints will have a radius that the buggy will need to get within to count as having reached that waypoint, and it will travel between waypoints using a "travel" and "safe" corridor system.

5.5.2 Concepts

First, the team defines a series of waypoints, a "tag" radius, a "travel" corridor width, and a "safe" corridor width. Then the buggy calculates heading based on the last 3-5 valid GPS locations, calculates a heading from its current position to the next waypoint, and then takes the difference between those two headings to figure out both which direction the buggy needs to turn, and how "urgent" that need is with some allowable amount of inaccuracy (e.g. if the heading is within 5 degrees of going directly towards the waypoint, the need value will be set to lowest priority).

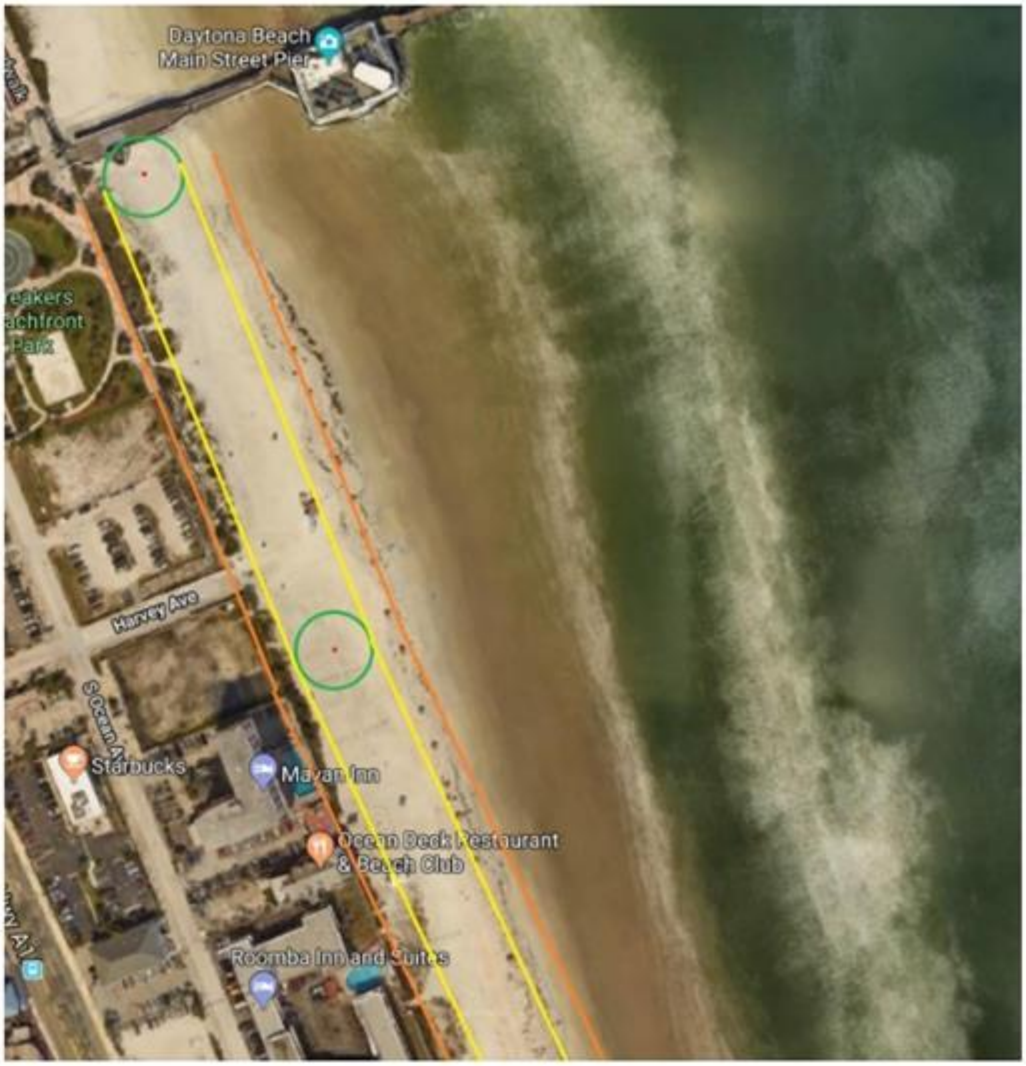

Figure 41: Navigation Mock up.

In this mockup, the red points are the waypoints, the area in between the yellow lines is the travel corridor, and the area in between the orange lines is the safe corridor. The green circles indicate the tag radius, meaning the buggy counts as having reached the associated waypoint once it enters the green circle. It's important to note that in this example, the travel corridor is the same width as the tag circles, and the safe corridor is even wider than that; in the final version, the team may use a smaller tag radius, and potentially variable width travel/safe corridors (to account for a particularly narrow stretch of beach for example). Furthermore, the travel corridor is a "soft" border that the buggy can cross (but avoids crossing) whereas the safe corridor is a "hard" border, meaning the buggy will stop and turn around rather than cross the border. Final decisions related to corridor width and associated information will have to be based on prototyping and testing, to get an idea of what works and what doesn't.

In general navigation mode, the buggy will try to stay within the travel corridor; and, within that corridor, navigation is going to be relatively low priority, especially weighed against object avoidance. When it leaves the travel corridor and is only in the safe corridor however, navigation will have a gradually increasing weight proportional to how close it is to the safe border to keep it from driving into the ocean or into the street; this may include some concept of completely stopping, turning around, and driving away from the next waypoint if the buggy thinks it has reached a dead-end. Fortunately, this should be possible to do as a zero-point turn with the planned differential steering system, which should resolve any safety concerns.

5.5.3 Design

Figure 45 shows the block diagram for the navigation design.

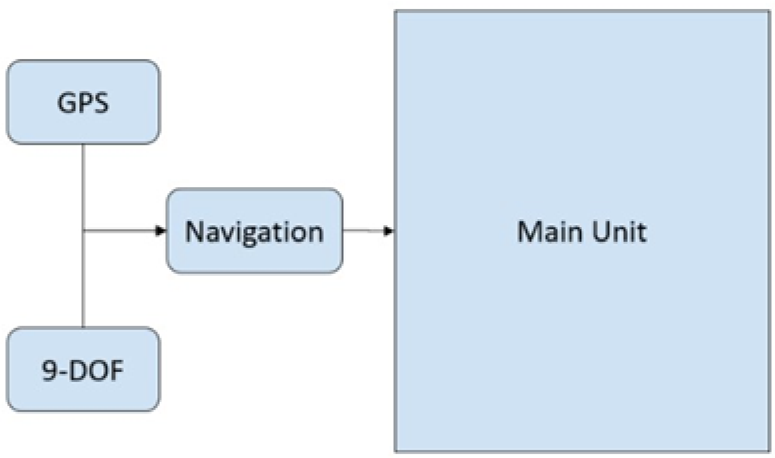

Figure 42: Navigation Design.

6.0 Course of Action Moving Forward

After an intensive, semester long study of this design project and all of it's requisite components, we believe we have a very firm understanding of the challenges we face as engineers, and the methods and parts we have identified as solutions to them. Our buggy must be completely self-sufficient, relying only on solar panels, and to that end we have identified some of the most efficient, cost effective circuit components we could find, in order to assemble a system which can create a large enough current to power two motors and a host of necessary computer systems. Our buggy must be able to identify and avoid collision with objects, and it will be able to, once we assembly and install our Lidar system and program the Arduino to recognize objects from the cloud of distance points it generates. It will be aided in this by a robust navigational system and an advanced microcontroller. Our buggy must be able to operate for a distance of 20 miles, and it will be able to, as a careful analysis of the power costs vs. the power generated by our solar cells will allow us to design around our power limitations.

Our ECE group will be taking Senior Design II in the summer term of 2018, while the portions of our larger group, consisting of mechanical engineers and computer scientists, will be taking the course in the fall. As a result of this discrepancy, we will be unable to produce the buggy chassis designed by the mechanical members of our team. Therefore, we will seek out a substitute vehicle of comparable complexity and design, and attempt to tailor our power and detection systems to the substitute vehicle's design. In doing this, we hope to create a working model car that demonstrates the validity and effectiveness of our Lidar and solar power systems, both with regards to providing the ability for a vehicle to autonomously detect obstacles and drive around them, and in general operational terms. If we can demonstrate that our designs are functional on a smaller scale vehicle, it would stand to reason that they would be applicable on the full-scale buggy that we had originally intended.

7.0 Administrative Content

This chapter describes the agreed time schedule and budget of the team. These were agreed upon through both discussions within the team, and discussions among the other teams in the buggy project. The section also lists references consulted in the planning and organization of this project.

7.1 Milestone Discussion

This section breaks down the time allotment planned for the completion of the project. Table 19 lists major project milestones and their approximate times of completion.

Senior Design 1		
Number	Milestone	Planned Completion Week
1	Brainstorming	1-2
2	Project selection	2
3.	Divide and conquer	3
4.	Research and documentation	4-11
5.	Table of contents	12
6.	Writing	13
7.	Design	14
8.	Final Senior Design 1 Paper	15
Senior Design 2		
Number	Milestone	Planned Completion Week
9.	Order PCB and parts	1-2
10.	Build prototype	3-4
11.	Testing and revisions	5-9
12.	Final Testing	10-11

13.	Final Report	11-12
14.	Presentation	12

Table 19. Major Project Milestones

7.2 Budget and Finance Discussion

The budget of $2000 provided by Duke Energy is split between the Mechanical Engineering team and the Electrical and Computer Engineering team. The size of the split is dependent on the basis of importance of parts that falls under a team, to the overall function of the system. It has been agreed upon that since the mechanical system is a vital and also the most expensive part of the project, a good portion of the budget will fall under the Mechanical Engineering team, with the motors and tires being the most expensive parts of the buggy.

7.3 References

1) http://forums.bajasae.net/forum/monoshock_topic723.html

2) AutoNEWS. “Das ist der Leichtbau-Offroader Ariel Nomad.” *Irrer Offroad-Racer Ariel Nomad: Infos, technische Daten und Preis (Bild 2)*, www.auto-news.de/auto/news/bildergalerie_Irrer-Offroad-Racer-Ariel-Nomad-Infos,-technische-Daten-und-Preis_id_36251&picindex=1.

3) Bureau, The Masterbuilder. “Analysis of Space Frame Structure.” *The Masterbuilder*, 4 Nov. 2017, www.masterbuilder.co.in/analysis-space-frame-structure/.

4) Life of Riley. “Space frame.” *Wikipedia*, Wikimedia Foundation, 5 Nov. 2017, en.wikipedia.org/wiki/Space_frame#/media/File:Articulacion_malla.svg.

5) *Young's Modulus - Tensile and Yield Strength for common Materials*, www.engineeringtoolbox.com/young-modulus-d_417.html.

6) “How To Prep Your ATV For The Sand Dunes.” *MotoSport*, 31 Dec. 2013, www.motosport.com/blog/how-to-prep-your-atv-for-the-sand-dunes.

7) Ken962. “Brushless DC Electric Motor Torque-Speed Characteristics.” *Wikimedia Commons*, 6 Nov. 2010, commons.wikimedia.org/wiki/File:Brushless_DC_Electric_Motor_Torque-Speed_Characteristics.png.

8) kennybobby. “Ev Conversion Torque Calculation and Motor Specifications.” *DIY Electric Car Forums RSS*, 14 Oct. 2013, www.diyelectriccar.com/forums/showthread.php/ev-conversion-torque-calculation-and-motor-89694.html

9) Hymel, Shawn. “Alternating Current (AC) vs. Direct Current (DC).”*Alternating Current (AC) vs. Direct Current (DC)*, SparkFun Electronics, learn.sparkfun.com/tutorials/alternating-current-ac-vs-direct-current-dc.

10) “4x4 Buggy Building & Tubing - 4Wheel & Off-Road Magazine.” *Four Wheeler*, 1 Feb. 2006, www.fourwheeler.com/how-to/body-chassis/131-0602-4x4-buggy-building-tubing/.

11) “Switching Regulator Fundamentals,” TI , Texas Instruments , Sept. 2016

http://www.ti.com/lit/an/snva559a/snva559a.pdf

12) “AmpFlow Wheels & Gearmotors.” Robot MarketPlace. The Robot MarketPlace, n.d. Web. 11 Apr. 2018. http://www.robotmarketplace.com/products/ampflow-motors.html

13) ”BatteryUniversity,”Battery Cofiguration. N.p., n.d. Web.
http://batteryuniversity.com/learn/article/serial_and_parallel_battery_configurations

14) DimensionEngineering,” User’s Guide. N.p., n.d. Web.
https://www.dimensionengineering.com/datasheets/Sabertooth2x60.pdf

15) “A sparse signal reconstruction approach for sequential equivalent time sampling” published in Instrumentation and Measurement Technology Conference Proceedings (I2MTC), 2016 IEEE International

16) Weitkamp C. *Lidar. [Electronic Resource] : Range-Resolved Optical Remote Sensing Of The Atmosphere* [e-book]. New York : Springer, c2005.; 2005. Available from: UCF Libraries Catalog, Ipswich, MA.

17) Lightware OSLRF datasheet
http://www.lightware.co.za/shop2017/download/Documents/OSLRF-01%20-%20Laser%20Rangefinder%20Manual%20-%20Rev%202.pdf

18) “*ROS: Wiki Documentation*”. N.p., n.d. Web. http://wiki.ros.org/.

19) *“OpenCV 2.4.8.0 documentation - Welcome to opencv documentation!”* N.p., n.d. Web. https://docs.opencv.org/2.4.8/

20) *“ISO/IEC/IEEE 29119 Software Testing -- The international standard for software testing”* N.p., n.d. Web. http://www.softwaretestingstandard.org/index.php

21) IPC. *“IPC-221B Generic Standard Generic Standard on Printed Board Design”* Web. http://www.ipc.org/TOC/IPC-2221B.pdf

8.0 Appendix

8.1 An Explanation of Neural Networks

This paper assumes that the reader has a rudimentary understanding of neural networks. Since neural networks are an emerging technology this may not be the case. This section attempts to explains neural networks. This does not explain all the facets of neural network. Instead, the information in this section should provide enough of an explanation to understand the design choices.

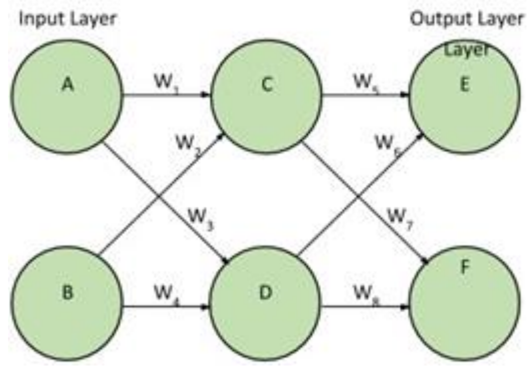

Figure 46 - A visual representation of a neural network with 1 hidden layer

Neural networks are a form of program that attempts to mimic the thought process of animals. Computers are normally discrete, meaning there is a set pattern to how they process data. Most programs make use of control flow statements such as if, while or for. A programmer must provide a set behavior for every possible input. This is very powerful, but it is not very flexible; especially when the input is more abstract like an image. Neural networks allow decision making without hard coded behaviors. The neural network is trained using data that simulate the inputs that are expected. When properly trained, a neural network can process data that it has never seen before.

8.1.1 <u>The General Structure</u>

Neural Networks are composed of components called nodes or neurons. These nodes are arranged in layers. All neural networks begin with an input layer. This layer has a node for each input into the neural network. For example, if the only inputs are two integers, there are two input nodes. For images, this is a little more complicated. Each pixel of an image is given a node. An image that is 640x480 would have 307,200 input nodes. All neural networks also have an output layer. This layer has a node for every expected output. These nodes can be used to encode any kind of information. It can be an integer, a probability calculation or something as complex as an image. In Nvidia's case, it had an output node that described how much the vehicle had to turn. Between the input and output layers there may be any number of extra layers of calculation. Since these layers are not directly interacted with, they are called hidden layers. For very basic problems, it may be fine to have only an input and an output layer. As problems get more complex, more layers are generally required. The term deep neural network refers to a neural network that makes use of multiple hidden layers. Generally, each node has an associated connection to every node in the previous and next layer. In the example diagram, each layer has 2 nodes which means each node has at least 2 connections. Node C is in a hidden layer, so it has 4 connections; 2 to the input layer and 2 to the output layer. These connections have associated weights which are used during calculations.

Calculations begin at the input layer. When the neural network is given an input, the next layer must be calculated. First, a sum of products is calculated for each node. This consists of the values for each node in the previous layer multiplied by the weight of the connection between that node and the node to be calculated. The sum of these products is then fed into the activation function of the node. This is a very simple function that adds an element of non-linearity to the network. Without the activation function, the relationship between the input and output of the network would be linear. This may be fine for something very simple but most problems that benefit from a neural network are not simple. There are multiple types of activation functions that can be used. The main ones are: a sigmoid, tanh, Rectified Linear Unit(ReLU) and Leaky ReLU. Each function has its own properties that make it useful. The function that is used depends on the needs of the network. Each node has its own activation function. As a general rule, the activation functions should be the same for each node. There may be a reason to make them different on a node to node basis, but you should already know why you are doing so. The output of the activation function is the new value for the node. Once all the values are calculated for that layer, the next layer, if there is one, can be calculated in the same way. This continues until the output layer is reached.

8.1.2 The Training Process

For a neural network to function properly, it must first be trained. When the network is initially created, the connections between each node are given random weights. The only caveat is that none of the weights should be zero. If a weight is assigned 0, it essential kills the node associated to it. The network is trained by adjusting the weights until the outputs are accurate. The most widely used method is back propagation. The new neural network is given inputs with desired outputs associated with them. The output of the neural network is compared to our desired output using an error function. This function determines how off the neural network's output was from the expected output. There are numerous types of error functions each with their own merits. The change in the weight values must be calculated one by one. It is found by finding the partial derivative of the error function with respect to the specific weight. For example, imagine the example neural network uses the error function:

$$Error = \frac{1}{2}(ExpectedOutput - ActualOutput) \qquad (1)$$

Now imagine that we want to calculate the amount that the weight w5 should change. This requires both the sum of products that reaches the node E and the sum of products after it has been put through the activation function. For clarity, the sum of products before the activation function is designated RawOutput and the sum afterwards is labeled Output. The calculation would be:

$$\frac{\delta Error}{\delta w_5} = \frac{\delta Error}{\delta Output} * \frac{\delta Output}{\delta w_5} = \frac{\delta Error}{\delta Output} * \frac{\delta Output}{\delta RawOutput} * \frac{\delta RawOutput}{\delta w_5} \qquad (2)$$

While this may seem intimidating, these partial derivations are values that are already known. $\frac{\delta Error}{\delta Output}$ is the derivative of the error function. Since w1 only affects the output of E, we are only concerned about the error of E. $\frac{\delta Output}{\delta RawOutput}$ is the derivative of the activation function that converts the sum of products to the output of E. $\frac{\delta RawOutput}{\delta w_5}$ is the output of the nodes that contribute to the raw output. Since only node C is affected by w1, it is only the output of node C. The equation for each weight is unique. Once the error has been calculated for each node, the weights are adjusted by subtracting the error from them. Many neural networks multiply the error by a Learning Rate before subtracting. The value of this constant determines how drastic the changes to the neural network's weights are. It is crucial that the Learning Rate. Is set properly. If it is too high, the neural network will bounce around the ideal weight settings without ever getting close to them. If it is set too low, the neural network will take too long to train.

The problem of programming these calculations is generally a solved one. There are many libraries in many languages that allow the creation of neural networks without specifically programming these calculations. Instead, the programmer only has to select components like number of layers, layer size, activation functions and error functions. The main impact that a programmer has over training is selecting appropriate training data. The purpose of training data is to "teach" a neural network how to do something given a type of input. It is important that the training data includes all the possibilities. Ideally, there should be lots of variation in the training data. It should contain lots of data so the neural network can "learn" its job completely. In addition, the data should be varied so it is able to handle a wide variety inputs. For example, if a neural network is meant to identify images with a cat in them, the training data should include many images with cats in them and images without cats in them. For the images with cats in them, there should ba a wide variety of images at multiple distances and angles to the subject. In addition, the background of the images should be varied. It may be beneficial to include data that the programmer believes may lead to confusion. Using the cat example, some of the images that don't contain cats could have other animals that

8.1.3 Image Processing

Images are very interesting to handle with Neural Networks. One of the main processes performed on an image is Normalization. Some images may be brighter or darker than others. Image normalization changes the range of brightness in an image by subtracting each pixel by the image's minimum value and then multiplying the new values by the desired range divided by the current range. The standard range in intensity is 0 to 255. Before an image is put through a neural network, it should be normalized. A good neural network should be able to handle images at any brightness. Normalizing images before processing makes sure that the input into the neural network is more uniform.

Each pixel in an image is represented by at least one number. As a result, the input layer of a neural network that handles images is huge. Since each node in a layer is connected to every node in adjacent layers the increase in the number of connections is even larger. While it is feasible to process images using a normal neural network, this method suffers greatly due to long computation times. Instead, it may be useful to use a convolution layer. Essentially, this means that a smaller neural network is made to handle a small section of the image called a kernel. Normally, this is a small square with a single digit amount of pixels on each side. The convolution layer takes the full image as an input. The convolution layer neural network begins at one corner of the image and performs its calculation. After, it shifts by a set amount, normally smaller than the kernel size, and takes the new square as its input. This creates an array of processed squares that is considered the output of the convolution layer. The array of outputs can then be used as the input into another neural network. The convolution layer acts as feature detector in the image. Nvidia used convolution layers in their autonomous car. The output of these layers highlighted key features in the image such as the edge of the road. Convolution layers are generally used in conjunction with pooling. Pooling involves reducing the data from a kernel to a single value. There are multiple methods for pooling. The output could be an average of each pixel or the maximum value.

8.2 Review of Relevant Papers

8.2.1 Navigator Design Report 2011 Intelligent Ground Vehicle Competition

This was a paper discovered early on in the design process. Initial designs of the autonomous system involved stereo vision to detect obstacles in the surrounding area. The robot discussed in this report exhibited many features that seemed relevant to this initial design. The robot utilized LiDAR to detect and measure the distance to nearby obstacles. It used a three camera setup in addition to the LiDAR system by detecting narrow objects that the LiDAR misses and collecting even more data for more detailed mapping of the surrounding area. This design utilizes the ROS navigation package. One of the main drawbacks of this design is the cost. The budget for this robot was listed at $4708. In addition, key components of the system such as LiDAR were listed as costing $0 implying that they were either sponsored or they already possessed them. The LiDAR system used by itself is over the allocated budget for the entire buggy.

8.2.2 End to End Learning for Self Driving Cars

This paper was written by Nvidia which is a leader in computer vision and machine learning. Here they attempt to create a vehicle capable of driving on roads safely. What is very interesting is the only kind of sensor used was a camera. This is done using a trained Convolutional Neural Network. It works by taking input from three separate cameras and feeding the stream into the neural network. First the images, which are initially only 66x200 pixels, are normalized and passed through three layers of convolution. These layers reduce the images to 64 separate 3x20 images that together are trained to mark the features of the road. These images are then fed into another three layers which convert them into steering controls.

The results of this experiment are very interesting. The neural network was able to learn to drive entirely from video training data. The programmers did not need to define road markers at all. It learned to distinguish the boundaries of the road entirely on its own. The conditions we will be driving under will be very different. We will not be able to rely on a defined road. Instead, we will be driving through unmarked land while avoiding any obstacles that may be present. The solution should be relatively similar though. Instead of training the buggy to follow a path, we will need it to avoid obstacles. In addition, we should be able to add a node to the input layer that feeds the neural network GPS data. This should allow the buggy to avoid obstacles with a tendency to turn towards our destination.

8.2.3 End-to-end Driving via Conditional Imitation Learning

The abstract of this paper explains the high-level concept; using deep networks trained to drive a vehicle in the sense of staying on the road and avoiding obstacles, combined with imitation learning for driving policies, ultimately creating a vehicle that can follow directions like “turn right at the next intersection”.

Practically speaking, the problem the paper is solving has to do with imitation learning. Imitation learning works under the assumption that by watching an expert perform a task, a network can be trained to imitate the expert and will then perform as well as the expert. This relationship is described in sets of observations and associated actions; that is, when the expert observes X it does Y, which is what the network seeks to replicate. However, an “implicit assumption ... is that the expert’s actions are fully explained by the observations” [2]. The problem this creates is that an imitation trained network can successfully drive a car and keep it on the road, and follow lanes- but, for example if it come to a fork in the road, it’s steering commands oscillate between the two options because it has no concept of intention. The solution in this paper was to provide an additional “command” argument that provided that intention, in addition to a clever method of training the model with a limited dataset by applying a variety of transformations to good data in order to create noisy training data, which allows the model to generalize better.

8.2.4 Autonomous Off-Road Vehicle Control Using End-to-End Learning

Though dated, this paper is an early and fairly effective example of endto-end learning being used to drive a vehicle in unknown terrain. This paper is particularly relevant because it focused on off-road driving, with obstacles like rocks, ditches, and ponds. Furthermore, it specifically used a stereo camera design, which is one of our potential detection options. Lastly, it includes a concept of live self-adjustment, in order to adapt to new and unknown obstacles.

Overall, the utility of the paper comes from its similarity to our project – cameras for input, ultrasonic rangefinders for close range detection, a magnetometer compass – and from their method of getting useful training data, which is to record a human driving the vehicle around based on the camera feed only. Fortunately, the age of the paper may act in our favor - even though they had a $30,000 budget, in 2004 that got them a 2-core CPU with 512 MB of RAM. This means that ideally their performance should be worse than or similar to our single-board computer, giving us an idea of what we can expect. Lastly, because this paper was so early in the development of end-to-end learning as a practical solution, everything is explained at an extremely accessible level, very thoroughly.

8.3 Development Environment Setup Instructions

This setup guide is starting from a brand new VM. The team used VirtualBox, because it is free and widely supported, even though it is lacking compared to other available virtualization options. The VM is used for development in an

Ubuntu environment, and so that team members can develop without physical access to the Nvidia Jetson TK1.

8.3.1 VM Setup

Download the preconfigured ROS VM from Ubiquity Robotics, linked in Appendix G. Extract the downloaded zip to your VirtualBox VMs folder, then double-click the Workstation 1.0.1.vbox file to start the virtual machine. Once it is running, the first thing to do is change the password by opening a terminal and running:

passwd sudo passwd

The default username and password is ”ubuntu”. Then, run

sudo apt-get update

to make sure everything is ready to go.

8.3.2 ROS (BSD License)

This section covers the last bits of ROS setup still needed on the VM. First, update the package key by running:

wget https://raw.githubusercontent.com/ros/rosdistro/master/ros.key sudo apt-key add ros.key

At this point it should be safe to delete the downloaded ros.key file. Note, this part isn’t strictly necessary, it’s just to make sure there are no problem with the rest of setup. Next, run

rosdep update

to update the ROS packages. To verify that everything is set correctly, run;

export — grep ROS

This should print several lines that look like declare -x ROSLISP —

PACKAGE DIRECTORIES ””

To verify that ROS is working, open a new terminal to run each of the following commands;

roscore rosrun turtlesim turtlesim node
rosrun turtlesim turtle teleop key

There should now be three terminal windows open, in addition to a window with a small turtle in it, that can be moved around using the arrow keys on your keyboard.

8.3.3 Rosserial Arduino (BSD License)

This section covers the setup of the Arduino IDE and installation of rosserial so that Arduino output appears as a node in ROS.

First, install the Arduino IDE from their website, found in Appendix G. The pre-installed VM needs the Linux 64 bits version. It will take you to a page asking for donations, but you can click ”Just Download”. Extract the files into ‘/home/ubuntu‘, then open the created folder and run the ‘install.sh‘ file in terminal.

We will now need to ”unblock” serial communication; run

sudo usermod -a -G dialout ubuntu

You will need to log out and back in for this to take effect. The last bit of Arduino IDE setup is, open the IDE, and under Tools, set the Board and Port to the correct board and port; the Port setting only matters if you have an actual physical Arduino to plug in, but the Board should match the actual board for correct compilation and verification. Now, install rosserial by running:

sudo apt-get install ros-kinetic-rosserial-arduino sudo apt-get install ros-kinetic-rosserial

Now that rosserial is installed on the ROS side, we can install it on the Arduino side; installing Arduino should have created a folder called ”Arduino” in ‘/home/Ubuntu/‘; ‘cd‘ to ‘/Arduino/libraries/‘ and run

rosrun rosserial arduino make libraries.py .

Note the period after make libraries.py, that is an argument needed to indicate that we’re installing ”here” rather than giving it a directory path to install in. To verify that this installed correctly, restart any Arduino IDEs you may have open and look in File → Examples for ros lib to be listed.

8.3.4 Adafruit Arduino libraries (BSD License)

This section covers installing the Adafruit libraries required to run the breakout boards.

‘cd‘ to the same ‘/home/Ubuntu/Arduino/libraries/‘ folder that the rosserial library is installed in, and run the following commands:

git clone http://github.com/adafruit/Adafruit GPS

git clone http://github.com/adafruit/Adafruit 10DOF
git clone http://github.com/adafruit/Adafruit Sensor
git clone http://github.com/adafruit/Adafruit LSM303DLHC
git clone http://github.com/adafruit/Adafruit BMP085 Unified
git clone http://github.com/adafruit/Adafruit L3GD20 U

All of these can be verified at once, by checking under File → Examples to see that their example code is available. Using the GPS as an example, open the Arduino IDE, and look under File → Examples for ”Adafruit GPS Library”.

8.3.5 Clone the Repo

This section covers getting the repo downloaded and working. Note that this is a private repo, and you must be added as a contributor to the repo before this section (or anything after this section) will work.

Open a terminal and make sure you're in '/home/ubuntu'; then, run git

clone http://github.com/pH34r-pH/SolarBuggy

'cd' into the SolarBuggy folder you just made and run 'git checkout [somebranch]' if you're working on something outside of 'master'. You can 'git pull' to ensure everything is up to date, but the checkout/clone should handle that. Next, inside the SolarBuggy folder, run

catkin make

This should take a bit to run, but it verifies that the project is building correctly on your system. It may throw a few warnings, but those are from packages within ROS- everything should otherwise finish correctly. Lastly, (and this must be done after every 'catkin make' that adds a new node or package), run

source ./devel/setup.bash

so that bash can find any new packages you've added. Installation can be verified by running the following, each in different terminals;

roscore rosrun buggybrain hello

The buggybrain hello command should “reply” with something like '[INFO] [numbers]: Hello, ROS¡.

8.3.6 Test (with an Arduino)

Plug in the Arduino via USB to the host computer. On the VirtualBox, click Devices -¿ USB and check the Arduino; this connects it to the VM. Open the Arduino IDE and under Tools, select the correct Arduino model and port (there should only be one available) to connect the IDE to the Arduino. Open and upload the ros hello.ino file from the Arduino folder inside the SolarBuggy project. Run the following commands, each in a separate terminal;

roscore

rosrun rosserial python serial node.py /dev/ttyACM0

Changing the port at the end of the second command to match what you're connected to. Open a third terminal and run

rostopic list

You should see '/chatter' and '/diagnostics' which means everything is working.

8.3.7 Errata

It may be necessary to also run 'sudo usermod -a -G video ubuntu' once a USB camera is set up, in order to actually get video.

8.4 Development Environment Resources

1. VirtualBox VM, downloadable at https://www.virtualbox.org
2. Ubiquity Robotics Virtual Machine Image, downloadable at https://downloads.ubiquityrobotics.com/
3. Arduino IDE, downloadable at https://www.arduino.cc/en/Main/Software

8.5 SolidWorks CAD Iteration Information

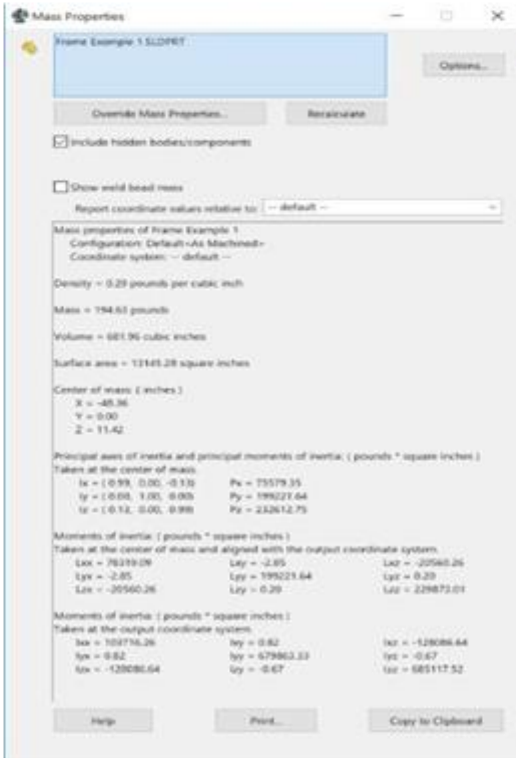

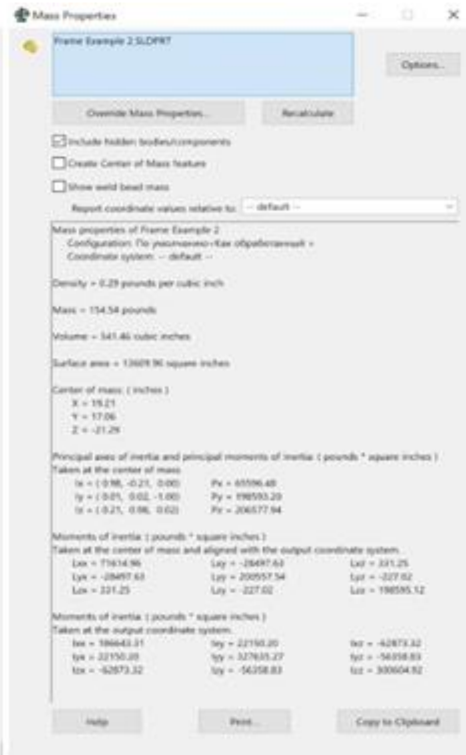

(a) Iteration 1 Mass Properties (b) Iteration 3 Mass Properties

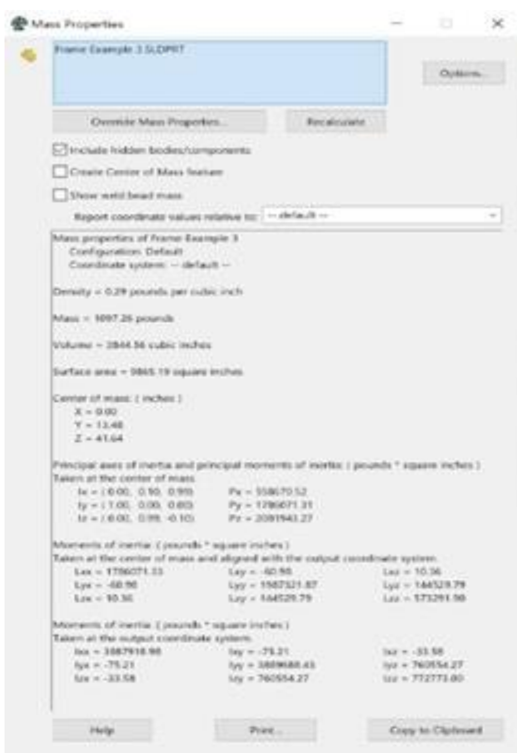

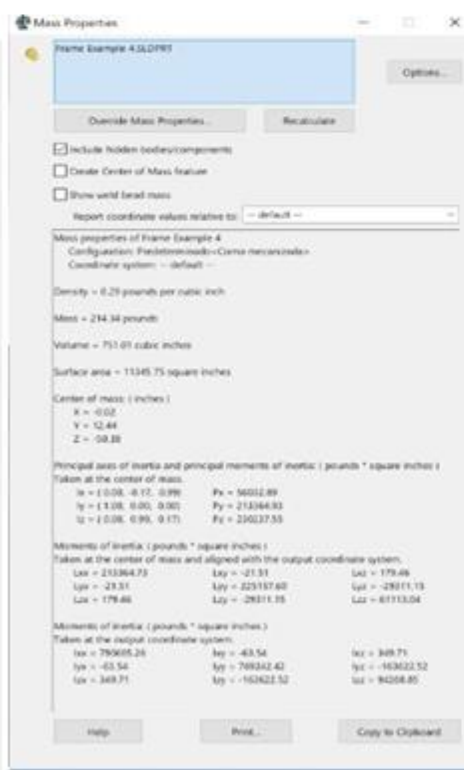

(a) Iteration 3 Mass Properties (b) Iteration 4 Mass Properties

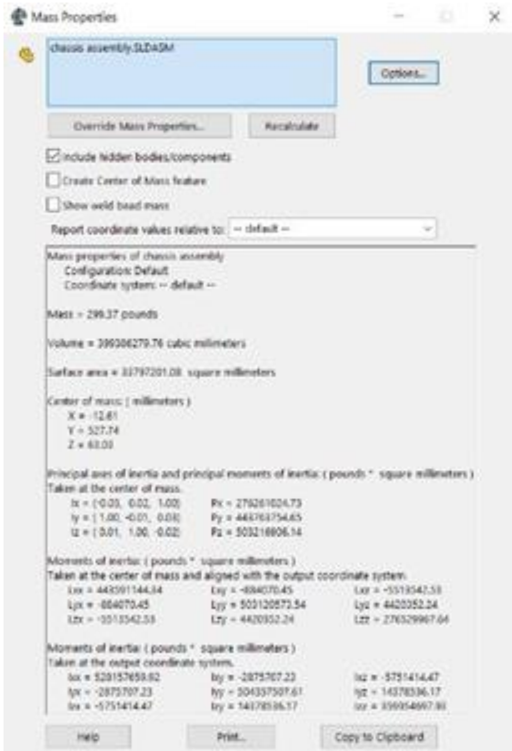

(a) Iteration 6 Mass Properties

(b) Iteration 7 Mass Properties

8.6 Ansys Analysis Data

1. Factor of Safety

Time [s]	Minimum	Maximum
1	1.7666	15

Table 20 - Static Structural Safety Factor

Object Name	Stress Tool
State	Solved
Definition	
Theory	Max Equivalent Stress

Stress Limit Type	Tensile Yield Per Material

Table 21 - Static Structural Stress Safety Tools

Object Name	Safety Factor
State	Solved
Scope	
Scoping Method	Geometry Selection
Geometry	All Bodies
Definition	
Type	Safety Factor
By	Time
Display Time	Last
Calculate Time History	Yes
Identifier	
Suppressed	No
Integration Point Results	
Display Option	Averaged
Average Across Bodies	No
Results	
Minimum	1.7666
Minimum Occurs On	chassis Default<As Machined>
Information	
Time	1. s

Load Step	1
Substep	1
Iteration Number	1

Table 22 - Static Structural Stress Tool Results

Object Name	Stress Tool 2
State	Solved
Definition	
Theory	Max Shear Stress
Factor	0.5
Stress Limit Type	Tensile Yield Per Material

Table 23 - Static Structural Stress Safety Tools

Object Name	Safety Factor
State	Solved
Scope	
Scoping Method	Geometry Selection
Geometry	All Bodies
Definition	
Type	Safety Factor
By	Time
Display Time	Last
Calculate Time History	Yes
Identifier	

Suppressed	No
Integration Point Results	
Display Option	Averaged
Average Across Bodies	No
Results	
Minimum	1.5343
Minimum Occurs On	chassis Default<As Machined>
Information	
Time	1. s
Load Step	1
Substep	1
Iteration Number	1

Table 24 - Static Structural Stress Tool 2 Results

Time [s]	Minimum	Maximum
1	1.5343	15

Table 25 - Static Structural Stress Tool 2 Safety Factor

2. Material Data

Density	0.2836 lbm in^-3
Coefficient of Thermal Expansion	6.6667e-006 F^-1
Specific Heat	0.10366 BTU lbm^-1 F^-1
Thermal Conductivity	8.0917e-004 BTU s^-1 in^-1 F^-1

Resistivity	8.5235 ohm cmil in^-1

Table 26 - Structural Steel Constants

Compressive Ultimate Strength psi
0

Table 27 - Structural Steel Compressive Ultimate Strength

Compressive Yield Strength psi
36259

Table 28 - Structural Steel Compressive Yield Strength

Tensile Yield Strength psi
36259

Table 29 - Structural Steel Tensile Yield Strength

Tensile Ultimate Strength psi
66717

Table 30 - Structural Steel Tensile Ultimate Strength

Zero-Thermal-Strain Reference Temperature F
71.6

Table 31 - Structural Steel Isotropic Secant Coefficient of Thermal Expansion

Alternating Stress psi	Cycles	Mean Stress psi
5.80E+05	10	0
4.10E+05	20	0

2.75E+05	50	0
2.05E+05	100	0
1.55E+05	200	0
63962	2000	0
38000	10000	0
31038	20000	0
20015	1.00E+05	0
16534	2.00E+05	0
12502	1.00E+06	0

Table 32 - Structural Steel Alternating Stress Mean Stress

Relative Permeability
10000

Table 33 - Structural Steel Isotropic Relative Permeability